BORDER COLLISION BIFURCATIONS

IN PIECEWISE SMOOTH SYSTEMS

A THESIS SUBMITTED TO THE UNIVERSITY OF MANCHESTER

FOR THE DEGREE OF DOCTOR OF PHILOSOPHY

IN THE FACULTY OF ENGINEERING AND PHYSICAL SCIENCES

2011

Chi Hong Wong

School of Mathematics

Contents

List of Tables

List of Figures

6

The University of Manchester

Chi Hong Wong
Doctor of Philosophy
Border Collision Bifurcations in Piecewise Smooth Systems
December 12, 2011

Piecewise smooth maps appear as models of various physical, economical and other systems. In such maps bifurcations can occur when a fixed point or periodic orbit crosses or collides with the border between two regions of smooth behaviour as a system parameter is varied. These bifurcations have little analogue in standard bifurcation theory for smooth maps and are often more complex. They are now known as "border collision bifurcations".

The classification of border collision bifurcations is only available for one-dimensional maps. For two and higher dimensional piecewise smooth maps the study of border collision bifurcations is far from complete. In this thesis we investigate some of the bifurcation phenomena in two-dimensional continuous piecewise smooth discrete-time systems.

There are a lot of studies and observations already done for piecewise smooth maps where the determinant of the Jacobian of the system has modulus less than 1, but relatively few consider models which allow area expansions. We show that the dynamics of systems with determinant greater than 1 is not necessarily trivial.

Although instability of the systems often gives less useful numerical results, we show that snap-back repellers can exist in such unstable systems for appropriate parameter values, which makes it possible to predict the existence of chaotic solutions. This chaos is unstable because of the area expansion near the repeller, but it is in fact possible that this chaos can be part of a strange attractor. We use the idea of Markov partitions and a generalization of the affine locally eventually onto property to show that chaotic attractors can exist and are fully two-dimensional regions, rather than the usual fractal attractors with dimension less than two. We also study some of the local and global bifurcations of these attracting sets and attractors. Some observations are made, and we show that these sets are destroyed in boundary crises and some conditions are given. Finally we give an application to a coupled map system.

Declaration

No portion of the work referred to in this thesis has been submitted in support of an application for another degree or qualification of this or any other university or other institute of learning.

Copyright Statement

Publications

- Paul Glendinning and Chi Hong Wong. Border collision bifurcations, snap-back repellers, and chaos. Phys. Rev. E (3), 79(2):025202, 4, 2009.

- Paul Glendinning and Chi Hong Wong. Two-dimensional attractors in the border-collision normal form. Nonlinearity, 24(4):995-1010, 2011.

Acknowledgements

Dedication

To my Parents and Brothers

Chapter 1

Introduction

Many systems in physics, economics and various other areas involve discontinuity or sudden change, such as impact mechanical systems and switching electrical circuits. As smooth maps may not describe the non-smoothness in the systems accurately, piecewise smooth maps are often used to model such situations. By piecewise smooth systems we mean systems that are smooth everywhere except along borders separating regions of smooth behaviour. These borders divide the phase space into countably many regions.

There has been a lot of research on the theory of bifurcation in smooth dynamical systems since the 1970s and the subject is quite well understood nowadays. However, a lot of the theories do not apply to piecewise smooth systems. In smooth maps, a local bifurcation occurs when a real eigenvalue or a complex conjugate pair of eigenvalues of a fixed point crosses the unit circle. On the other hand, in a piecewise smooth map, a bifurcation may also occur when a fixed point (or a periodic orbit) crosses or collides with the border between the two regions of smooth behaviour. This involves a discontinuous change in the eigenvalues of the Jacobian matrix evaluated at the fixed point (or at a periodic point), which can lead to a new class of bifurcations different from the standard bifurcations in smooth systems. This is known as border collision bifurcation. This term was first used by Nusse and Yorke [71], though it had been studied in the Russian literature under the name C-bifurcation [26, 27] in the

1970s.

In fact, there have been a lot of studies on piecewise smooth systems over the years. Lozi introduced in the late 1970s a family of two-dimensional piecewise affine map (now known as the Lozi map), similar to the Hénon map, which was soon later proved to have strange attractors for some set of parameters [69, 62, 13, 10, 12]. There are also a large number of French publications in the 1970s and 80s by Gumowski and Mira. Since the 1990s, Gardini et.al. have been working on two-dimensional endomorphisms and piecewise smooth maps.

However, comparing with the study of smooth systems, there is relatively little research in the piecewise smooth case and border collision bifurcations, and the results obtained so far are rather preliminary. Most of this research assumes that the map is continuous across the borders, the study of discontinuous piecewise smooth maps is relatively sparse [76, 53, 6, 51, 75]. The goal of this thesis is to enrich the bifurcation theory for continuous piecewise smooth discrete-time systems.

To investigate the local behaviour near a border collision bifurcation, one needs to study the piecewise linear approximation of the map in the neighbourhood of a fixed point on the border. For one-dimensional discrete-time systems the classification of border collision bifurcations is complete [72, 5]. To study multi-dimensional systems, the non-differentiability of piecewise smooth maps does not allow the use of dimension reduction techniques such as the centre manifold theorem for smooth systems. That is why there are some differences between the bifurcations in one and two-dimensional systems, and very little is known about bifurcations in systems of arbitrary dimension. For two-dimensional maps, Nusse and Yorke [71] gave a general criterion for the occurrence of border collision bifurcations based on index theory. Moreover, a normal form for border collision bifurcations in two-dimensional piecewise smooth maps was derived [4, 7]. Since then a lot of studies of border collision bifurcations have been done using the normal form. Banerjee et. al. [4, 7] proposed a classification of border collision bifurcations for two-dimensional maps that are globally contractive. There are some bifurcations analogous to the standard ones such as saddle-node or periodic

doubling in smooth systems. Some other interesting dynamics can also occur in two-dimensional piecewise smooth maps. It has been shown that for some parameter values multiple attractors can coexist [71, 23, 7]. Chaotic dynamics is also possible, in particular, it can be robustly chaotic [9], so that for its parameter values, there exists a neighbourhood in the parameter space with no periodic attractor and the chaotic attractor is unique in that neighbourhood.

Some recent textbooks in piecewise smooth systems include [8, 87, 54, 17].

The theory of border collision bifurcations developed so far usually assumes area contractions on both sides of the border, so stable dynamics are likely to be observed numerically. When the determinant of the Jacobian matrix has modulus greater than one, the instability of the fixed point often complicates the dynamics of the system. Recently some work has been done on cases where local area expansions are allowed. When a pair of complex conjugate eigenvalues jump discretely from the inside to the outside of the unit circle as the fixed point moves across the border, the resulting dynamics is sometimes similar to the Neimark-Sacker bifurcation of a smooth map in which an attracting periodic or quasiperiodic orbit is created as the fixed point loses stability. However, the bifurcation is often much more complex, with multiple (chaotic) attractors, saddles, and repellers created or destroyed [89, 88, 79, 80, 81]. [74, 82, 83] analyze the bifurcations when a fixed point of one of the linear maps loses stability through the standard fold, flip and Neimark-Sacker bifurcations which occur in smooth maps. In the presence of the switching surface in phase space and non-smoothness of the map, these bifurcations again lead to more complicated dynamics.

In this thesis we investigate some of the bifurcation phenomena in two-dimensional systems that are area expanding and the thesis proceeds as follows.

In Chapter 2, some of the background material for border collision bifurcations is given. We introduce the border collision normal form for one and two-dimensional piecewise smooth maps, and summarize the key results of previous researchers.

In Chapter 3, we investigate the two-dimensional border collision normal form map, where there is area expansion in the phase space. We show that there can

be chaotic behaviour in the system, in particular, we use the concept of snap-back repeller and show that for appropriate parameter values there is a snap-back repeller immediately after the border collision bifurcation, and hence that the bifurcation creates chaos. Also, the idea of heteroclinic repellers, an extension of snap-back repeller, is briefly discussed at the end of the chapter.

In Chapter 4, some numerical examples are given to show that, in the area expanding case in the border collision normal form map, it is possible to have globally stable dynamics. Strange attractors can exist for such models. Although examples had already been shown in [82, 83], by using the results from Markov partition theory for two-dimensional systems and a generalization of the affine locally eventually onto (ALEO) property developed in [40], we prove that there are some parameter values for which the strange attractor can be a fully two-dimensional object, a polygonal region in fact, rather than the usual fractal attractors.

In Chapter 5, we discuss various bifurcation phenomena of the stable dynamics of the border collision normal form described in Chapter 4. A polygonal absorbing region can be constructed. When an eigenvalue of the Jacobian matrix of a piecewise smooth map crosses the unit circle, the presence of the switching surface can make the resulting motion more complicated than the standard saddle-node or period-doubling bifurcations. This is known as degenerate bifurcation. This bifurcation affects the basin of attraction of the attracting set. We also use an example to illustrate snap-back repeller bifurcation in the system, which occurs when a snap-back repeller is created or destroyed. We discuss how snap-back repeller bifurcation changes the geometry of the attracting set. We also analyze the ways these sets lose stability and give conditions for some particular cases.

In Chapter 6, a system coupled by a piecewise affine map is considered. We study its synchronization and the stability of the synchronized state using the theory of border collision bifurcations, and attempt to explain a bifurcation phenomenon described in [40]. We show that degenerate bifurcations and border collision bifurcations occur in this coupled system, which are responsible for the creation of the new

periodic orbits and the more complicated dynamics.

Finally conclusions are presented in Chapter 7.

Chapter 2

Preliminaries

2.1   Introduction

Consider $F : \mathbb{R}^m \to \mathbb{R}^m$. A system of differential equations, $\dot{x} = F(x)$, or a map, $x_{n+1} = F(x_n)$, is said to be piecewise smooth if the phase space can be partitioned into a finite number J of disjoint non-empty open regions $R_i, i = 1, \ldots, J$, and a boundary Σ, which is made up of a union of continuously differentiable surfaces which separate these regions, so that $\mathbb{R}^m = (\cup_1^J R_i) \cup \Sigma$, and F is smooth in each R_i. Non-smoothness occurs on Σ, which is called switching surface or switching manifold. This is also known as hybrid system. Note that we do not need to impose any continuity conditions for F across the switching surface, if F is continuous across Σ then the system is piecewise smooth continuous. To introduce a parameter μ, we consider a continuous family of maps $F(x; \mu)$, $F : \mathbb{R}^m \times \mathbb{R} \to \mathbb{R}^m$, such that $F(x; \mu)$ is piecewise smooth for each μ, also the maps and their Jacobians with respect to x vary continuously in the parameter μ on each of the sets R_i.

In piecewise smooth systems the interaction of invariant sets with switching manifolds often produces bifurcations not observed in smooth systems. These are known as discontinuity-induced bifurcations. When a fixed point (or periodic point) meets the switching manifold and a bifurcation occurs, the bifurcation is called a border collision bifurcation [71, 70].

In this thesis, we study the bifurcation theory for continuous piecewise smooth discrete-time systems.

There are two main kinds of border collision bifurcation, namely, border collision pair bifurcation and border crossing bifurcation. Border collision pair bifurcation occurs when two fixed points of the system collide on the switching surface and disappear at the bifurcation. This can be regarded as an analogue of the standard saddle-node bifurcation in smooth systems. The second type is border crossing bifurcation. A fixed point is a border crossing fixed point if it crosses the border between two regions in which the map is smooth. Bifurcation occurs when the nature of the fixed point is changed as it crosses the switching surface. Various examples of both bifurcations can be found in [71, 7].

Nusse and Yorke [71, 70] gave a general criterion for the occurrence of border crossing bifurcations based on index theory. Before we state their border collision bifurcation theorem, we have some necessary definitions.

Consider a system $X_{n+1} = F(X_n)$ where $F : \mathbb{R}^m \to \mathbb{R}^m$ is piecewise smooth continuous in two regions U and V separated by a smooth surface Σ, and

$$F(X) = \begin{cases} F_U(X) & X \in U \\ F_V(X) & X \in V \end{cases}$$

and $F_U(X) = F_V(X)$ for $X \in \Sigma$. Suppose that F depends smoothly on a parameter μ. Let X_μ be a fixed point of F and suppose that at $\mu = \mu^*$, X_{μ^*} is on the border separating U and V. We can assume $\mu^* = 0$ without loss of generality. Suppose that X_μ exists for $-\epsilon < \mu < \epsilon$, the fixed point X_μ is called a border crossing fixed point if it crosses Σ as μ varied through 0. Similarly for periodic orbits. An orbit of period p is called typical if none of the points of the orbit are on the border, so that the Jacobian matrix exists (i.e. the Jacobian matrix of the p-th iterate of the map at a point of the orbit) and neither $+1$ nor -1 is an eigenvalue of this Jacobian matrix. The orbit index is a number associated with a periodic orbit.

Definition 2.1.1. *Suppose a typical periodic orbit PO of a map F has minimum period p. Let A_p be the Jacobian matrix of the p-th iterate of F at one of the points in PO. Let m be the number of real eigenvalues of A_p smaller than -1, and let n be the number of real eigenvalues of A_p greater than $+1$ (counting multiplicities). The orbit index is defined by*

$$I_{PO} = \begin{cases} 0 & \text{if } m \text{ is odd} \\ -1 & \text{if } m \text{ is even and } n \text{ is odd} \\ +1 & \text{if both } m \text{ and } n \text{ are even} \end{cases}$$

The orbit index is a bifurcation invariant in the sense that if one examines the periodic orbits that collapse to the fixed point X_μ as $\mu \to 0$, and adds the orbit indices of the periodic orbits that exist just before a bifurcation, then that sum equals the corresponding sum just after that bifurcation. A periodic orbit PO is called an isolated border crossing orbit if PO includes a point that is a border crossing fixed point under some iterate of the map; and the orbit PO is isolated in phase space when $\mu = 0$, that is, there exists a neighborhood U of the orbit PO such that PO is the only periodic orbit in U when $\mu = 0$.

Theorem 2.1.2 (Border Collision Bifurcation, [71]). *For each two-dimensional piece-wise smooth map that depends smoothly on a parameter μ, if the index of an isolated border crossing orbit changes as μ crosses 0, then at $\mu = 0$ a bifurcation occurs at this point, a bifurcation involving at least one additional periodic orbit.*

This result says that additional fixed points or periodic orbits must bifurcate from X_μ at $\mu = 0$ if the orbit index changes. As an example consider the supercritical period-doubling border collision bifurcation.

Example. Consider a two-dimensional system

$$
\begin{pmatrix} x_{n+1} \\ y_{n+1} \end{pmatrix} = \begin{cases} \begin{pmatrix} 1.20 & 1 \\ -0.30 & 0 \end{pmatrix} \begin{pmatrix} x_n \\ y_n \end{pmatrix} + \begin{pmatrix} 1 \\ 0 \end{pmatrix} \mu & x_n \leq 0 \\[2em] \begin{pmatrix} -0.75 & 1 \\ 0.30 & 0 \end{pmatrix} \begin{pmatrix} x_n \\ y_n \end{pmatrix} + \begin{pmatrix} 1 \\ 0 \end{pmatrix} \mu & x_n \geq 0 \end{cases}
$$

The border of this system is the line $x = 0$. At $\mu = 0$ there is a fixed point on the border at $(0,0)$. For $\mu < 0$ there is a fixed point in $x < 0$, which has eigenvalues 0.355 and 0.845 and so it is an attractor with orbit index $+1$. For $\mu > 0$ the fixed point has eigenvalues 0.289 and -1.039 and so it becomes a flip saddle with orbit index 0. Thus Theorem 2.1.2 implies that there is a bifurcation at $\mu = 0$. Indeed, for $\mu > 0$, there is a period 2 orbit that collapses to $(0,0)$ as $\mu \to 0$. This orbit has eigenvalues 0.091 and -0.991 and so is an attractor. The orbit index is $+1$, note that the two points of this period 2 orbit are collectively assigned $+1$. Hence, both the sum of the orbit indices before the bifurcation and the sum after are $+1$.

Note that Theorem 2.1.2 gives a sufficient condition for the occurrence of border collision bifurcation, and this condition is not necessary. Also, this theorem considers only the case where the fixed point (or periodic orbit) crosses the switching surface as μ crosses 0, which is border crossing bifurcation.

2.2   Border collision bifurcations in one-dimensional piecewise smooth maps

Suppose that the map F is one-dimensional, and suppose for simplicity that the map involves only two regions of smooth behaviour, then the border is a point x_b. So,

$$
F(x; \mu) = \begin{cases} F_1(x; \mu) & x \leq x_b \\ F_2(x; \mu) & x \geq x_b \end{cases} \tag{2.1}
$$

Since the local structure of border collision bifurcations depends only on the local properties of the map in the neighborhood of the border, we study such bifurcations with the help of a normal form: the piecewise affine approximation of F in the neighborhood of the border [5]. The normal form is derived as follows. We change the coordinate by letting $\bar{x} = x - x_b$, then the border is transformed to $\bar{x} = 0$, and the phase space is divided into $L = (-\infty, 0]$ and $R = [0, \infty)$. For simplicity we drop the bar on $\bar{x}$. Suppose that a fixed point is on the border when $\mu = 0$ (if the fixed point is on the border at $\mu = \mu^*$, then we can transform the parameter by letting $\mu' = \mu - \mu^*$), then we expand $F(x; \mu)$ to first order about $x = \mu = 0$ and obtain

$$
\begin{aligned}
F_L(x; \mu) &= ax + \mu v_L + o(x; \mu) & x \leq 0 \\
F_R(x; \mu) &= bx + \mu v_R + o(x; \mu) & x \geq 0
\end{aligned}
\tag{2.2}
$$

where

$$
\begin{aligned}
a &= \lim_{x \to 0^-} \frac{\partial}{\partial x} F(x; 0) \\
b &= \lim_{x \to 0^+} \frac{\partial}{\partial x} F(x; 0) \\
v_L &= \lim_{x \to 0^-} \frac{\partial}{\partial \mu} F(x; 0) \\
v_R &= \lim_{x \to 0^+} \frac{\partial}{\partial \mu} F(x; 0).
\end{aligned}
$$

The continuity of the map $F(x; \mu)$ for all μ requires that $v_L = v_R = v$, which we assume is nonzero. We can then eliminate v by rescaling the parameter μ. Therefore we obtain the one-dimensional normal form of F

$$
x_{n+1} = \begin{cases} ax_n + \mu & x \leq 0 \\ bx_n + \mu & x \geq 0 \end{cases}
\tag{2.3}
$$

As μ is varied, the local bifurcation of the original map F is the same as that of the normal form (2.3).

The map for $x \leq 0$ has a fixed point $x_L = \mu/(1-a)$, which exists if $\mu/(1-a) \leq 0$, which is satisfied if and only if either $\mu \leq 0$ and $a < 1$ or $\mu \geq 0$ and $a > 1$; and the map for $x \geq 0$ has a fixed point $x_R = \mu/(1-b)$ which exists if $\mu/(1-b) \geq 0$, which
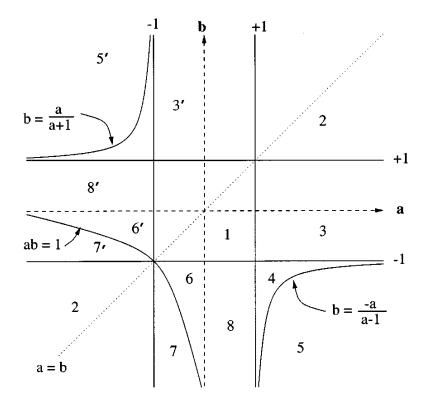
Figure 2.1: (sourced from [5]) Partitioning of the parameter space into regions with the same qualitative phenomena. The labeling of regions refers to various bifurcation scenarios. 1) persistence of stable fixed points, 2) persistence of unstable fixed points, 3) no fixed point to stable and unstable fixed points, 4) no fixed point to two unstable fixed points and chaotic attractor, 5) no fixed point to two unstable fixed points, 6) supercritical border collision period doubling, 7) subcritical border collision period doubling, 8) a stable fixed point to periodic or chaotic attractor. The regions shown in primed numbers have the same bifurcation behaviour as the unprimed ones when μ is varied in the opposite direction.

is satisfied if and only if either $\mu \geq 0$ and $b < 1$ or $\mu \leq 0$ and $b > 1$.

Note that this normal form map is invariant under the transformation $x \rightarrow -x, \mu \rightarrow -\mu, a \rightleftharpoons b$. In other words, the bifurcation behaviour when we have parameter (b, a) is the same as the case with (a, b) when μ is varied in the opposite direction. Thus it suffices to consider only the case $a > b$.

It has been shown [72, 5, 49] that various combinations of the parameters a and b lead to different kinds of bifurcation behaviour as μ is varied.

1. If $-1 < b \leq a < 1$, then there is no bifurcation and a stable fixed point for $\mu < 0$ persists and remains stable for $\mu > 0$;

2. If $1 < b \leq a$ or $b \leq a < -1$, then there is no bifurcation and an unstable fixed point for $\mu < 0$ persists and remains unstable for $\mu > 0$;

3. If $-1 < b < 1 < a$, then there is a bifurcation from no fixed point for $\mu < 0$ to two fixed points x_L (unstable) and x_R (stable) for $\mu > 0$;

4. If $a > 1$ and $-\frac{a}{a-1} < b < -1$, then there is a bifurcation from no fixed point to two unstable fixed points plus a chaotic attractor as μ is increased through zero;

5. If $a > 1$ and $b < -\frac{a}{a-1}$, then there is a bifurcation from no fixed point to two unstable fixed points as μ is increased through zero, and there is an unstable chaotic orbit for $\mu > 0$;

6. If $b < -1 < a < 0$ and $-1 < ab < 1$, then there is a bifurcation from a stable fixed point x_L to an unstable fixed point x_R plus a stable period-2 orbit as μ is increased through zero;

7. If $b < -1 < a < 0$ and $ab > 1$, then there is a bifurcation from a stable fixed point x_L plus an unstable period-2 orbit to an unstable fixed point x_R as μ is increased though zero;
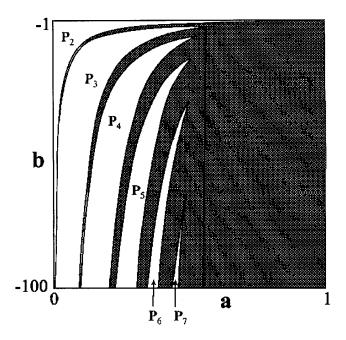
Figure 2.2: (sourced from [72]) The parameter region $0 < a < 1$ and $b < -1$, showing the type of attractor for $\mu > 0$. Regions P_n correspond the existence of stable period n orbit, inside the shaded region there exists chaotic attractors.

8. If $0 < a < 1, b < -1$ and $ab < -1$, then there is a bifurcation from a stable fixed point x_L to an unstable fixed point x_R plus a period-n attractor, $n \geq 2$ or a chaotic attractor as μ is increased through zero.

Note that in cases 3, 4 and 5, there is a border collision pair bifurcation at $\mu = 0$; in cases 6, 7 and 8, there is a border crossing bifurcation at $\mu = 0$. The possible bifurcation scenarios are summarized in Figure 2.1 [5]. In the last scenario, whether a stable period-n orbit or a chaotic attractor is created, depends on the pair of parameters (a, b) as shown in Figure 2.2 [72].

2.3   Two-dimensional border collision normal form

The results outlined above give a complete description of the bifurcations of the one-dimensional normal form as μ is varied. In more than one dimension, piecewise smooth systems may exhibit extremely complicated dynamics.

It has been shown [71, 4, 7] that, for two-dimensional piecewise smooth maps, a normal form for border collision bifurcation can again be written.

Consider a general two-dimensional piecewise smooth map $g(\hat{x}, \hat{y}; \rho)$, which depends on a single parameter ρ. Let $\hat{x} = h(\hat{y}; \rho)$ denote a smooth curve that divides the phase plane into two regions R_1 and R_2. The map is given by

$$g(\hat{x}, \hat{y}; \rho) = \begin{cases} g_1(\hat{x}, \hat{y}; \rho) & (\hat{x}, \hat{y}) \in R_1 \\ g_2(\hat{x}, \hat{y}; \rho) & (\hat{x}, \hat{y}) \in R_2 \end{cases} \qquad (2.4)$$

where g_1 and g_2 are both by assumption continuous and have continuous derivatives in their corresponding regions.

Define

$$\tilde{x} = \hat{x} - h(\hat{y}; \rho), \quad \tilde{y} = \hat{y}.$$

This change of variables moves the border to the $\tilde{y}$-axis. Then the map $g(\hat{x}, \hat{y}; \rho)$ can be written

$$g(\tilde{x} + h(\hat{y}; \rho), \tilde{y}; \rho) = f(\tilde{x}, \tilde{y}; \rho),$$

and the border is $\tilde{x} = 0$. Suppose that when $\rho = \rho_*$ the map $f(\tilde{x}, \tilde{y}; \rho)$ has a fixed point $P_* = (0, \tilde{y}_*(\rho_*))$ on the border.

Let e_1 be a tangent vector in the $\tilde{y}$ direction and suppose that the vector e_1 maps to a vector e_2. We assume e_2 is not parallel to e_1. Define new coordinates again. Choose the point P_* as the new origin for e_1 in the $\bar{y}$ direction and e_2 in the $\bar{x}$ direction. In these $\bar{x} - \bar{y}$ coordinates, the fixed point P_* is now $(0, 0)$ and the border is given by $\bar{x} = 0$. We define the new parameter $\bar{\mu} = \rho - \rho_*$, so $\bar{\mu}_* = 0$. Rescale $\bar{x}$ and $\bar{y}$ again such that at $\bar{\mu} = 0$ a unit vector along the $\bar{y}$-axis maps to a unit vector along the $\bar{x}$-axis. The phase space is now divided into two halves L and R (for left and right). Now the map can be written $F(\bar{x}, \bar{y}; \bar{\mu}) = F_\alpha(\bar{x}, \bar{y}; \bar{\mu})$ for $\bar{\mathbf{x}} \in \alpha = L, R$ where

$$F_L(\bar{x}, \bar{y}; \bar{\mu}) = \begin{pmatrix} F_1(\bar{x}, \bar{y}; \bar{\mu}) \\ F_2(\bar{x}, \bar{y}; \bar{\mu}) \end{pmatrix}, \qquad F_L(0, 0; 0) = \begin{pmatrix} 0 \\ 0 \end{pmatrix}$$

and similarly for F_R. Linearizing $F_L(\bar{x}, \bar{y}; \bar{\mu})$ in the neighbourhood of $(0, 0, 0)$, we have

$$F_L(\bar{x}, \bar{y}; \bar{\mu}) = \begin{pmatrix} J_{11} & J_{12} \\ J_{21} & J_{22} \end{pmatrix} \begin{pmatrix} \bar{x} \\ \bar{y} \end{pmatrix} + \bar{\mu} \begin{pmatrix} v_{Lx} \\ v_{Ly} \end{pmatrix} + o(\bar{x}, \bar{y}; \bar{\mu}) \qquad (2.5)$$

where

$$J_{11} = \lim_{\bar{x} \to 0^-, \bar{y} \to 0} \frac{\partial}{\partial \bar{x}} F_1(\bar{x}, \bar{y}; 0),$$

$$J_{12} = \lim_{\bar{x} \to 0^-, \bar{y} \to 0} \frac{\partial}{\partial \bar{y}} F_1(\bar{x}, \bar{y}; 0),$$

$$J_{21} = \lim_{\bar{x} \to 0^-, \bar{y} \to 0} \frac{\partial}{\partial \bar{x}} F_2(\bar{x}, \bar{y}; 0),$$

$$J_{22} = \lim_{\bar{x} \to 0^-, \bar{y} \to 0} \frac{\partial}{\partial \bar{y}} F_2(\bar{x}, \bar{y}; 0),$$

$$v_{Lx} = \lim_{\bar{x} \to 0^-, \bar{y} \to 0} \frac{\partial}{\partial \bar{\mu}} F_1(\bar{x}, \bar{y}; 0),$$

$$v_{Ly} = \lim_{\bar{x} \to 0^-, \bar{y} \to 0} \frac{\partial}{\partial \bar{\mu}} F_2(\bar{x}, \bar{y}; 0).$$

Since a unit vector along the $\bar{y}$ axis maps to a unit vector along the $\bar{x}$ axis at $\bar{\mu} = 0$, this choice of coordinates makes $J_{12} = 1$ and $J_{22} = 0$. Further, we note that J_{11} is the trace (denoted T_L) and J_{21} is the negative of the determinant (denoted D_L) of the Jacobian matrix. Thus (2.5) becomes

$$F_L(\bar{x}, \bar{y}; \bar{\mu}) = \begin{pmatrix} T_L & 1 \\ -D_L & 0 \end{pmatrix} \begin{pmatrix} \bar{x} \\ \bar{y} \end{pmatrix} + \bar{\mu} \begin{pmatrix} v_{Lx} \\ v_{Ly} \end{pmatrix} + o(\bar{x}, \bar{y}; \bar{\mu}), \qquad \bar{x} \le 0 \qquad (2.6)$$

and similarly for $\bar{\mathbf{x}} = (\bar{x}, \bar{y}) \in R$

$$F_R(\bar{x}, \bar{y}; \bar{\mu}) = \begin{pmatrix} T_R & 1 \\ -D_R & 0 \end{pmatrix} \begin{pmatrix} \bar{x} \\ \bar{y} \end{pmatrix} + \bar{\mu} \begin{pmatrix} v_{Rx} \\ v_{Ry} \end{pmatrix} + o(\bar{x}, \bar{y}; \bar{\mu}), \qquad \bar{x} \ge 0 \qquad (2.7)$$

where the corresponding quantities in R are defined in a similar way to these in L.

Continuity of the map implies

$$\begin{pmatrix} v_{Lx} \\ v_{Ly} \end{pmatrix} = \begin{pmatrix} v_{Rx} \\ v_{Ry} \end{pmatrix} = \begin{pmatrix} v_x \\ v_y \end{pmatrix}.$$

Finally we make another change of variables so that the choice of axes is independent of the parameter. Let $x = \bar{x}, y = \bar{y} - \bar{\mu} v_y$, and $\mu = \bar{\mu}(v_x + v_y)$ (assuming $(v_x + v_y) \neq 0$), then we have the normal form

$$\mathbf{x}_{n+1} = F(\mathbf{x}_n) = \begin{cases} A_L \mathbf{x}_n + \mathbf{m} & x \leq 0 \\ A_R \mathbf{x}_n + \mathbf{m} & x \geq 0 \end{cases} \tag{2.8}$$

where the matrices A_L and A_R, and the vector $\mathbf{m}$ are defined as

$$A_\alpha = \begin{pmatrix} T_\alpha & 1 \\ -D_\alpha & 0 \end{pmatrix}, \qquad \mathbf{m} = \begin{pmatrix} \mu \\ 0 \end{pmatrix} \tag{2.9}$$

for $\alpha = L, R$, the left and right half-plane.

The normal form map is again the piecewise affine approximation of the original map in the neighbourhood of the border, and the switching surface is transformed to be the y-axis.

The fixed points of the system on both sides of the border are given by

$$\mathbf{x}_*^\alpha = \left(\frac{\mu}{1 - T_\alpha + D_\alpha}, \frac{-D_\alpha \mu}{1 - T_\alpha + D_\alpha} \right). \tag{2.10}$$

for $\alpha = L, R$. Then if $\frac{\mu}{1 - T_L + D_L} < 0$, the fixed point $\mathbf{x}_*^L$ exists, or "admissible". If $\frac{\mu}{1 - T_L + D_L} > 0$, $\mathbf{x}_*^L$ is in R and does not exist, but iterations of points in L are influenced by this "virtual" fixed point. Similarly, if the x-component of $\mathbf{x}_*^R$ is positive, the fixed point is admissible, otherwise it is a virtual fixed point. At $\mu = 0$ the two fixed points meet at the origin, and this is clearly on the border $x = 0$.

The stability of the fixed points is determined by the eigenvalues of the map,
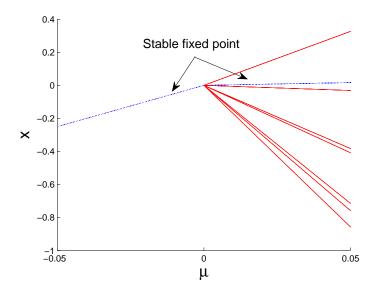
Figure 2.3: Bifurcation diagram for a two-dimensional border collision normal form. A stable fixed point bifurcates to a stable fixed point and a stable period 7 orbit. $T_L = 1.6, D_L = 0.8, T_R = -1.4, D_R = 0.6$.

which are the solutions of the quadratic equation $s^2 - T_\alpha s + D_\alpha = 0$. The dynamics of the system is governed by five parameters, T_L, D_L, T_R, D_R, μ.

Some research has been done for dissipative systems, where $|D_L| < 1$ and $|D_R| < 1$, so areas are decreased by iterations. In [18, 4, 7], some classification has been shown for such systems, and similar partitionings as for the one-dimensional case shown in Figure 2.1 are given. However, two-dimensional systems can exhibit more complicated dynamics than one-dimensional systems. References [71, 23, 7, 25] show that multiple attractors can coexist in a system. Figure 2.3 shows an example where a stable fixed point bifurcates to another stable fixed point and a stable period 7 orbit in a border crossing bifurcation as μ is increased through 0.

As in the one-dimensional case, chaotic dynamics is possible in the two-dimensional normal form [71, 9, 23, 7, 24, 25]. In particular, it can be robustly chaotic [9], so that for its parameter values, there exists a neighbourhood in the parameter space with no periodic attractor and the chaotic attractor is unique in that neighbourhood. Chaotic attractors can also exist when the map is globally contractive. When the eigenvalues of the Jacobian matrix at every point in the phase space are within the unit circle, the map is called globally contractive. In a piecewise smooth map, this
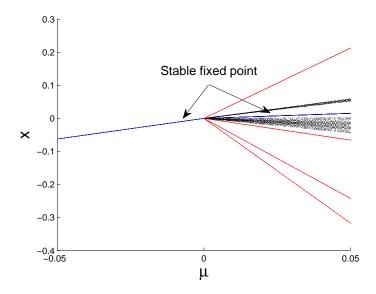
Figure 2.4: Bifurcation diagram for a two-dimensional border collision normal form. A stable fixed point bifurcates to a stable fixed point, a stable period 4 orbit and a chaotic attractor. $T_L = 0.9, D_L = 0.7, T_R = -1.59, D_R = 0.7$.

implies that the fixed points are stable on both sides of the border. In such a map, one usually does not expect the occurrence of chaos for which a stretching behaviour is necessary. Figure 2.4 is an example of such a system. A stable fixed point bifurcates to a coexistence of a stable fixed point, a stable period 4 orbit and a chaotic attractor in a border crossing bifurcation.

It was believed that when a stable fixed point occurs on both sides of a border collision there will be no observable change in the system behaviour. However, it has been later shown that border collision bifurcations can also lead to a peculiar situation where the system collapses at the point of bifurcation, so all orbits starting from all points other than the fixed point diverge to infinity, even though the fixed point remains stable on both sides of the bifurcation point.

For example, consider the normal form (2.8) and (2.9) with parameters [49]

$$T_L = -0.3, \quad D_L = 0.9, \quad T_R = -1.6, \quad D_R = 0.9.$$

The eigenvalues of A_L are $-0.15 \pm 0.9367i$ and the eigenvalues of A_R are $-0.80 \pm 0.5099i$. For $\mu < 0$ there is a fixed point in L and it is locally stable; for $\mu > 0$ there
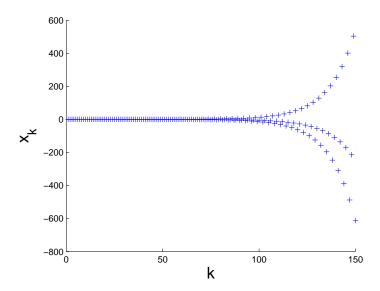
Figure 2.5: Time series for x_k for the example of dangerous border collision bifurcation. $T_L = -0.3, D_L = 0.9, T_R = -1.6, D_R = 0.9$ and $\mu = 0$, with initial point $(-0.03, 0.01)$.

is a fixed point in R and it is also locally stable. However the basin of attraction of the fixed point shrinks to the single point $(0, 0)$ as the parameter is varied toward the bifurcation value $\mu = 0$, and at the bifurcation point the basin of attraction has zero size. Therefore, at $\mu = 0$, the trajectory of the map diverges for any nonzero initial condition. A sample trajectory of x_k at $\mu = 0$ is shown in Figure 2.5.

This phenomenon leads to a new class of bifurcations, which is now called dangerous border collision bifurcations [49, 50, 32, 20, 19, 21].

Recently some researchers have shown [89, 88, 79, 80, 81, 74, 82, 83] that many interesting dynamics can occur when on one side of the border the determinant of the Jacobian matrix is greater than one.

Suppose that $|D_L| < 1, D_R > 1, -(1 + D_L) < T_L < (1 + D_L)$ and $-2\sqrt{D_R} < T_R < 2\sqrt{D_R}$, then the fixed point is attracting for $\mu < 0$ and is an unstable spiral for $\mu > 0$. As μ is increased through 0, the fixed point moves from L to R in a border crossing bifurcation. When $\mu > 0$, if we start from any point in R, the orbit spirals outward and crosses the switching surface to L after some iterations, where the motion is governed by the virtual attracting fixed point $\mathbf{x}_*^L$ in R. Since the virtual fixed point attracts orbits from the left, the outward motion eventually returns to

the right and so the system shows some kind of rotating motion. For some initial conditions, the outward motion dominates and the orbit diverges; for some other initial conditions the orbit is trapped in this rotating motion. Therefore, between these two set of initial conditions one may expect there is an invariant closed curve which is stable. But the orbit occurring on the closed invariant curve could be a mode-locked periodic orbit or a quasiperiodic orbit, depending on the parameters. It has been shown [89, 88, 80, 81] that these transitions between the mode-locked dynamics and quasiperiodicity is extremely complex.

In smooth systems, when a stable fixed point (or periodic orbit) loses its hyperbolicity and becomes unstable, i.e. when an eigenvalue of the Jacobian matrix moves out of the unit circle, it undergoes one of the standard bifurcations such as saddle-node, period-doubling and Neimark-Sacker bifurcation which are now very well-known. However, in piecewise smooth systems, because of the switching surface and the non-smoothness of the map, these bifurcations can be different from the smooth case and they are often more complicated. References [74, 82, 83] analyze these bifurcations for piecewise smooth systems, which are named degenerate bifurcation, degenerate flip bifurcation and centre bifurcation respectively.

We here give an example of a centre bifurcation from [82].

Consider the normal form with parameters

$$T_L = 0.7, \quad D_L = 0.9, \quad T_R = -0.2, \quad D_R = 1.057.$$

When $\mu < 0$, there is a stable fixed point in L; when $\mu > 0$, there is a fixed point in R which is unstable. Numerical solutions show that for $\mu > 0$, there is a coexistence of a stable period 4 orbit and a stable period 25 orbit. In particular, this period 4 orbit $LLRR$ (which represents a periodic orbit where there are two points in L followed by two points in R under iteration) has eigenvalues $0.821 \pm 0.480i$, and the orbit becomes an unstable spiral when the determinant of $A_R^2 A_L^2$ becomes 1, that is, $D_R = 1/D_L = 1.1111\ldots$. It was shown [82] that at this value of D_R, when the

complex-conjugate eigenvalues of the attracting 4-cycle reach the unit circle, the 4-cycle undergoes a center bifurcation, where in the phase space there are four cyclic repelling invariant regions filled with the invariant ellipses. After the bifurcation the 4-cycle becomes unstable and nothing is born.

Therefore, in terms of the border collision bifurcation of the fixed point of the map as μ varies through 0, there is a bifurcation from a stable fixed point to a cyclic repelling closed invariant curve coexisting with one or several attractors. This example may be considered as a piecewise-linear analogue of the NeimarkSacker bifurcation for smooth maps, and is still to be studied in detail.

We will return to these bifurcations in Chapter 5.

In the remaining chapters, we investigate two-dimensional border collision bifurcations where the determinant of at least one of the Jacobian matrices is greater than one.

Chapter 3

Snap-back Repellers in Border Collision Normal Form

3.1 Border collision bifurcations, snap-back repellers and chaos

In 1975, Li and Yorke [56] first introduced the term chaos, and proved the well-known theorem "period three implies chaos", a simple criterion for a one-dimensional discrete dynamical system $x_{n+1} = f(x_n), n = 0, 1, \ldots$ to be chaotic. Over the years there have been a lot of studies on chaos on a wide range of systems. Nowadays, one of the methods available to prove that a map has chaotic behaviour is to show the existence of a homoclinic orbit, i.e. a fixed point (or a periodic orbit, viewed as fixed points of a higher iterate) which another orbit approaches in both forwards and backwards time. If the fixed point is a saddle, this means that there are intersections of the stable and unstable manifolds of the fixed point. In parameterized families of maps, homoclinic orbits are typically created at some critical parameter value when the stable and unstable manifolds of a fixed point intersect tangentially, and on one side of this critical value there are no intersections, and hence no homoclinic orbit to the fixed point, and on the other side of this critical value there are two transversal

intersections.

If the fixed point is repelling, so all the eigenvalues of the Jacobian matrix lie outside the unit circle, then there is no local stable manifold. Thus, for invertible maps, homoclinic orbits cannot exist. However, for non-invertible maps, the fixed point can have more than one preimage and so it is possible that there exists a point (other than the fixed point) which maps to the fixed point, and from this point there is a sequence of preimages which tends to the fixed point in backwards time. Therefore there can be a homoclinic orbit to the fixed point even though it has no local stable manifold. Marotto [65] was the first to prove that such a homoclinic orbit can imply the existence of an unstable chaotic set, and the term "snap-back repeller" was given to the fixed point associated with this homoclinic orbit, even though there has been some controversy later about the definition of a snap-back repeller and the original proof of the theorem. Several papers [15, 60, 55, 14] provided a few alterations of the theorem and Marotto himself also gave a corrected version in 2005 [66]. Nonetheless, this theorem has been successfully used to predict and analyze chaos in multi-dimensional discrete systems.

In the border collision normal form map (2.8), when $|D_L|$ and $|D_R|$ are not both less than 1, the fixed points of the map can be repellers instead of attractors. Since the determinant of the Jacobian matrix of a map shows how areas are increased or decreased by iteration, in the case where the modulus of the determinant is less than one, we may expect to observe stable dynamics. On the other hand, one might imagine that if a fixed point is a repeller instead, the dynamics would be either uninteresting or could be obtained from the modulus less than one case by reversing time. However, neither of these is necessarily the case: if the map is not invertible we cannot simply reverse time, and the dynamics described below is certainly interesting and relevant to some examples. We here show how a snap-back repeller works in the area-expanding border collision normal form, then we give our result in [42] that in appropriate parameter regions there is a snap-back repeller immediately after the border collision bifurcation, and hence that the bifurcation creates chaos.

Definition 3.1.1. *Let $F : \mathbb{R}^n \to \mathbb{R}^n$ be differentiable. Suppose $\mathbf{z}$ is a fixed point of F and all the eigenvalues of the Jacobian matrix $DF(\mathbf{z})$ have modulus greater than 1. Suppose that there exists a point $\mathbf{y}_0 \neq \mathbf{z}$ in a repelling neighbourhood of $\mathbf{z}$, such that $\mathbf{y}_M = \mathbf{z}$ for some M and $\det(DF(\mathbf{y}_k)) \neq 0$ for $1 \leq k \leq M$, where $\mathbf{y}_k = F^k(\mathbf{y}_0)$. Then $\mathbf{z}$ is called a regular snap-back repeller of F.*

For piecewise smooth systems, suppose that $\mathbb{R}^n$ is partitioned into disjoint open regions $R_i, i = 1, \ldots, J$ where F is smooth and Σ is the switching surface, then the definition of a regular snap-back repeller requires that $\mathbf{z}$ and each $\mathbf{y}_k$ do not intersect Σ so that the Jacobian matrices are defined.

Theorem 3.1.2 ([65])**.** *If F has a snap-back repeller then F is chaotic, in the sense of Li-Yorke. That is, there exists*

(i) *a positive integer N such that for each integer $p \geq N$, F has a point of period p;*

(ii) *an uncountable set S containing no periodic points of F such that:*

    (a) *$F(S) \subset S$,*

    (b) *for every $\mathbf{x}, \mathbf{y} \in S$ with $\mathbf{x} \neq \mathbf{y}$,*

$$\limsup_{k \to \infty} \| F^k(\mathbf{x}) - F^k(\mathbf{y}) \| > 0,$$

    (c) *for every $\mathbf{x} \in S$ and any periodic point $\mathbf{y}$ of F,*

$$\limsup_{k \to \infty} \| F^k(\mathbf{x}) - F^k(\mathbf{y}) \| > 0,$$

(iii) *a subset S^0 of S such that for every $\mathbf{x}, \mathbf{y} \in S^0$,*

$$\liminf_{k \to \infty} \| F^k(\mathbf{x}) - F^k(\mathbf{y}) \| = 0.$$

Li-Yorke chaos means that given any two orbits in S^0, they are at times (infinitely often) more than some specified distance apart, yet at different times (infinitely often) arbitrarily close to each other. This is a popular definition of chaos as well as Devaney's, which requires sensitive dependence on initial conditions, topological transitivity etc.. In [58, 77], it was proved that a system admitting a snap-back repeller is conjugate to a shift or a sub-shift of the finite type on some symbolic space, which leads to the conclusion that a snap-back repeller induces chaos in the sense of Devaney as well.

In [42], we consider the border collision normal form. Following the definition above, we say that the map has a simple snap-back repeller if there exists a fixed point $\mathbf{x}_*^R$ in $x > 0$ and

(i) the eigenvalues of A_R have modulus strictly greater than one and $D_L \neq 0$;

(ii) there is a point $\mathbf{x}_0^L$ in $x < 0$ such that $F_L(\mathbf{x}_0^L) = \mathbf{x}_*^R$;

(iii) there exists a sequence $\mathbf{x}_i^R$ in $x > 0$ which tends to $\mathbf{x}_*^R$ as $i \to \infty$ such that
$F_R(\mathbf{x}_{i+1}^R) = \mathbf{x}_i^R$, $i = 1, 2, 3, \ldots$ and $F_R(\mathbf{x}_1^R) = \mathbf{x}_0^L$.

Of course, more complicated connections are possible, with several passages across the switching surface Σ, or more than one path can exist, we here use the simplest one to show how the theory works.

We then need to define a set of neighbourhoods of these points in the orbit on which the chaotic dynamics can be defined. Note that since the system is not differentiable across $x = 0$, each of these neighbourhoods has to be chosen so that it does not contain any point on the y-axis. We start by choosing a closed ball of radius r centred on $\mathbf{x}_1^R$, $B(1, r)$, and take r small enough so that $B(1, r) \subset R$, $F_R(B(1, r)) = B(0, r) \subset L$, $F_L(B(0, r)) = N(r) \subset R$ and none of the other points $\mathbf{x}_i^R$, $i = 2, 3, \ldots$, are contained in $B(1, r)$. See Figure 3.1.

Now define $B(2, r)$ to be those points in R which map to $B(1, r)$ under one iteration of F_R. We might need to reduce the size of r so that $B(2, r) \subset R$ is
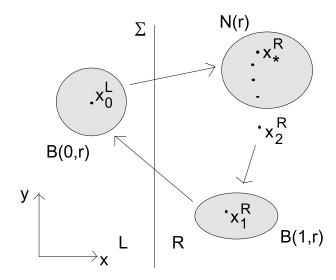
Figure 3.1: The geometry of a simple snap-back repeller.

closed and does not contain any point in Σ. Define $B(n, r) \subset R$ inductively so that

$F_R(B(n, r)) = B(n - 1, r)$ and $B(n, r)$ does not intersect Σ. Note that, by definition,

$\mathbf{x}_n^R \in B(n, r)$ for each $n \geq 1$, $\mathbf{x}_0^L \in B(0, r)$, $\mathbf{x}_*^R \in N(r)$, and since the eigenvalues

of A_R have modulus strictly greater than 1, the sets $B(n, r)$ converge to $\mathbf{x}_*^R$ while

their maximum widths tend to zero, in particular, there exists $K > 0$ such that

$B(k, r) \subset N(r)$ for all $k > K$. So after a finite number of steps the sets $B(n, r)$ will be

sufficiently close to x_*^R and sufficiently small so that no reduction of r will be necessary.

Moreover, by construction, $F_L \circ F_R^k(B(k, r)) = N(r)$ and $F_L \circ F_R^k$ restricted to $B(k, r)$

is a homeomorphism (in fact, affine) and hence there exists a fixed point of $F_L \circ F_R^k$ in

$B(k, r)$ for each $k > K$. Also, for every $k_0, k_1 > K$ there exists a closed connected set

$B(k_0, k_1, r) \subset B(k_0, r)$ such that $F_L \circ F_R^{k_0}(B(k_0, k_1, r)) = B(k_1, r)$. Similarly, for $k_2 >$

K there exists another closed connected set $B(k_0, k_1, k_2, r) \subset B(k_0, k_1, r) \subset B(k_0, r)$

such that $F_L \circ F_R^{k_0}(B(k_0, k_1, k_2, r)) = B(k_1, k_2, r) \subset B(k_1, r)$. Inductively, using the

same argument, for any $M > 0$ and any sequence $k_0, k_1, k_2, \ldots$ with $K < k_i < K + M$

there exists a non-empty set $B(k_0, k_1, k_2, \ldots, r) \subset \cdots \subset B(k_0, r)$ such that

$$F_L \circ F_R^{k_0}(B(k_0, k_1, k_2, \ldots, r)) = B(k_1, k_2, k_3, \ldots, r) \qquad (3.1)$$

and hence that there is an unstable chaotic invariant set containing infinitely many

periodic points and uncountably many aperiodic points close to the simple snap-back repeller.

Note that this system does not formally satisfy all the conditions imposed as F is not everywhere differentiable. A formalism which is applicable directly to the normal form can be found in [61].

Now return to the normal form. Recall from the previous chapter, for given T_α and D_α, $\alpha = L, R$, the fixed points of the maps are given by (2.10)

$$x_*^\alpha = \frac{\mu}{1 - T_\alpha + D_\alpha}, \qquad y_*^\alpha = -D_\alpha x_*^\alpha, \qquad \alpha = L, R$$

and $\mathbf{x}_*^R$ exists provided $x_*^R > 0$, with a similar inequality for the existence of $\mathbf{x}_*^L$. Given T_α and D_α these inequalities define the sign of μ for which these fixed points exist. The fixed points in R and L coincide at the origin (on Σ) if $\mu = 0$. Also, since $y_{n+1} = -D_\alpha x_n$, the images of L and R overlap if D_R and D_L have opposite signs (one positive and one negative), and do not overlap if they have the same signs. Clearly for a snap-back repeller to exist D_R and D_L must have opposite signs.

To fix ideas we will consider the case

$$D_R > 1, \qquad D_L < 0 \tag{3.2}$$

and aim to show the existence of a snap-back repeller to x_*^R. For geometric simplicity we will make the further assumption that $\mathbf{x}_R^*$ is an unstable node, so the eigenvalues of A_R are real and distinct and greater than one. This corresponds to the additional condition

$$T_R > 2, \qquad T_R^2 > 4D_R, \qquad 1 - T_R + D_R > 0 \tag{3.3}$$

which implies that the fixed point $\mathbf{x}_*^R \in R$ exists if $\mu > 0$. Since (3.2) implies that R and L are mapped to the lower half plane, there is a preimage of $\mathbf{x}_*^R$ in L if $y_*^R < 0$, which is automatically satisfied from (2.10) as $D_R > 0$.

Using the notation from above, this preimage $\mathbf{x}_0^L = (x_0, y_0)$ is given by

$$x_0 = \frac{D_R}{D_L}x_*^R, \quad y_0 = \frac{1}{D_L}(T_R D_L - T_L D_R - D_L D_R)x_*^R. \tag{3.4}$$

By definition the point $\mathbf{x}_1^R$ is a preimage of $\mathbf{x}_0^L$ in $x > 0$, and for this preimage to exist we must have $y_0 < 0$. Since $D_L < 0$ and $x_*^R > 0$ this implies that the condition

$$T_R D_L - T_L D_R - D_L D_R > 0 \tag{3.5}$$

must hold. In this case $\mathbf{x}_1^R = (x_1, y_1)$ exists and by definition $F_R(\mathbf{x}_1^R) = \mathbf{x}_0^L$ so

$$
\begin{aligned}
x_0 &= T_R x_1 + y_1 + \mu \\
y_0 &= -D_R x_1
\end{aligned}
\tag{3.6}
$$

and hence, using (2.8) and (3.4),

$$
\begin{aligned}
x_1 &= -\tfrac{1}{D_L D_R}(T_R D_L - T_L D_R - D_L D_R)x_*^R \\[1em]
y_1 &= \tfrac{1}{D_L D_R}\left(D_R(D_R - D_L - D_L D_R)\right. \\
    &\qquad\qquad \left. + T_R(T_R D_L - T_L D_R)\right)x_*^R
\end{aligned}
\tag{3.7}
$$

Note that (3.5) ensures that this point does exist in R.

Looking back to the definition of a snap-back repeller it remains to show that $\mathbf{x}_1^R$ lies in the two dimensional unstable manifold of $\mathbf{x}_*^R$, i.e. if $\mathbf{x}_1^R$ is iterated in backwards time using the map in $x > 0$ then this orbit remains in $x > 0$ and converges to $\mathbf{x}_*^R$.

By (3.3) the eigenvalues and eigenvectors of the linear part of the map in $x > 0$ are

$$s_\pm = \frac{1}{2}(T_R \pm \sqrt{T_R^2 - 4D_R}), \quad \mathbf{e}_\pm = \begin{pmatrix} s_\pm \\ -D_R \end{pmatrix} \tag{3.8}$$

with $1 < s_- < s_+$ and hence the eigenvectors both have negative slopes. Except for solutions on $\mathbf{e}_+$, orbits of the linear map therefore converge in backwards time to $\mathbf{x}_*^R$
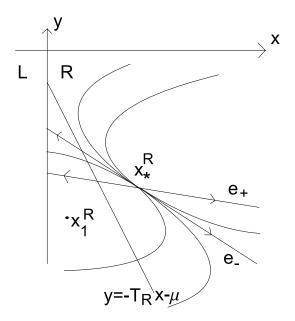
Figure 3.2: The geometry of the linear flow in R. Solutions lie on curves which (with the exception of $\mathbf{e}_+$) are linear transformations of generalized parabolas $y = x^{\ln s_+ / \ln s_-}$.

on generalized parabolas which are tangential to $\mathbf{e}_-$ (the eigenvector whose eigenvalue has smaller modulus) at the fixed point, and this is the eigenvector with the steeper slope. Thus solutions in backwards time lie on curves as sketched in Figure 3.2, and clearly all solutions in $y < 0$ which start to the left of $\mathbf{e}_+$ and $\mathbf{e}_-$ tend to the fixed point along solution curves which lie in $x > 0$ and $y < 0$ for all time and so there will be a simple snap-back repeller.

In [42] we give a sufficient but not necessary condition for this simple snap-back repeller to exist, that is $\mathbf{x}_1^R$ lies to the left of $\mathbf{e}_+$, but actually we can do better.

From (3.6), we see that $\mathbf{x}_1^R \in R$, if it exists, lies on the line $y = -T_R x - \mu + x_0, x > 0$. Since $x_0 < 0, \mathbf{x}_1^R$ is below the line

$$y = -T_R x - \mu. \tag{3.9}$$

This is in fact the preimage of the negative y-axis in $x > 0$. Geometrically, one can see that, since the fixed point is a regular unstable node, the two y-intercepts of the lines of the eigenvectors $\mathbf{e}_\pm$ have preimages in R to the left of the fixed point, hence the line (3.9) intersects both of the eigenvectors at points to the left of $\mathbf{x}_*^R$ as shown

in Figure 3.2. We can also see that, in backwards time of F_R, $\mathbf{x}_1^R$ converges to $\mathbf{x}_*^R$ without leaving $x > 0$ and $y < 0$ whether $\mathbf{x}_1^R$ is to the left of $\mathbf{e}_-$ or inside the triangle bounded by (3.9), $\mathbf{e}_-$ and $y = 0$. Therefore, the conditions (3.2), (3.3) and (3.5) ensure that $\mathbf{x}_*^R$ is a simple snap-back repeller in R; or, we can say, if $\mathbf{x}_*^R \in R$ is a regular unstable node and $D_L < 0$, it is a simple snap-back repeller if and only if we have (3.5).

Let's give some examples where the parameters satisfy all these conditions simultaneously. We start by setting

$$D_R = 10, \quad T_R = 7 \tag{3.10}$$

in which case (3.3) is satisfied and since $1 - T_R + D_R = 4$ the fixed point exists if $\mu > 0$. For $D_L < 0$, the last constraint (3.5) becomes

$$-3D_L - 10T_L > 0 \tag{3.11}$$

so we have a lot of freedom to choose D_L and T_L. We consider briefly several possibilities which satisfy these constraints.

First suppose that $T_L = 0$ and $-1 < D_L < 0$. Clearly both conditions are satisfied so the snap-back repeller exists if $\mu > 0$. The fixed point in L is stable and since $1 - T_L + D_L > 0$ it exists if $\mu < 0$. Hence, as μ increases through zero a stable fixed point is destroyed and an unstable fixed point with a strange invariant set from the snap-back repeller is created in a border crossing bifurcation. If $T_L = -1$ and $-2 < D_L < 0$ there is a similar bifurcation but in this case the stable fixed point in $\mu < 0$ is replaced by a saddle.

In the cases where $\mathbf{x}_*^R$ is a flip node or a spiral, similar arguments for the existence of snap-back repeller can still be made. Assuming (3.2) again, we need $T_R < -2, T_R^2 > 4D_R, 1 + T_R + D_R > 0$ for a flip node, $T_R^2 < 4D_R$ for a spiral, and (3.5) needs to hold for both cases. However, because the local structure of the map in $x > 0$ is more
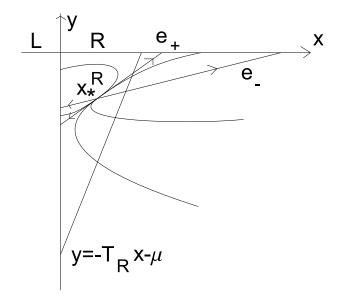
Figure 3.3: In the case where $\mathbf{x}_*^R$ is a flip node, $\mathbf{x}_1^R$ lies below the line $y = -T_R x - \mu$.

complicated, the preimages of $\mathbf{x}_1^R$ may not tend to the fixed point without leaving R like the regular node case discussed above. (One should note that again, even if this is the case, there may be other possible routes, with several passages across the boundary, for $\mathbf{x}_0^L$ to tend to the fixed point, which still imply the existence of the snap-back repeller) For example, if $\mathbf{x}_*^R$ is a flip node, then $s_- < s_+ < -1$. $\mathbf{x}_1^R$, if it exists, is below the line (3.9). As shown in Figure 3.3, although we can again write down a sufficient condition for the existence of a simple snap-back repeller that $\mathbf{x}_1^R$ lies to the left of $\mathbf{e}_-$, this is less helpful because there is a large unbounded region to the right of $\mathbf{e}_-$ where $\mathbf{x}_1^R$ can exist.

Of course, given any example it is straightforward to determine whether (x_1, y_1) given by (3.7) exists and lies in the two dimensional unstable manifold of $\mathbf{x}_*^R$ in R by backwards iteration of one branch of the map. Since $y_{n+1} = -D_R x_n$ in $x > 0$, so only if a point has $y > 0$ it has a preimage in $x < 0$. We thus can write down conditions for $y_i < 0$ for $i = 1, 2, \ldots$ and note that it takes only a finite number of steps and then a preimage of $\mathbf{x}_1^R$ will be sufficiently close to the fixed point.
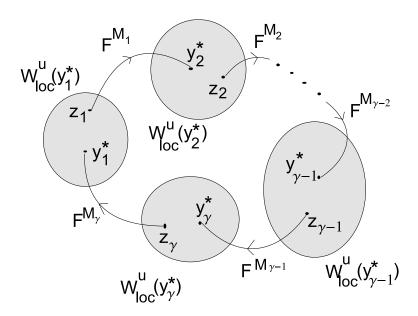
Figure 3.4: The geometry of γ (≥ 2) heteroclinic repellers.

3.2 Heteroclinic repellers

Continue the example above, another interesting transformation occurs if $T_L = -1$ and $D_L < -2$. This again satisfies (3.11) so the snap-back repeller exists in $\mu > 0$. But $1 - T_L + D_L < 0$ and so the fixed point in L also exists if $\mu > 0$. So in this case we know of no recurrent dynamics if $\mu < 0$, but two fixed points and the strange invariant set exist if $\mu > 0$. Moreover, since the fixed point $\mathbf{x}_*^L \in L$ is a repeller itself, simple calculations show that $\mathbf{x}_*^L$ is also a snap-back repeller, but more importantly $\mathbf{x}_*^L$ together with $\mathbf{x}_*^R$ possess the so-called "heteroclinic repellers" proposed by [59]. This is an extension of a snap-back repeller, and since the concept and the proof of the theorem are so similar to the snap-back repeller we only state here the definition of heteroclinic repellers and the theorem along with a diagram illustrating its geometry in the system. The details of the theorem can be found in [59, 57].

Definition 3.2.1 ([59]). *In a system* $\mathbf{y}_{n+1} = F(\mathbf{y}_n), n = 1, 2, \ldots$ *where* $F : \mathbb{R}^n \to \mathbb{R}^n$, *the* γ (≥ 2) *fixed points* $\mathbf{y}_1^*, \mathbf{y}_2^*, \ldots, \mathbf{y}_\gamma^*$ *are called heteroclinic repellers (see Figure 3.4) if the following three conditions hold:*

   (i) for all i, $\mathbf{y}_i^*$ *is expanding;*

(ii) there exist γ points $\mathbf{z}_i$ in each local unstable manifold of $\mathbf{y}_i^*$ and γ natural numbers $M_i, i = 1, \ldots, \gamma$, such that

$$F^{M_j}(\mathbf{z}_j) = \mathbf{y}_{j+1}^*, \quad j = 1, \ldots, \gamma - 1,$$
$$F^{M_\gamma}(\mathbf{z}_\gamma) = \mathbf{y}_1^*;$$

(iii) for all i, $\mathbf{z}_i$ satisfies the non-degenerate property, that is, $DF^{M_i}(\mathbf{z}_i)$ exists and $\det(DF^{M_i}(\mathbf{z}_i)) \neq 0$.

Let's suppose, for simplicity, that $\gamma = 2$.

Theorem 3.2.2 ([59])**.** *If F has one pair of heteroclinic repellers then F is chaotic. That is, there exists*

(i) *a positive integer N such that for each integer $p \geq N$, F has a point of period p;*

(ii) *two uncountable sets $S_1, S_2, S_1 \cap S_2 = \emptyset$ which contain no periodic points of F such that for $i = 1, 2$:*

    (a) *$F(S_i) \subset S_i$,*

    (b) *for every $\mathbf{x}, \mathbf{y} \in S_i$ with $\mathbf{x} \neq \mathbf{y}$,*

$$\limsup_{k \to \infty} \|F^k(\mathbf{x}) - F^k(\mathbf{y})\| > 0,$$

    (c) *for every $\mathbf{x} \in S_i$ and any periodic point $\mathbf{y}$ of F,*

$$\limsup_{k \to \infty} \|F^k(\mathbf{x}) - F^k(\mathbf{y})\| > 0,$$

(iii) *a subset S_i^0 of S_i such that for every $\mathbf{x}, \mathbf{y} \in S_i^0$,*

$$\liminf_{k \to \infty} \|F^k(\mathbf{x}) - F^k(\mathbf{y})\| = 0.$$
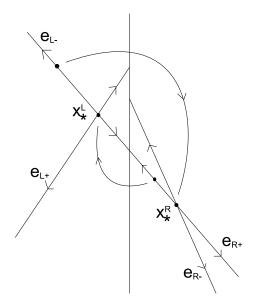
Figure 3.5: When $T_L = -1, D_L = -6, T_R = 7, D_R = 10, \mu = 1$, the fixed points $\mathbf{x}_*^L$ and $\mathbf{x}_*^R$ are heteroclinic repellers.

We can return to the example above. Let

$$T_L = -1, \quad D_L = -6, \quad T_R = 7, \quad D_R = 10, \quad \mu = 1. \tag{3.12}$$

Then $\mathbf{x}_*^R = (0.25, -2.5)$ and $\mathbf{x}_*^L = (-0.25, -1.5)$ and $\mathbf{x}_*^R$ is a snap-back repeller. The eigenvalues of F_L and F_R are $s_{L+} = 2, s_{L-} = -3$ and $s_{R+} = 5, s_{R-} = 2$ respectively, so $\mathbf{x}_*^L$ is a flip node while $\mathbf{x}_*^R$ is a regular node. By direct calculations, one can check that the lines of the eigenvectors $\mathbf{e}_{L-}$ and $\mathbf{e}_{R+}$ coincide. Thus, as shown in Figure 3.5, the preimage of $\mathbf{x}_*^R$ in $x < 0$ is on the eigenvector of $\mathbf{x}_*^L$ and converges to $\mathbf{x}_*^L$ in backwards time. Similarly, the preimage of $\mathbf{x}_*^L$ in $x > 0$ is on the eigenvector of $\mathbf{x}_*^R$ and converges to $\mathbf{x}_*^R$ in backwards time. Hence the fixed points $\mathbf{x}_*^L$ and $\mathbf{x}_*^R$ are a pair of heteroclinic repellers.

3.3   Snap-back repeller bifurcations

So far we know that snap-back repellers can exist in piecewise smooth systems, and this implies chaotic dynamics. The next question is how snap-back repellers are created. Suppose that a system has a expanding fixed point, and a parameter, say

λ^*, such that when a parameter value λ is less than λ^* (respectively $\lambda > \lambda^*$) the fixed point is expanding but not a snap-back repeller; for $\lambda \geq \lambda^*$ (respectively $\lambda \leq \lambda^*$) the fixed point is a snap-back repeller. Then we say there is a snap-back repeller bifurcation at $\lambda = \lambda^*$. It has been shown [34, 41] that a regular snap-back repeller of a map is persistent (or structurally stable) as a function of a parameter. This is,

Theorem 3.3.1. *If F_λ is a continuous family of piecewise smooth maps and has a regular snap-back repeller when λ equals to, say 0, then there is an open neighbourhood $\mathcal{M}$ of $\lambda = 0$ such that F_λ has a regular snap-back repeller for all $\lambda \in \mathcal{M}$.*

Therefore, a snap-back repeller bifurcation occurs when a homoclinic orbit, associated with an expanding fixed point, of the map is degenerate, i.e. there is a point $\mathbf{y}_k$ in the homoclinic orbit where $DF(\mathbf{y}_k)$ is not defined or $\det(DF(\mathbf{y}_k)) = 0$. For piecewise smooth systems, this can happen when some point in the orbit is on the switching surface. Some research [61, 78, 35, 41] shows that with various extra assumptions, an expanding fixed point with a degenerate homoclinic orbit can still exhibit chaotic dynamics.

Recall our example above for the border collision normal form, where we assume (3.2) and (3.3), a snap-back repeller $\mathbf{x}_*^R \in R$ exists for $\mu > 0$ if we have (3.5). We want to know what happens if $\mu > 0$ (by rescaling $\mu = 1$ may be assumed) and $T_R D_L - T_L D_R - D_L D_R$ changes sign. We use this expression as a bifurcation parameter.

If

$$T_R D_L - T_L D_R - D_L D_R = 0 \tag{3.13}$$

then (3.4) becomes $\mathbf{x}_0^L = (\frac{D_R}{D_L} x_*^R, 0)$ and (3.7) becomes

$$x_1 = 0, \quad y_1 = \frac{1}{D_L}(D_R - D_L - D_R D_L + T_R D_L) x_*^R \tag{3.14}$$

which is on the switching surface $x = 0$. The approach of the solution to the fixed point in reverse time is determined by the position of $\mathbf{x}_1^R$ relative to the intersections

of the lines of eigenvectors through the fixed point $\mathbf{x}_*^R$ with the y-axis. Recall (3.8),
then the eigenvectors through $\mathbf{x}_*^R$ are the lines

$$y = -\frac{D_R}{s_{\pm}}(x - x_*^R) - y_*^R \tag{3.15}$$

which intersect the y-axis at $(0, y_{\pm})$ where

$$y_{\pm} = -D_R\left(1 - \frac{1}{s_{\pm}}\right)x_*^R. \tag{3.16}$$

If $y_+ > y_1$ then backward iterates tend to the fixed point in $x > 0$ tangential to
the branch of the eigenvector of s_- above and to the left of the fixed point, whilst if
$y_1 < y_+$ then the accumulation is to the right and below the fixed point.

Consider a family of disjoint closed (with non-empty interior) neighbourhoods of
the preimages of $\mathbf{x}_1^R$ in $x > 0$, chosen so that they map onto each other. The image
of these sets maps to a region around $\mathbf{x}_1^R$ part of which lies in R and part in L. Both
of these sets will be mapped (in fact "folded over") to $y < 0$ close to $\mathbf{x}_0^L$ with $\mathbf{x}_0^L$ on
the boundary of the image. In the standard argument for the existence of chaos in
a snap-back repeller neighbourhoods can be chosen to map over the original sets in
a small neighbourhood of the fixed point allowing a symbolic description of orbits
using established techniques. If the preimage is on the boundary of the set, however,
there is a chance that the image of this set does not contain a countable number of
the preimages which converge on the fixed point, making it impossible to argue for
chaotic solutions.

Consider a half-disc of radius ϵ and with boundary

$$x_0 - \epsilon \leq x \leq x_0 + \epsilon, \quad y = 0 \tag{3.17}$$

and

$$(x_0 + \epsilon \cos\theta, y_0 - \epsilon \sin\theta), \quad 0 \leq \theta \leq \pi \tag{3.18}$$
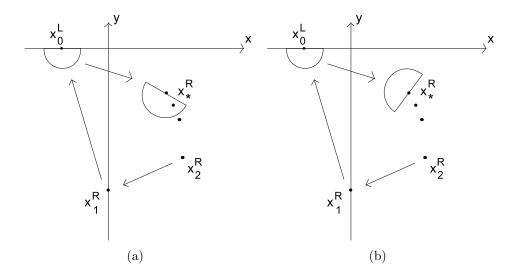
Figure 3.6: Schematic diagram of phase space at the snap-back repeller bifurcation point. The half-disc with $\mathbf{x}_0^L$ on its boundary maps to the half-disc with $\mathbf{x}_*^R$ on its boundary, which (a) is on the same side of the fixed point as the preimages of $\mathbf{x}_1^R$ (b) is on the opposite side of the fixed point from the preimages of $\mathbf{x}_1^R$.

for some small ϵ as shown in Figure 3.6. $\mathbf{x}_0^L$ is on the boundary of this set. One can check that the image of the semi-circle is to the left of the image of the line, which is

$$y - y_*^R = -\frac{D_L}{T_L}(x - x_*^R). \tag{3.19}$$

Hence if the gradient of the line, $-\frac{D_L}{T_L}$, is positive or more negative than the gradient of the eigenvector $\mathbf{e}_-$ the region will contain preimages accumulating on the fixed point in $x > 0$ tangential to the branch of $\mathbf{e}_-$ above and to the left of the fixed point, and if $-\frac{D_L}{T_L}$ is negative but greater than (i.e. more positive than) the gradient of $\mathbf{e}_-$ then it will contain the accumulation to the right and below the fixed point.

Four different cases arise depending on whether preimages of $\mathbf{x}_0^L$ accumulate on the fixed point from above or below, and depending on whether the image of a half-disc containing $\mathbf{x}_0^L$ contains this accumulation or not. If the preimages converge to the fixed point on the same side of the fixed point as is covered by the image of a neighbourhood of $\mathbf{x}_0^L$ in $y < 0$, the standard arguments for the existence of chaos can be made (Figure 3.6 (a)). On the other hand, if the preimages converge on the opposite side of the fixed point as is covered by the neighbourhood of $\mathbf{x}_0^L$ then we

cannot use standard arguments to create infinitely many recurrent points (Figure 3.6 (b)).

Moreover, Gardini [34] and Glendinning [41] both proved that in the process of the creation of a regular snap-back repeller, there is an infinite cascade of more complicated snap-back repellers involving higher periods. That is, there is a sequence of snap-back bifurcations which accumulate on the parameter at which the first snap-back repeller is created. This cascade is in many ways analogous to the cascade of saddle-node bifurcations near a homoclinic tangency [36].

In this chapter we have shown that snap-back repellers exist in the normal form for unstable border collision bifurcations, which makes it possible to predict the existence of chaotic solutions. This chaos is unstable because of the area expansion near the repeller, but we will see in the next chapter, this chaos can actually be part of a strange attractor. Specifically, we show that for appropriate parameter values there is an attracting two-dimensional region in phase space in which periodic orbits are dense and there is a dense orbit.

Chapter 4

Two-dimensional Attractors in Border Collision Normal Form

4.1   Introduction

As we have described in Chapter 2, in the stable case of border collision bifurcations, a number of possible bifurcations can occur depending on the values of the parameters, and strange attractors are known to exist over some regions in the parameter space. For the two-dimensional normal form this is known as "robust chaos" [9]. These robust chaotic sets created in the normal form are associated with the unstable manifold of a saddle fixed point or periodic orbit, and there is only one positive Lyapunov exponent. The attractor is the closure of the one-dimensional unstable manifold with a fractal structure which has dimension less than one in the orthogonal direction. Since the determinant of the Jacobian matrix of a map shows how areas are increased or decreased by iteration, attractors are easily observed in the area contracting (determinant less than one) case, and for this reason these results have found a number of applications.

Intuitively, locally unstable systems may still exhibit globally stable dynamics. Suppose that $D_R > 1$ and $-2\sqrt{D_R} < T_R < 2\sqrt{D_R}$, then there is an unstable spiral in R for $\mu > 0$. As we have discussed at the end of Chapter 2, if $|D_L| < 1$ and
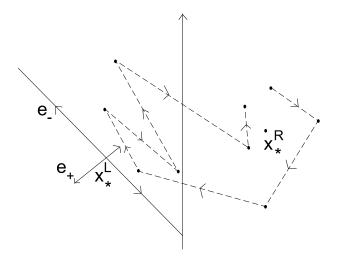
Figure 4.1: A schematic diagram showing how the unstable motions from both sides of the switching surface can create stable dynamics.

$-(1+D_L) < T_L < (1+D_L)$, then the left fixed point is a virtual attractor in R when $\mu > 0$. Any orbit in R spirals outward initially, and as it crosses the switching surface and comes into L, it is attracted to R again eventually. It is possible that there is some set of points in R for which the orbits are trapped in this rotating motion.

Now suppose that $D_L < -1$. If $(1+D_L) < T_L < -(1+D_L)$, then the left fixed point $\mathbf{x}_*^L$ is admissible in L for $\mu > 0$. This is a flip node which has eigenvalues $s_+ > 1$ and $s_- < -1$. The corresponding eigenvectors $\mathbf{e}_+$ and $\mathbf{e}_-$ have slopes $-D_L/s_+ > 0$ and $-D_L/s_- < 0$ respectively. As shown in Figure 4.1, points in L to the right of $\mathbf{e}_-$ are pushed towards R. Thus, similar to the case above, it is possible to have recurring dynamics if the orbits are trapped between the fixed points. Similarly for $T_L > -(1+D_L)$, where the left fixed point is a flip saddle, admissible in L.

In this chapter we show that attractors can exist for models which allow area expansion, and prove that there are some parameter values for which the strange attractor can be a fully two-dimensional object, a polygonal region in fact, rather than the usual fractal attractors.

Two-dimensional attractors in the border collision normal form have been observed numerically, and the existence of invariant regions has been proved in a variety of cases [11, 33, 67, 68]. Figure 4.2 shows an example given in [33], rewritten in the normal form. Different attractors exist as the parameters change. The bifurcations

involved are discussed in the next chapter. For some parameter values, multiple attractors can coexist. An example is shown in Figure 4.3, a period 3 window coexists with a period 6, each attracts a different set of points.

A series of papers has investigated these two-dimensional chaotic regions which can arise if at least one of the determinants has modulus greater than one. However, there are very few proofs of the existence of two-dimensional attractors for these cases, i.e. two-dimensional regions with infinitely many unstable periodic orbits and dense orbits. We know of two exceptions to this statement, the Cournot map cases $(T_L = T_R = 0)$ covered in [11] and the special case considered by Dobryiskiy [22]. The former case can be treated by analyzing an appropriate one-dimensional map using the standard theory of one-dimensional maps, and the latter is based on a proof that the unstable manifold of a saddle is dense and the attractor is the closure of this one-dimensional unstable manifold. We aim to develop techniques which do not rely on one-dimensional techniques, and hence have a broader application. We [43] extend the range of examples for which two-dimensional attractors can be proved to exist using two-dimensional Markov partitions. In the case of Dobryiskiy [22], the attractor is constructed with the unstable manifold of a saddle, so the fixed point is on the boundary of the set. On the other hand, in our examples below the attractors contain a repeller.

If $T_L = T_R = 0$ then the normal form becomes

$$
\begin{aligned}
x_{n+1} &= y_n + \mu \\
y_{n+1} &= \begin{cases} -D_L x_n & \text{if} \quad x_n \leq 0 \\ -D_R x_n & \text{if} \quad x_n \geq 0. \end{cases}
\end{aligned}
\tag{4.1}
$$

This is a Cournot map [11], i.e. a map of the form $x_{n+1} = g(y_n), y_{n+1} = h(x_n)$, which implies that $x_{n+2} = g \circ h(x_n)$ and $y_{n+2} = h \circ g(y_n)$. These maps for the second iterate are one-dimensional maps, and so they can be analyzed using the standard

Figure 4.2: Attractors in border collision normal form for various parameter values. $T_R = 1.93, D_R = 1.2204, \mu = 38.36$.

(a)   (b)
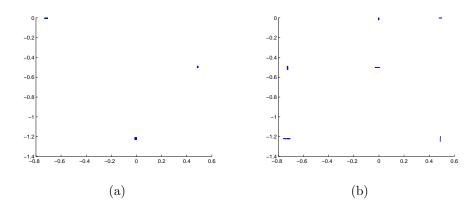
Figure 4.3: Coexistence of multiple attractors in border collision normal form. $T_L = 0.01, D_L = -0.69, T_R = -0.021, D_R = 2.5, \mu = 0.5$. (a) initial point $(0, -1.22)$ leads to a period three window; (b) initial point $(0, -0.5025)$ leads to a period six window.

one-dimensional techniques, which can then be re-interpreted for the original two-dimensional maps. In our case (4.1) gives

$$
x_{n+2} = \begin{cases} \mu - D_L x_n & \text{if } x_n \leq 0 \\ \mu - D_R x_n & \text{if } x_n \geq 0. \end{cases} \tag{4.2}
$$

If $D_R D_L < 0$ then this map can have chaotic dynamics with motion dense on an interval, and this translates to two-dimensional regions in the full two-dimensional map.

The existence of polygonal invariant regions and some of the changes which can occur as parameters vary has been studied for many years (see [67] and references therein), where the polygonal construction is used to prove the existence of two-dimensional invariant regions in a variety of cases. We are not aware of a rigorous proof of the existence of a two-dimensional transitive attractor except in the Cournot case we have outlined above.

In our normal form, according to [33], an invariant region can be constructed by considering the images of the switching surface. Recall that $y_{n+1} = -D_\alpha x_n$, the images of L and R overlap if D_R and D_L have opposite signs, and do not overlap if they have the same signs. Note that, if $|D_R|$ or $|D_L|$ is greater than one, there can be, on average, area expansion along orbits. The contraction required to keep orbits

bounded and hence create invariant regions or attractors is provided by this folding action across the switching surface. So let's assume that D_R and D_L have opposite signs. The boundary $x = 0$ is mapped to $y = 0$, and the image of the origin O is $P_1 = F(O) = (\mu, 0)^T$. Then since the map is piecewise affine, the line segment OP_1 is mapped to another line segment $P_1 P_2$. Let $P_n = F(P_{n-1}) = F^n(O)$. Let $N > 0$ be the first integer such that the segment $P_N P_{N+1}$ intersects the boundary. We assume that such a finite N exists and suppose that $P_N P_{N+1}$ intersects the boundary at Q_0. Then the image of Q_0, Q_1, is on the x-axis, and the polygon $D = P_1 P_2 \ldots P_{N+1} Q_1$ is an $(N+2)$-sided polygon with the sides being made up of segments of the images of the switching surface (see Figure 4.4). If there exists an integer $M \geq 0$ such that $F^M(D) = F^{M+1}(D)$ then $F^M(D)$ is an invariant set by construction. In particular, if P_{N+1} and Q_1 are mapped inside D then D is invariant.
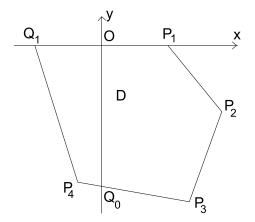
Figure 4.4: Each side of the polygon D is made up of a segment of some image of the y-axis. (e.g. $N = 3$)

In the remainder of this chapter, we give our results in [43] that for some parameter values, this invariant set D can be constructed. Moreover, we use the results from standard Markov partition theory of dynamical systems and a generalization of the affine locally eventually onto (ALEO) property developed in [40] to show that this set is a chaotic attractor.

4.2   Markov partitions, expansion and the ALEO property

In this section we develop some general theory for piecewise affine maps. We begin with a definition.

Definition 4.2.1. ([52]) *Given $D \subseteq \mathbb{R}^2$ and $F : D \to D$, an affine subdivision is a finite collection $\mathcal{M} = M_1, \ldots, M_N$ of pairwise disjoint open sets in D whose boundary $\cup \partial M_i$ is a finite union of closed line segments (possibly infinite or semi-infinite) such that $\cup M_i$ is dense in D and $F|_{M_i}$ is an affine map, $i = 1, \ldots, N$.*

If such a subdivision exists we say F is a piecewise affine map, the subdivision is minimal if the domains M_i are the largest domains on which $F|_{M_i}$ is affine. It is worth noting that, even though the border collision normal form itself is continuous on the boundary, this definition does not assume continuity, this means that piecewise affine maps may be multi-valued.

Next we use the affine locally eventually onto property introduced by Guckenheimer and Williams [47] in the context of expanding maps of the interval. This was used in [40] to prove strong expansion properties of a piecewise affine map originally introduced by Pikovsky and Grassberger [73]. The definition below is slightly weaker than the version introduced in [40], but we show that it is enough to imply standard chaotic properties.

Definition 4.2.2. *A piecewise affine map $F : D \to D$ has the ALEO (affine locally eventually onto) property on the subdivision $(M_i)_{i=1}^N$ of D if for every open set $U \subseteq D$ and $i \in \{1, \ldots, N\}$ there exists $V \subseteq U$ and $n > 0$ such that $F^n(V) = M_i$ and $F^n|_V$ is affine.*

In our examples below we prove this property by showing the existence of finite Markov partitions, but we believe that the ALEO property holds in many examples which do not have Markov partitions (cf. [40]). Let $cl(U)$ denotes the closure of U and $int(U)$ denotes the interior of U. The definitions below follow [1, 84, 85].

Definition 4.2.3. *Let F be a piecewise affine map. A finite Markov partition of an F-invariant set D is a finite subdivision*

$$\mathcal{M} = \{M_1, M_2, \ldots, M_n\}$$

such that $F(M_i)$ is a union of elements of $\mathcal{M}$, $i = 1, \ldots, N$. If every set in $\mathcal{M}$ is convex then we say $\mathcal{M}$ is a convex Markov partition.

The existence of a Markov partition makes it possible to use symbolic dynamics to describe the behaviour of orbits under F in terms of passages through the different elements of $\mathcal{M}$. This labelling may not be unique (points may have non-trivial stable manifolds, and points on the boundary lie in two sets). This will cause us some technical difficulties below when proving the existence of chaotic properties for the maps. These difficulties will be resolved in one of two ways - either by proving an expansion result which ensures that there is a unique correspondence between trajectories and allowed symbol sequences, or by making an additional (weak) assumption on the Markov partition.

Definition 4.2.4. *Let F be a piecewise affine map and let $\mathcal{M}$ be a finite Markov partition with N elements. Then the associated graph $\mathcal{G}$ is the directed graph with vertices labelled $\{1, \ldots, N\}$ and edges from i to j if and only if $M_j \subseteq F(M_i)$. The transition matrix for this graph is $H_\mathcal{G} = (h_{ij})$ where $h_{ij} = 1$ if there is an edge from i to j and $h_{ij} = 0$ otherwise. The graph is strongly connected if there is a path from each vertex to every other vertex, so for each i and j there exists n (depending on i and j) such that $(H^n)_{ij} > 0$; such a transition matrix is called irreducible.*

The graph of a Markov partition defines a symbolic dynamics in the following standard way. Let $\Sigma(n)$ denote the set of all words $\omega = \omega_0 \ldots \omega_n \in \{1, \ldots, N\}^{n+1}$ such that

$$h_{\omega_i \omega_{i+1}} = 1, \quad i = 0, \ldots, n-1,$$

i.e. each ω_i labels a vertex of the associated graph or, equivalently, an element of the

Markov partition. Then for each $\omega \in \Sigma(n)$ the set

$$R_\omega = \{\mathbf{x} \in D | \mathbf{x} \in M_{\omega_0}, F(\mathbf{x}) \in M_{\omega_1}, \ldots, F^n(\mathbf{x}) \in M_{\omega_n}\}$$
$$= M_{\omega_0} \cap F^{-1}(M_{\omega_1}) \cap \cdots \cap F^{-n}(M_{\omega_n})$$

is closed and non-empty, where the inverse maps are chosen such that if $M_{\omega_{k+1}} \subseteq F(M_{\omega_k})$ then $F^{-1}(M_{\omega_{k+1}})$ is defined using the inverse of the map F_α, proceeding inductively along the word. Taking the limit as $n \to \infty$ we obtain a one-sided infinite sequences of symbols and as a countable intersection of closed nested sets is non-empty, if $\omega \in \Sigma(\infty)$ then

$$R_\omega = \bigcap_{k=0}^{\infty} F^{-k}(M_{\omega_k})$$

(with the convention on the definition of the inverse described above) is non-empty and if $\mathbf{x} \in R_\omega$ then $F(\mathbf{x}) \in R_{\sigma(\omega)}$ where σ is the shift map (just delete the first term in the sequence and relabel the resulting sequence).

Most of the following lemma is again standard for continuous maps and also applies to piecewise affine maps [1]. The final statement about convexity follows as the image or preimage of a convex set under a non-singular affine map is convex, and a non-empty intersection of convex sets is convex.

Lemma 4.2.5. *Let $F : D \to D$ be a piecewise affine map with a finite Markov partition $\mathcal{M}$. Then for $2 \leq n \leq \infty$*

(i) if $\omega \in \Sigma(n)$ then R_ω is closed and non-empty;

(ii) $\bigcup_{\omega \in \Sigma(n)} R_\omega = D$;

(iii) if $\omega \in \Sigma(n), n < \infty$ then F^n restricted to R_ω is affine;

(iv) if $n = \infty$ then F^j restricted to R_ω is affine for all $j \in \mathbb{N}$;

(v) $F(R_\omega) = R_{\sigma(\omega)}$.

In addition, if $\mathcal{M}$ is convex then for all $\omega \in \Sigma(n)$, R_ω is convex.

Ideally, for each $\omega \in \Sigma(\infty)$, the set R_ω is a point, for then the map $\Sigma(\infty)$ to D is surjective, so that there is a symbol sequence corresponding to each orbit. This is usually proved using some expansive property (or conversely, a contraction property on the inverse), but as we will see below, the border collision normal form is not expanding. It may well be that a better theory from the one developed below is possible, but the results here do allow us to prove the ALEO property in the examples considered here.

Definition 4.2.6. *A Markov partition (or its transition graph H) is said to be contracting if R_ω is a point for all $\omega \in \Sigma(\infty)$.*

For a contracting Markov partition, points with nearby symbol sequences are close in D.

Proposition 4.2.7. *Let $F : D \to D$ be piecewise affine and suppose that F has a finite Markov partition $\mathcal{M} = \{M_1, \ldots, M_N\}$ with irreducible transition matrix H. If for all open sets $U \subset D$ there exists $i \in \{1, \ldots, N\}, k \geq 0$ and $V \subseteq U$ such that $F^k(V) = M_i$ and $F^k|_V$ is affine, then F is ALEO on $\mathcal{M}$.*

Proof. H is irreducible, so for every M_i and M_j there exists $n > 0$ such that in the partition $\mathcal{M}$ there exists $V_{ij} \subset M_i$ such that $F^n(V_{ij}) = M_j$ and $F^n|_{V_{ij}}$ is affine (H is irreducible so there is an allowed path from i to j and by taking preimages backwards along this path we obtain V_{ij}).

By assumption, for all open U there is $V \subseteq U$ and i and k such that $F^k(V) = M_i$ and $F^k|_V$ is affine, so for any M_j let $\hat{V} \subseteq V$ be such that $F^k(\hat{V}) = V_{ij}$ and note that $F^{k+n}(\hat{V}) = F^n(V_{ij}) = M_j$ and the map is affine by construction. Hence F is ALEO on $\mathcal{M}$. $\qquad\square$

Finally, we need to show that a piecewise affine map F which is ALEO and has a finite Markov partition is chaotic. Recall that a map F is chaotic on some set D if

(i) F is topologically transitive on D, i.e. for all open sets $U, V \in D$ there exists n such that $F^n(U) \cap V \neq \emptyset$;

(ii) F has sensitive dependence on initial conditions on D, i.e. there exists $\delta > 0$ such that for all $\mathbf{x} \in D$ and $\epsilon > 0$ there exists $n \geq 0$ and $\mathbf{y} \in D$ with $|\mathbf{x} - \mathbf{y}| < \epsilon$ such that $|F^n(\mathbf{x}) - F^n(\mathbf{y})| > \delta$;

(iii) the periodic points of F are dense in D.

But if a continuous map on a metric space has an uncountable invariant set on which it is topologically transitive and for which periodic orbits are dense, then it also has sensitive dependence on initial conditions [37].

Proposition 4.2.8. *Let $F : D \to D$ be piecewise affine and suppose that F has a finite Markov partition $\mathcal{M} = \{M_1, \ldots, M_N\}$ with irreducible transition matrix H. If F is ALEO on $\mathcal{M}$ then periodic points are dense in D and F is topologically transitive on D. Thus F also has sensitive dependence on initial conditions in D.*

Proof. We start with dense periodic orbits. Let U be an open neighbourhood of any point $\mathbf{x} \in D$, and as U is open $U \cap M_i \neq \emptyset$ for some i; denote one of these non-empty intersections as W. Then the ALEO property implies that there exists $V \subseteq W$ and $n \geq 1$ such that $V \subseteq W \subseteq M_i = F^n(V)$. Hence V contains a periodic point.

For topological transitivity: for any open V again $V \cap M_r \neq \emptyset$ for some r, and any open U contains a subset V_1 such that $F^k(V_1) = M_r$ for some k by the ALEO property. □

We can see that, if there is a contracting Markov partition with positive topological entropy (i.e. there is an irreducible transition matrix), then for any open set there is a point which is mapped inside some M_i after some iterations. Hence for a piecewise affine map there is some neighbourhood of this point which is mapped to M_i. This implies the ALEO property.

However, in many cases this is not enough as neither A_R nor A_L can be expanding. Note that A is expanding if $|\mathbf{x}^T A^T A \mathbf{x}| > k|\mathbf{x}^T \mathbf{x}|$ for some $k > 1$, in other words the

eigenvalues of the symmetric matrix $A^T A$ is greater than 1. For our normal form map,

$$A_\alpha^T A_\alpha = \begin{pmatrix} T_\alpha^2 + D_\alpha^2 & T_\alpha \\ T_\alpha & 1 \end{pmatrix}$$

with trace $T_\alpha^2 + D_\alpha^2 + 1$ and determinant D_α^2 ($\alpha = L, R$). Since $A_\alpha^T A_\alpha$ is symmetric a necessary condition for A_α being expanding is $Tr(A_\alpha^T A_\alpha) \geq 2$ and $\det(A_\alpha^T A_\alpha) - Tr(A_\alpha^T A_\alpha) + 1 \geq 0$. Since the last inequality is $T_\alpha^2 \leq 0$ the only possible expanding matrices of the normal form have trace zero, which brings us back to the Cournot cases (4.1).

We have developed two different techniques to get around this problem. In the next section we show that although F itself is not expanding, there are some situations for which an appropriate iterate of F is expanding, and that this is enough to prove that the Markov partition is contracting. This is the approach used in the next section. In the following section we use a different strategy, showing that any open interval eventually maps over an element of the Markov partition and thus proving the ALEO property directly.

Before we move on to the next section, we need some notions of invariance and attracting behaviour.

Definition 4.2.9. *Given a continuous map $F : \mathbb{R}^2 \to \mathbb{R}^2$, a compact closed set D is an invariant region if $int(D)$ is connected, D is the closure of its interior and $F(D) \subseteq D$. An invariant region is an attracting invariant region if it is contained in an open set U such that for all $\mathbf{x} \in U$, $F^n(\mathbf{x}) \in D$ as $n \to \infty$. Finally, an attracting invariant region D is a chaotic attractor if periodic points are dense in D and F is topologically transitive on D.*

4.3 Example 1 - a finite Markov partition with local expansion

Suppose that the parameters of the border collision bifurcation can be chosen as shown in Figure 4.5, where $P_1 = F(O)$ and $P_2 = F(P_1)$ are in $x > 0$ and $P_3 = F(P_2)$ has $x = 0$. Moreover, $P_4 = F(P_3)$ is in $x < 0$, $F(P_4) = P_2$ and the line P_2P_4 intersects the y-axis at W, which is the preimage of O. Suppose that P_2P_4 intersects P_1P_3 at V and P_1P_3 intersects OP_2 at U. Then by definition (points of intersection of lines map to the points of intersection of the images of the lines) $F(U) = V$ and $F(V) = W$. Consider the Markov partition involving the sets

$$
\begin{aligned}
M_1 &= OUVW, & M_2 &= OP_1U, & M_3 &= P_1P_2U, & M_4 &= P_2UV \\
M_5 &= P_2P_3V, & M_6 &= P_3VW, & M_7 &= P_3P_4W, & M_8 &= P_4OW
\end{aligned}
\tag{4.3}
$$

Then

$$
\begin{aligned}
F(M_1) &= M_1 \cup M_2, & F(M_2) &= M_3 \cup M_4, \\
F(M_3) &= M_5, & F(M_4) &= M_6 \\
F(M_5) &= M_7, & F(M_6) &= M_8, \\
F(M_7) &= M_1 \cup M_4 \cup M_8, & F(M_8) &= M_2 \cup M_3
\end{aligned}
\tag{4.4}
$$

which shows that $D = P_1P_2P_3P_4$ is an invariant region.

Theorem 4.3.1. *Suppose $\mu > 0$ in the border collision normal form. If $T_R = t$ where t is the solution of*

$$
t^3 + t^2 + t - 1 = 0
\tag{4.5}
$$

in $[0, 1]$, and

$$
D_R = t^2 + t + 1 = \frac{1}{t}
\tag{4.6}
$$

and

$$
T_L = -t^2, \quad D_L = -1,
\tag{4.7}
$$

then the quadrilateral $D = P_1P_2P_3P_4$ is formed as described above, and M_1 to M_8
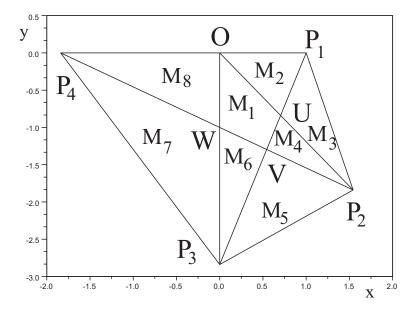
Figure 4.5: Attracting region for parameter values (4.8) with $F(O) = P_1$, $F(P_k) = P_{k+1}$, $k = 1, 2, 3$, $F(P_4) = P_2$, $F(W) = O$, $F(V) = W$ and $F(U) = V$; the Markov partition used to prove the region is transitive and has dense periodic orbits is labelled M_i.

form a Markov partition with covering (4.4) and F is ALEO on D.

The equations above give approximate values

$$T_R \approx 0.543689, D_R \approx 1.839287, T_L \approx -0.295598, D_L = -1. \tag{4.8}$$

Proof. Without loss of generality choose $\mu = 1$. Direct calculation shows that $P_1 = (1, 0)^T$, $P_2 = (T_R + 1, -D_R)^T$ and

$$P_3 = \begin{pmatrix} T_R^2 + T_R + 1 - D_R \\ -D_R(T_R + 1) \end{pmatrix}, \tag{4.9}$$

so the x-component of P_3 is zero if

$$D_R = T_R^2 + T_R + 1 \tag{4.10}$$

in which case $P_4 = (-D_R(T_R + 1) + 1, 0)^T$. The preimage of O is $W = (0, -1)^T$, so

the line P_2P_4 intersects the y-axis at W if

$$\frac{1}{D_R(T_R+1)-1} = \frac{D_R}{T_R+1+D_R(T_R+1)-1} \tag{4.11}$$

using similar triangles. Rewriting this as $(D_R+1)(T_R+1)-1 = D_R^2(T_R+1)-D_R$, and using (4.10) gives

$$T_R^5 + 3T_R^4 + 4T_R^3 + 2T_R^2 - T_R - 1 = (T_R^3 + T_R^2 + T_R - 1)(T_R^2 + 2T_R + 1) = 0$$

and hence (4.5) holds. By direct evaluation this has a solution $T_R \in [0,1]$ and then D_R given by (4.6) is greater than one, and P_2 is in $x > 0$ as required.

The conditions (4.7) on D_L and T_L ensure that $F(P_4) = P_2$.

To prove the ALEO property we want to show that every allowed symbol sequence corresponds to a unique orbit. We do this by supposing, for contradiction, that there are two points always in the same element of the Markov partition, and show that their distance eventually expands under iteration, and hence they cannot be in the same element infinitely long. Finally it is easy to see from (4.4) that there are paths from each element of the partition to every other element, so the associated transition matrix is irreducible.

If the orbit of $\mathbf{x}$ lies entirely in $x > 0$ then the point is the fixed point of the affine map in R and is unique - it corresponds to the allowed path $M_1 M_1 M_1 \dots$.

Suppose that $x < 0$. If $\mathbf{x} \in M_8$ then the allowed path starts in one of these ways

$$M_8 M_2 M_4 M_6 M_8 \dots, \quad M_8 M_2 M_3 M_5 M_7 \dots, \quad \text{or} \quad M_8 M_3 M_5 M_7 \dots.$$

In each case there is one iterate in L followed by either two or three iterates in R before returning to L. Similarly if $\mathbf{x} \in M_7$ the allowed path starts

$$M_7 M_1^p M_2 M_4 M_6 M_8 \dots, \quad M_7 M_1^p M_2 M_3 M_5 M_7 \dots, \quad \text{or} \quad M_7 M_4 M_6 M_8 \dots$$

operator B	$\delta = \det(B^T B)$	$\tau = \text{Trace}(B^T B)$	$\tau - 2$	$\delta - \tau + 1$
$A_R^2 A_L^2$	11.44	7.06	5.06	5.38
$A_R^3 A_L^2$	38.71	14.21	12.21	25.51
$A_R^2 A_L$	11.44	6.77	4.77	5.68
$A_R^3 A_L$	38.71	15.83	13.82	23.89
A_R^2	11.44	7.06	5.06	5.38

Table 4.1: Expansion properties for higher iterates of the map.

with $p \geq 1$ (including $p = \infty$), or M_7 is followed by M_8 and we have one of the cases for M_8 with an extra iteration in L at the beginning. From these cases we can see that the orbit of a point is made up of only a few particular routes. The sequence of visits to the left and right can be obtained by joining the following

$$LLRR, \quad LLRRR, \quad LRR, \quad LRRR, \quad \text{and} \quad RR.$$

For example,

$$M_7 M_1^4 M_2 M_4 M_6 M_8 M_3 M_5 M_7 M_8 M_3 M_5 M_7 \ldots$$

corresponds to $(LRRR)(RR)^2(LRR)(LLRR)L\ldots$. Hence if each of the five combinations of Ls and Rs corresponds to an effective expansion by a factor greater than one, then the distance between two point in the same element expands until they are mapped to different elements of the partition, so an infinite allowed path corresponds to a unique point.

As shown earlier, a 2×2 matrix B is expanding if the trace τ and determinant δ of the symmetric matrix $B^T B$ satisfy $\tau \geq 2$ and $\delta - \tau + 1 \geq 0$. We have checked numerically that each of the five combinations for B

$$A_R^2 A_L^2, \quad A_R^3 A_L^2, \quad A_R^2 A_L, \quad A_R^3 A_L, \quad \text{and} \quad A_R^2$$

(note that the order of the operators is reversed here from the order of the symbol sequences) do indeed correspond to expanding matrices. See Table 4.1 for numerical results.
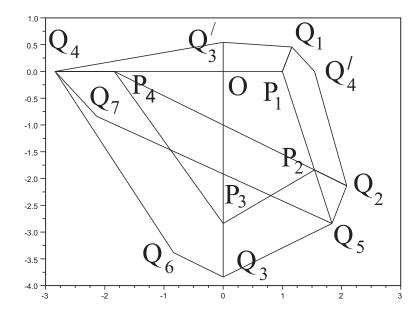
Figure 4.6: Basin of attraction for the quadrilateral attractor $P_1P_2P_3P_4$.

Thus since the transition graph has positive topological entropy, the map is ALEO.

$\square$

It remains to be shown that this invariant set is an attractor.

Corollary 4.3.2. *For parameters defined in Theorem 4.3.1 the quadrilateral $P_1P_2P_3P_4$ is an attractor.*

Proof. By Theorem 4.3.1 and Proposition 4.2.8, periodic orbits are dense and the map is topologically transitive in the quadrilateral $P_1P_2P_3P_4$, which is an invariant region. It therefore remains to prove that the region is attracting.

We construct a polygon $Q_3'Q_1Q_4'Q_2Q_5Q_3Q_6Q_4$ containing $P_1P_2P_3P_4$ and such that iterates of all points in the polygon tend to the quadrilateral. See Figure 4.6.

Let $Q_3 = P_3 + \epsilon(0,-1)^T$, Q_4, Q_5, Q_6, Q_7 be images of Q_3, i.e. $Q_{3+k} = F^k(Q_3), k = 1, 2, 3, 4$, and Q_1 and Q_2 be the preimages of Q_3 in R, so that $F(Q_1) = Q_2$ and $F(Q_2) = Q_3$. A simple calculation gives

$$
\begin{aligned}
Q_1 &= P_1 + \epsilon(t^3, t^2(1+t))^T, & Q_2 &= P_2 + \epsilon(t, -t^2)^T, \\
Q_4 &= P_4 + \epsilon(-1, 0)^T, & Q_5 &= P_2 + \epsilon(t^2, -1)^T, & (4.12) \\
Q_6 &= P_3 + \epsilon(-t(1+t), -t)^T, & Q_7 &= P_4 + \epsilon(-t^2, -t(1+t))^T.
\end{aligned}
$$

Note that Q_5 is on the extension of $P_1 P_2$ in $x > 0$, and Q_6 and Q_7 in $x < 0$ (Q_6 is on the extension of $P_2 P_3$).

Now let Q_4' be the preimage of Q_5 in $x > 0$ and Q_3' be the preimage of Q_4'. Since Q_5 is on the extension of $P_1 P_2$, Q_4' is on the x-axis the extension of OP_1, similarly Q_3' is on the positive y-axis. Calculations give

$$Q_3' = \epsilon(0, t)^T, \quad Q_4' = P_1 + \epsilon(t, 0)^T.$$

Let $N_0 = OQ_4Q_3'$, $N_1 = OQ_3'Q_1P_1$, $N_2 = Q_1P_1P_2Q_2Q_4'$, $N_3 = Q_2P_2P_3Q_3Q_5$ and $N_4 = Q_3P_3P_4Q_4Q_6$ and note that the polygon $Q_3'Q_1Q_4'Q_2Q_5Q_3Q_6Q_4$ is the union of the sets $N_i, i = 0, 1, 2, 3, 4$ and the quadrilateral $P_1P_2P_3P_4$. Also, $F(N_0) \subset N_2 \cup N_3$, $F(N_1) \subset N_2$, $F(N_2) = N_3$ and $F(N_3) = N_4$.

Calculation shows that Q_7 lies in $x < 0$ to the right of Q_6Q_4 and to the left of P_3P_4, and recall that $F(P_4) = P_2$. Hence the image of N_4 is the polygon $Q_4P_4P_2Q_5Q_7$ which, at least for sufficiently small ϵ, intersects N_4 on a set A near P_4, has a strip across $P_1P_2P_3P_4$ and intersects N_3 on a set B near P_2. By choosing $\epsilon > 0$ small enough the image of A which does not map to the quadrilateral is mapped into B; and $F(B) = C$, a subset of N_4 in $x \le 0$ near P_3. $F(C)$ lies in the image of N_4 but does not stretch as far as B. Thus any recurrent dynamics in the large polygon which does not map to the invariant quadrilateral is confined to B in $x > 0$ and two disjoint regions (for ϵ sufficiently small) A and C in $x \le 0$; the third iterate of F restricted to these regions is an affine map with determinant $1/t$. As $|t| \ne 1$ the only non-trivial dynamics can be the fixed point of the third iterate (as the motion is bounded by the polygon) and hence any solution either maps into the attractor $P_1P_2P_3P_4$ or tends to the period three cycle $P_2P_3P_4$, which is also in the closed quadrilateral. Hence the closed quadrilateral is an attractor. $\square$

Figure 4.7 illustrates this strange attractor.

The argument above is simple but a little long and tedious in the case of this section, but considerably easier for the cases described in the next section.
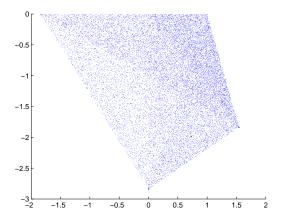
Figure 4.7: Strange attractor with parameters (4.8). 20000 points on an orbit are shown.

4.4 Example 2 - a countable set of examples

The example of the previous section demonstrates that the Markov partition technique can be applied effectively to study attractors of the border collision normal form, here we give an example which shows how to generate a countable set of parameters for which a Markov partition exists. An example is illustrated in Figure 4.8.

Suppose $\mu > 0$, so again we take $\mu = 1$ without loss of generality. The fixed point P^* in R is

$$P^* = \frac{1}{1 - T_R + D_R} \begin{pmatrix} 1 \\ -D_R \end{pmatrix}$$

and A_R has complex conjugate eigenvalues $re^{\pm i\theta}$, if

$$T_R = 2r\cos\theta, \quad D_R = r^2 \quad (r > 0, \ 0 < \theta < \pi). \tag{4.13}$$

Note that the fixed point P^* is then a spiral. We will choose r and θ so that there exists $n > 1$ such that $P_n = F^n(O)$ is on $x = 0$, with $P_k = F^k(O)$ in $x > 0$ for $k = 1, \ldots, n-1$. Then $P_{n+1} = F(P_n)$ lies on the x-axis. Let's assume that P_{n+1} is in $x < 0$. Suppose also that the line $P_{n+1}P^*$ intersects the y-axis at $W = (0, -1)^T$ which is the preimage of the origin O. These two conditions fix T_R and D_R. For T_L and D_L we choose them so that $F(P_{n+1}) = P^*$. This yields the geometry shown in Figure 4.8,
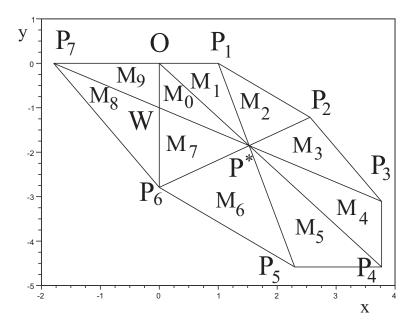
Figure 4.8: Attracting region showing the construction of the Markov partition used to prove the region is transitive and has dense periodic orbits. The case $n = 6$ is illustrated with $T_R \approx 1.55842898$, $D_R \approx 1.21435044$ with T_L and D_L given by (4.21), i.e. $T_L \approx -0.2929366$ and $D_L \approx -1.0338562$. $F(O) = P_1$; $F(P_i) = P_{i+1}$, $i = 1, \ldots, 6$; $F(P^*) = F(P_7) = P^*$; and $F(W) = O$.

creating an $n + 1$-sided polygon $D = P_1 P_2 \ldots P_{n+1}$ and regions $M_0, \ldots, M_{n+3}$ which form a Markov partition of D. We begin by proving that parameters at which these conditions hold do exist for each $n > 2$.

By definition

$$F^k(O) = (A_R^{k-1} + \cdots + A_R + I) \begin{pmatrix} 1 \\ 0 \end{pmatrix} = (A_R - I)^{-1}(A_R^k - I)) \begin{pmatrix} 1 \\ 0 \end{pmatrix}$$

provided $A_R - I$ is non-singular. Using (4.13) and recall that $0 < \theta < \pi$, so $\sin\theta \neq 0$,

calculation shows that

$$P_n = F^n(O)$$

$$= \frac{r^n}{(1 - T_R + D_R)\sin\theta} \begin{pmatrix} r\sin(n\theta) - \sin(n+1)\theta \\ D_R\sin(n+1)\theta - (T_R - 1)r\sin(n\theta) \end{pmatrix}$$

$$+ \frac{1}{1 - T_R + D_R} \begin{pmatrix} 1 \\ -D_R \end{pmatrix} \tag{4.14}$$

The condition that P_n has $x = 0$ is therefore

$$r^{n+1}\sin(n\theta) - r^n\sin(n+1)\theta + \sin\theta = 0. \tag{4.15}$$

This simplifies P_n to $P_n = (0, q_n)^T$ where

$$q_n = \frac{r^{n+1}\sin(n\theta)}{\sin\theta} = -1 + \frac{r^n\sin(n+1)\theta}{\sin\theta} \tag{4.16}$$

and so $P_{n+1} = (1+q_n, 0)^T$. We will need to check that $q_n < -1$. The second condition that W is on the line $P_{n+1}P^*$ is equivalent to the statement that the slope of the line $P_{n+1}W$ equals the slope of WP^*. After some manipulation, we get

$$\frac{r^{n+1}\sin(n\theta) + \sin\theta}{\sin\theta} = \frac{1}{1 - T_R} \tag{4.17}$$

or

$$2r^{n+1}\cos\theta\sin(n\theta) - r^n\sin(n\theta) + 2\sin\theta\cos\theta = 0. \tag{4.18}$$

Multiply (4.15) by $2\cos\theta$ then subtract from (4.18) gives

$$2\cos\theta\sin(n+1)\theta - \sin(n\theta) = 0,$$

and by using trigonometric formulae we have $\sin(n+2)\theta = 0$, therefore we choose

the solution with

$$\theta_n = \frac{2\pi}{n+2}.$$ (4.19)

Substituting this into (4.15) and simplifying we find that (4.15) is satisfied if and only if

$$g_n(r) = 2r^{n+1}\cos\theta_n - r^n - 1 = 0.$$ (4.20)

For large r, $g_n(r) > 0$, and if $r = 1$,

$$g_n(1) = -2(1 - \cos\theta_n) < 0.$$

Hence, by the intermediate value theorem g_n has a zero at some $r_n > 1$. Moreover, since $\sin(n+1)\theta_n = \sin 2\pi(n+1)/(n+2) = -\sin\theta_n$, $q_n = -1 - r_n^n < -1$ hence P_{n+1} indeed lies in L as assumed.

Now we know that, for any given $n > 1$, $P_n = (0, q_n)^T$ and $P_{n+1} = (1 + q_n, 0)^T$ with q_n given by (4.16) for parameters (r_n, θ_n). The condition $F(P_{n+1}) = P^*$ is thus

$$T_L(1 + q_n) + 1 = \frac{1}{1 - T_R + D_R}, \quad D_L(1 + q_n) = \frac{D_R}{1 - T_R + D_R}$$ (4.21)

which determines T_L and D_L.

Theorem 4.4.1. *Suppose $\mu > 0$ in the border collision normal form. For each $n > 0$ sufficiently large let (T_R, D_R, T_L, D_L) be determined from (4.13), (r_n, θ_n) and (4.21) above. Then the border collision normal form is ALEO on a two dimension region $D = P_1 \ldots P_{n+1}$.*

Numerical calculations suggest that "sufficiently large" means $n \geq 6$.

As illustrated in Figure 4.8, the Markov partition will be constructed using the sets $M_0, \ldots, M_{n+3}$ defined by $M_0 = WOP^*$, $M_1 = OP_1P^*$ and $M_k = P_{k-1}P_kP^*$, $k =$

$2, \ldots, n$, $M_{n+1} = WP_nP^*$, $M_{n+2} = WP_nP_{n+1}$ and $M_{n+3} = WP_{n+1}O$. Then by construction,

$$F(M_{k-1}) = M_k, \quad k = 1, \ldots, n,$$
$$F(M_n) = M_{n+1} \cup M_{n+2}, \quad F(M_{n+1}) = F(M_{n+2}) = M_{n+3} \cup M_0, \qquad (4.22)$$
$$F(M_{n+3}) = M_1.$$

The union of these regions, the polygon $D = P_1 \ldots P_{n+1}$, is invariant and $M_0, \ldots, M_{n+3}$ form an irreducible Markov partition.

To prove Theorem 4.4.1, we first need to define a skew-tent map.

Let $a < b < c$. Then a skew-tent map $S : [a, c] \to [a, c]$ is a continuous map such that $S([a, b]) = S([b, c]) = [a, c]$, and such that S is affine on both $[a, b]$ and $[b, c]$. The point b is called the turning point of the map. (Figure 4.9)
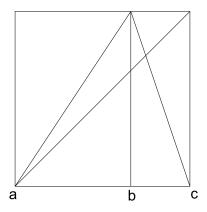
Figure 4.9: A skew-tent map.

Proposition 4.4.2. *Let $S : [a, c] \to [a, c]$ be a skew-tent map with turning point b, then for any interval $I \subseteq [a, c]$ there exists $J \subseteq I$ and $n > 0$ such that $S^n|_J$ is affine and $S^n(J) = [a, c]$.*

Proof. Suppose that $I = [\alpha, \gamma] \subseteq [a, c]$ and contains b. Consider $[\alpha, b] \subseteq [a, b]$. Since $S|_{[a,b]}$ is affine, $S([\alpha, b]) = [S(\alpha), c]$. If $S(\alpha) \leq b < c$ then we are done, since we can choose $\beta \in [\alpha, b]$ such that $S(\beta) = b$ and $J = [\beta, b] \subset I$, so $S(J) = [b, c]$ and $S^2(J) = [a, c]$ and $S^2|_J$ is affine.

If $b < S(\alpha)$, then $S^2([\alpha, b]) = [a, S^2(\alpha)]$. If $S^2(\alpha) \geq b$ then again we are done.

Suppose not, then since the gradients of the map $S|_{[a,b]}$ and $S|_{[b,c]}$ are greater than 1 in modulus, the interval is expanded under each iteration, until eventually $S^{n-1}([\alpha, b]) = [a, S^{n-1}(\alpha)]$ for some $n - 1$ such that $S^{n-1}(\alpha) \geq b$. Then again we can choose $J = [\beta, b] \subseteq [\alpha, b]$, so that $S|_J$ is affine and $S^n(J) = [a, c]$.

For any interval $I \subseteq [a, c]$ not containing b, i.e. I is contained in either $[a, b]$ or $[b, c]$, we again note that interval is then expanded under each iteration until some image contains the turning point b, then above argument applies. $\qquad \square$

Now return to our example, we have two useful lemmas.

Lemma 4.4.3. *Consider the normal form for parameters defined in Theorem 4.4.1. Then F^{n+2} restricted to the line segment $P_{n+1}P^*$ is a skew tent map with turning point at W.*

Proof. This follows easily from the observation that $F(P_{n+1}W) = F(WP^*) = OP^*$ and $F^{n+1}(OP^*) = P_{n+1}P^*$ and $F^{n+1}|_{OP^*}$ is affine, so $F^{n+2}(P_{n+1}W) = F^{n+2}(WP^*) = P_{n+1}P^*$. $\qquad \square$

Lemma 4.4.4. *Consider the normal form for parameters defined in Theorem 4.4.1. Let Q be any region in $M_k, k = 0, \ldots, n + 1$, which contains an entire neighbourhood of P^* within M_k. Then there exists $Q_1 \subseteq Q$ and m such that $F^m(Q_1) = M_0$ and $F^m|_{Q_1}$ is affine.*

Proof. Consider the preimages of $M_0 = WOP^*$ under the map in R. The preimage of the point W, W_{-1} lies on the line segment P_nP^*, so the preimage of M_0 in R is the set $W_{-1}WP^* \subset M_{n+1}$. Similarly its preimage is $W_{-2}W_{-1}P^* \subset M_n$ where W_{-2} is on the segment $P_{n-1}P^*$. Continuing in this way we see that $F^{-(n+2)}(M_0) \subset M_0$ and contains the angle $\angle P_{n+1}P^*O$, and more generally the sets $F^{-m(n+2)}(M_0) \subset M_0, m > 0$ form a nested sequence of such regions tending to P^*. Also with $k = 1, \ldots, n + 1$ fixed, $F^{-m(n+2)+k}(M_0)$ is in M_k containing the angle at P^* and tends to P^* as $m \to \infty$. $\qquad \square$

Note that this shows that preimages of M_0 exist in any region filling the angle at P^* in $M_k, k = 0, \ldots, n + 1$.

Now we start proving Theorem 4.4.1.

Proof. First, from (4.22) one can see that the transition matrix associated with the Markov partition is irreducible, hence to apply Proposition 4.2.7 we only need to check that for all open sets U in the invariant region $D = \cup M_k$ there exists i, n and $V \subseteq U$ such that $F^n(V) = M_i$ and $F^n|_V$ is affine. We show this for $i = 0$.

First note that $r_n > 1$ and so $D_R = r_n^2 > 1$. Simplifying the expression for D_L in (4.21) using $q_n = -1 - r_n^n$ gives

$$D_L = -r_n^{-(n-2)}(1 - 2r_n \cos\theta_n + r_n^2)^{-1}.$$

Since, from (4.19) and (4.20), $\theta_n \to 0$ and $r_n \to 1$ as $n \to \infty$, $D_L \to -\infty$ as $n \to \infty$ and in particular $|D_L| > 1$ for sufficiently large n. Therefore for large n both $|D_R|$ and $|D_L|$ are greater than one and hence areas are increased under iteration. Numerical simulations show that $|D_L| > 1$ provided $n \geq 6$.

Let U be an open set in D and fix n large enough so that $|D_R|$ and $|D_L|$ are greater than one. Let $m_1 \geq 0$ be the smallest integer such that $F^{m_1}(U)$ intersects the y-axis (m_1 exists because otherwise $F^m|U$ would be affine for each m and the area of $F^m(U)$ would increase unboundedly, but $F^m(U)$ is in the finite invariant region D).

Suppose that $F^{m_1}(U)$ intersects WP_n and let $U_1 \in M_{n+1}$ be the component of $F^{m_1}(U)$ in R, so that $F^{m_1}(U) \cap WP_n$ is on its boundary. Let $U_2 \subseteq U$ such that $F^{m_1}(U_2) = U_1$ and $F^{m_1}|_{U_2}$ is affine.

Since $F(M_{n+1}) = M_{n+3} \cup M_0$ and WP_n maps to OP_{n+1}, $F(U_1) \cap M_{n+3} \neq \emptyset$ and by choosing U_1 and U_2 smaller if necessary we may assume that $F(U_1)$ is contained in M_{n+3}, so $F^{n+2}|_{U_1}$ is affine and $F^{n+2}(U_1) \subseteq M_{n+1} \cup M_{n+2}$ has a segment $I \subseteq P_{n+1}P^*$ on its boundary. By Lemma 4.4.3 and Proposition 4.4.2 there exists $J \subseteq I$ and m_2 such that $F^{m_2(n+2)}|_J$ is affine and $F^{m_2(n+2)}(J) = P_{n+1}P^*$, so there exists $U_3 \subseteq F^{n+2}(U_1)$ with J on the boundary such that $F^{m_2(n+2)}|_{U_3}$ is affine and $P_{n+1}P^*$, in particular W, is on the boundary of $F^{m_2(n+2)}(U_3)$. By (4.22), $F^{m_2(n+2)}(U_3) \subseteq M_{n+1} \cup M_{n+2}$, and since it contains W on its boundary it contains the intersection of an open neighbourhood

of W with M_{n+1}, i.e. it fills the angle $\angle P_n W P^*$. Let $U_4 \subseteq F^{m_2(n+2)}(U_3)$ be the component of $F^{m_2(n+2)}(U_3)$ in R so that $F(U_4)$ is contained in M_0 and fills the angle $\angle WOP^*$, then $F^{n+3}(U_4) \subseteq M_0$ and fills the angle WP^*O. Thus Lemma 4.4.4 ensures that there exists $U_5 \subseteq F^{n+3}(U_4)$ and m_3 such that $F^{m_3}(U_5) = M_0$ and $F^{m_3}|_{U_5}$ is affine. Therefore, given an open set U, there exists $V(\subseteq U_2) \subseteq U$ and $N = m_1 + (n+2) + m_2(n+2) + (n+3) + m_3$ such that $F^N|_V$ is affine and $F^N(V) = M_0$, and hence F is ALEO on the polygon $D = P_1 P_2 \ldots P_{n+1}$ by Proposition 4.2.7.

If $F^{m_1}(U)$ intersects WO, let U_1 be the component of $F^{m_1}(U)$ in R, then $F^{n+2}(U_1) \subseteq M_{n+3} \cup M_0$ and has a segment $P^* P_{n+1}$ on the boundary and the above argument applies. $\square$

Corollary 4.4.5. *For parameters such that Theorem 4.4.1 holds, the closed polygon* $D = P_1 P_2 \ldots P_{n+1}$ *is an attractor.*

The proof is similar but simpler than the one in the previous section, so we shall be brief.

Proof. Again, by Theorem 4.4.1 and Proposition 4.2.8, periodic orbits are dense and the map is topologically transitive in the invariant region $D = P_1 P_2 \ldots P_{n+1}$. We need to show that there is an open region containing D such that iterates of all points tend to D.

Let $Q_n = P_n + \epsilon(0, -1)^T$ for sufficiently small $\epsilon > 0$, its image Q_{n+1} is on the x-axis in L, then take preimages in $x > 0$ back to Q_1. Note that, since Q_n is close to but below $P_{n-1} P_n$, Q_1 is above the x-axis near P_1, hence the line segment $Q_1 Q_2$ intersects the x-axis at some point S_1, which has a preimage on the positive y-axis at S_0.

Consider the set $S_0 Q_1 Q_2 \ldots Q_{n+1}$. Let $N_0 = S_0 O Q_{n+1}, N_1 = S_0 Q_1 P_1 O$ and $N_k = Q_{k-1} Q_k P_k P_{k-1}, k = 2, \ldots, n+1$, and note that the polygon $S_0 Q_1 Q_2 \ldots Q_{n+1}$ is the union of $N_0, \ldots, N_{n+1}$ and the invariant region D. By construction, $F(N_1) \subset N_2$ and $F(N_k) = N_{k+1}, k = 2, \ldots, n$. For sufficiently small ϵ, S_0 is near O and Q_{n+1} is near P_{n+1} which is mapped inside D, hence $F(N_0) = S_1 P_1 Q_{n+2} \subset D \cup N_2$ and $F(N_{n+1}) =$

$Q_{n+1}Q_{n+2}P^*P_{n+1} \subset D \cup N_{n+1}$. But the image of N_{n+1} which is not contained in D is a small set near P_{n+1}, so its image, for sufficiently small ϵ, is contained in D near P^*, i.e. $F^2(N_{n+1}) \subset D$. Therefore iterates of points in $S_0Q_1Q_2\ldots Q_{n+1}$ tend to the invariant polygon $D = P_1P_2\ldots P_{n+1}$ and so D is an attractor. $\qquad\square$

We have here shown that using the ALEO property two-dimensional attractors with finite Markov partitions exist for the border collision normal form at some carefully chosen parameters. We believe that such attractors exist over much larger regions of parameter space (more numerical examples can be found in [33, 67]), that the ALEO property holds even if finite Markov partitions do not exist, though we have not yet developed the techniques to prove this. But our hope is that the use of the ALEO property will eventually allow us to provide a mathematical proof of the existence of these attractors.

Chapter 5

Bifurcations of Attractors in Border Collision Normal Form

5.1 Introduction

So far we have shown that invariant regions and attractors can exist for the border collision normal form with local area expansion, in this chapter we discuss some of the bifurcations these sets exhibit as the parameters change values.

As in the previous chapters we assume that $D_R D_L < 0$, so that the map F is non-invertible, and at least one of the determinants has modulus greater than one, so we let $D_R > 1$ and $D_L < 0$ throughout. Note that, by a change of scale only the sign of μ matters if $\mu \neq 0$.

Recall again from Chapter 2 that the fixed points $\mathbf{x}_*^\alpha$ of the normal form map are given by

$$x_*^\alpha = \frac{\mu}{1 - T_\alpha + D_\alpha}, \quad y_*^\alpha = -D_\alpha x_*^\alpha, \quad \alpha = L, R$$

and a fixed point is admissible if $\mathbf{x}_*^\alpha \in \alpha$ and virtual otherwise. We assume that $\mathbf{x}_*^R \in R$ when $\mu > 0$ (without loss of generality choose $\mu = 1$), so $1 - T_R + D_R > 0$. Also, the eigenvalues of the map for each side of the switching surface are the solutions of the quadratic $s^2 - T_\alpha s + D_\alpha = 0$, so $\mathbf{x}_*^R \in R$ is
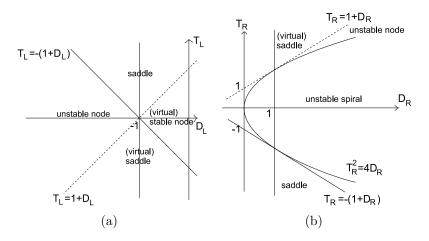
Figure 5.1: Parameter spaces (D_L, T_L) and (D_R, T_R) of the normal form map for each side of the switching surface.

- an unstable spiral if $-2\sqrt{D_R} < T_R < 2\sqrt{D_R}$;

- an unstable node if $-(1 + D_R) < T_R < -2\sqrt{D_R}$ or $2\sqrt{D_R} < T_R < 1 + D_R$; and

- a saddle if $T_R < -(1 + D_R)$ or $T_R > 1 + D_R$.

We can summarize these in a diagram in the (D_R, T_R) parameter space. Similarly, the same can be done for the fixed point $\mathbf{x}_*^L$. See Figure 5.1. The dotted lines in the figures represent the line $T_\alpha = 1 + D_\alpha$, on which the corresponding fixed point approaches infinity and ceases to exist. Hence there is a singularity for the fixed point on this line.

In this chapter we consider mainly the case where $\mathbf{x}_*^R$ is an unstable spiral and investigate some of the bifurcations of the attracting sets as the parameters change values. Note that in this case every point in R except the fixed point itself eventually maps to L. The other fixed point $\mathbf{x}_*^L$, since $D_L < 0$ and hence the eigenvalues are real and with opposite signs, is either a flip node or a flip saddle. The slopes of its eigenvectors are given by $-D_L/s_\pm$, so there is an eigenvector with positive slope, corresponding to the positive eigenvalue. Therefore, if $\mathbf{x}_*^L$ is an unstable node in L, there is an unstable manifold of the fixed point that "pushes" points in L towards R; if $\mathbf{x}_*^L$ is a virtual stable node in R, a stable manifold "pulls" orbits from L to R again, the same happens when the fixed point is a saddle or a virtual saddle. So it is likely that there exist some globally recurrent dynamics.
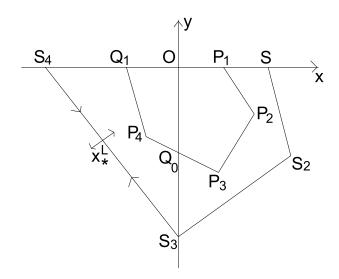
Figure 5.2: An attracting set and its basin of attraction when $\mathbf{x}_*^L$ is an admissible saddle.

An example is illustrated in Figure 5.2.

Let

$$T_L = 0.3, \quad D_L = -0.8, \quad T_R = 1, \quad D_R = 1.8.$$

The polygon $V = P_1 P_2 P_3 P_4 Q_1$ is constructed as described in the previous chapter. $\mathbf{x}_*^L$ is an admissible saddle, $S_3 S_4$ is the stable manifold of the fixed point, $S_2 S_3$ and $S S_2$ are the preimages of $S_3 S_4$ in R (below the x-axis). Since $F(S_3) = S_4$ and S_4 is mapped on the segment $\mathbf{x}_*^L S_3$, $F(O S_3 S_4) \subset S S_2 S_3 S_4$ and hence $S S_2 S_3 S_4$ is an invariant set. Note that the polygon $P_1 P_2 P_3 P_4 Q_1$ depends on T_R and D_R only (the images of the points P_4 and Q_1 depend on T_L and D_L though), so there always exists T_L and D_L such that $\mathbf{x}_*^L$ is sufficiently far to the left of the polygon and the set bounded by its stable manifold contains V and hence its images, thus the set $\cup_k F^k(V)$ is bounded and invariant. With the parameters above, one can check that P_4 and Q_1 are mapped inside V, so $F(V) \subset V$. Moreover, orbits in $S S_2 S_3 S_4$ are pushed towards V by the unstable manifold of $\mathbf{x}_*^L$, so V is in fact an attracting set, with a polygonal basin of attraction $S S_2 S_3 S_4$. When the fixed point $\mathbf{x}_*^L$ is an admissible saddle, by considering the stable manifold and its preimages in R, we can obtain a basin of attraction for an attracting set in this way, provided the constructed attracting set does not intersect the stable manifold of the fixed point $\mathbf{x}_*^L$, otherwise points from the set eventually

map over the other side of the stable manifold and diverge. This bifurcation where the boundary of an attracting set meets the boundary of its basin of attraction and causes a destruction of the attracting set is an example of boundary crisis or contact bifurcation [44, 45, 46].

We shall next investigate what happens if (D_L, T_L) crosses the line $T_L = -(1 + D_L)$, where one of the eigenvalues of F_L is equal to -1, and $\mathbf{x}_*^L$ becomes an admissible unstable node.

5.2 Degenerate bifurcations

For one-dimensional systems $x_{n+1} = F(x_n), F : \mathbb{R} \to \mathbb{R}$, a period-doubling bifurcation (also known as flip bifurcation) occurs when a stable fixed point (or periodic orbit) p loses its hyperbolicity such that $F'(p) = -1$ at some parameter value, after which its nature changes and becomes unstable.

Theorem 5.2.1 ([83]). *Let $F_\mu : \mathbb{R} \to \mathbb{R}$ be a family of C^3-maps depending smoothly on the parameter μ. Let p_μ be a fixed point of F_μ and $F'_{\mu_0}(p_{\mu_0}) = -1$. If, at $\mu = \mu_0$ and $x = p_{\mu_0}$,*

(i) $(d^3/dx^3)F^2_{\mu_0}(p_{\mu_0}) \neq 0$, and

(ii) $(d/d\mu)F'_{\mu_0}(p_{\mu_0}) \neq 0$,

then there is a period-doubling bifurcation, that is, a period two orbit is created while a fixed point changes its stability.

For maps on the real line, this local bifurcation is one of the most common bifurcations, a lot of examples can be found in most text books, e.g. [16, 2]. One of them is the logistic map. Let $F_\mu(x) = \mu x(1 - x), x \in [0, 1]$ with $\mu > 1$. F_μ has two fixed points one at 0 and the other at $p_\mu = (\mu - 1)/\mu$. $F'_\mu(0) = \mu$ and $F'_\mu(p_\mu) = 2 - \mu$, hence 0 is a repelling fixed point for $\mu > 1$ and p_μ is attracting for $1 < \mu < 3$. When $\mu = 3$, $F'_\mu(p_\mu) = -1$. Figure 5.3 shows the graphs of F^2_μ for μ near 3. Note that

two new fixed points for F_μ^2 appear as μ increases through 3. These are periodic points of period two, created in the bifurcation. Moreover, as μ increases further, there is a period-doubling cascade as the period 2 orbit bifurcates into period 4 by period-doubling, followed by a further period-doubling into period 8, and so on.

(a)   (b)   (c)
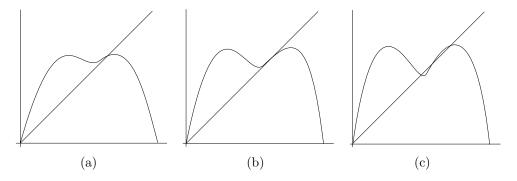
Figure 5.3: The graphs of $F_\mu^2(x)$ where $F_\mu(x) = \mu x(1 - x)$ for (a) $\mu < 3$, (b) $\mu = 3$, and (c) $\mu > 3$.

It is obvious that, if F is an affine map, (i) of Theorem 5.2.1 is not satisfied, not only at a fixed point, but in the whole region of definition. Thus the bifurcation as the derivative F' equal to -1 for linear maps does not lead to the creation of an orbit of double period. For example, let $F(x) = \alpha x + \epsilon$, then at $\alpha = -1$ any point $x \in \mathbb{R}$, except for the fixed point $p = \epsilon/(1 - \alpha)$, is periodic of period 2, while for $\alpha < -1$ the trajectory of any point $x \neq p$ tend to infinity. So, for affine maps in bifurcation with eigenvalue equal to -1, there are infinitely many period 2 orbits at the bifurcation value, and it gives rather trivial results after the bifurcation. If we have a piecewise affine map (or piecewise smooth map, with components not necessarily all affine), however, the same bifurcation may occur, at fixed points or periodic orbits, when the eigenvalue equals -1. In this case what occurs after the bifurcation is not necessarily trivial. Depending on other components of the map, it can give rise to rather complicated dynamics. Sushko and Gardini [83] defined the following:

Definition 5.2.2. *Let $F_\mu : \mathbb{R} \to \mathbb{R}$ be a family of piecewise C^3-smooth maps depending smoothly on the parameter μ. Let p_μ be a fixed point of F_μ, $\delta > 0$ be such that for $\mu \in (\mu_0 - \delta, \mu_0 + \delta)$ the fixed point does not coincide with a switching point of F_μ*

and $F'_{\mu_0}(p_{\mu_0}) = -1$. At $\mu = \mu_0$ a degenerate flip bifurcation occurs if

(i) $SF_{\mu_0}(x) = 0$ for all x in a neighbourhood of p_{μ_0}, where $SF = (F'''/F') - (3/2)(F''/F')^2$ is the Schwarzian derivative of F; and

(ii) $(d/d\mu)F'_{\mu_0}(p_{\mu_0}) \neq 0$.

In other words, a fixed point (or a periodic orbit) of a piecewise smooth map undergoes a degenerate flip bifurcation when the fixed point does not coincide with any switching point of F_μ, the eigenvalue crosses -1 as μ crosses μ_0 and at the bifurcation value the map F_μ (or F_μ^k for periodic orbit of period k) is locally affine (in some neighbourhood of the fixed point). This means that at the bifurcation value the map has locally (in some neighbourhood of the fixed point) infinitely many period 2 orbits.

From the example above, suppose we now have

$$F(x) = \begin{cases} \alpha x + \epsilon, & x \leq 0, \\ \beta x + \epsilon, & x \geq 0, \end{cases}$$

where α and β have opposite signs, so F is a skew-tent map. Suppose that $\epsilon < 0$, then at $\alpha = -1$ every point in the interval $[\epsilon, 0]$ except the fixed point $p = \epsilon/(1 - \alpha) < 0$ is period 2 orbit, points in $x < \epsilon$ are mapped to $x > 0$ and do not have period 2. The difference between this and the trivial example above is that at the bifurcation value, one of the period 2 orbits created coincides with the switching point $x = 0$, so there is a border collision at this degenerate flip bifurcation. It has been shown in [64] that the degenerate flip bifurcation of an attracting period k orbit, $k \geq 3$, of the skew-tent map leads to $2k$ cyclical chaotic intervals. The degenerate flip bifurcation of a period 2 orbit leads to 2^i cyclical chaotic intervals, where $i \geq 2$ can be any integer depending on parameters. A fixed point that undergoes a degenerate period doubling bifurcation can have a period doubling, or it can lead to 2^i periodic chaotic intervals, $i \geq 1$.
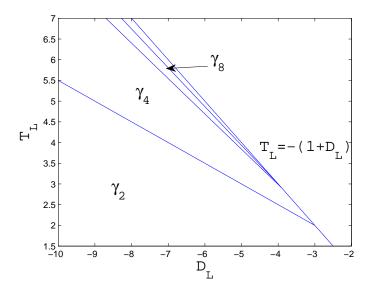
Figure 5.4: Degenerate flip bifurcations. Regions γ_i for $i = 2, 4, 8$ in the (D_L, T_L) space where period i orbit exists at $T_R = 2$ and $D_R = 2$ are shown.

The idea of degenerate bifurcation can be extended to higher dimensional systems. It has been shown in [63, 83] that in the two-dimensional border collision normal form a degenerate flip bifurcation of a stable fixed point $\mathbf{x}_*^R$ (while $\mathbf{x}_*^L$ is also stable but virtual) can lead to similar results: a period-doubling to a stable period 2 orbit, or to a 2^i cyclic chaotic attractor for any $i \geq 1$; while the degenerate flip bifurcation of an attracting period 2 orbit can lead to a 2^i cyclical chaotic attractor for $i \geq 2$. However, in the parameter region that we are interested in, where the fixed point $\mathbf{x}_*^R$ is an unstable spiral in R and $\mathbf{x}_*^L$ is admissible in L, $\mathbf{x}_*^L$ is unstable. The fixed point changes from a saddle to an unstable node as (D_L, T_L) crosses the line $T_L = -(1 + D_L)$, where one of the eigenvalues of the fixed point, s_-, equals to -1. When $T_L = -(1 + D_L)$, the line of the eigenvector through $\mathbf{x}_*^L$ is $y = D_L(x - x_*^L) + y_*^L$, which intersects the axes at S and S'. Every point on this segment SS' except the fixed point has period 2. This bifurcation creates a period 2 orbit which has eigenvalues

$$s_{2\pm} = \frac{1}{2}(T_L T_R - D_L - D_R \pm \sqrt{(T_L T_R - D_L - D_R)^2 - 4D_L D_R}).$$

So, depending on the parameter values, this orbit can undergo further degenerate flip bifurcation as one of the eigenvalues is equal to -1. Calculations show that $s_{2+} = -1$

(and $s_{2-} > 1$) when $T_L T_R = -(1 - D_L)(1 - D_R)$. This bifurcation creates a period 4 orbit, where one of the points is in R and the rest in L. The period-doubling cascade can go on depending on the four parameters. We shall not go into detail here, but we give an example in Figure 5.4.

Thus, the bifurcation of the fixed point $\mathbf{x}_*^L$ is similar to the stable case described in [83], but the instability makes it impossible to observe the results numerically. By continuity, this degenerate flip bifurcation of the saddle $\mathbf{x}_*^L$ does not affect the stability of the attracting set contained inside (if it exists), but it changes the shape of the basin of attraction. As described at the beginning of the chapter, if $\mathbf{x}_*^L$ is an admissible saddle, by considering the stable manifold and its preimages, we get a polygonal basin of attraction for the attracting set if it exists. After the degenerate flip bifurcation, the fixed point becomes a repeller and new unstable orbits are created, hence the dynamics around these orbits complicates the geometry of the basin boundary. See Figure 5.5.

Apart from degenerate flip bifurcations, Sushko and Gardini [83] also defined degenerate fold bifurcations and centre bifurcations as analogies with the fold bifurcations and Neimark-Sacker bifurcations for the smooth maps. These also occur in the border collision normal form map at various parameter values [82, 83].

5.3 Example revisited

Recall the example of a border collision normal form that we presented in the previous chapter from [33] again (see Figure 5.6). As the parameters change from Figure 5.6 (a) to (f), a number of local and global bifurcations take place.

Figure 5.6 (a) shows that there is a stable period 13 orbit. The numerics show that the orbit is of the form $R^9 L^4$, in other words the induced map $F_L^4 F_R^9$ has a stable fixed point with the parameters given. By direct calculations, the eigenvalues of $A_L^4 A_R^9$ at the fixed point are a pair of complex conjugates with modulus less than 1, while the fixed point $\mathbf{x}_*^R$ is an unstable spiral. As the eigenvalues of this period 13
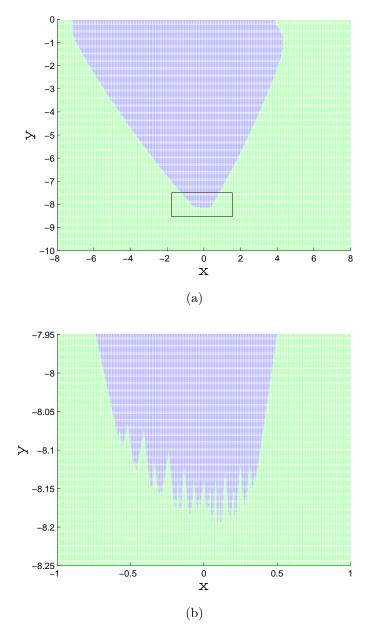
(a)

(b)

Figure 5.5: (a) Basin of attraction (blue) when $\mathbf{x}_*^L$ is a admissible repeller, (b) enlargement of the region indicated. $T_L = 0.1, D_L = -1.2, T_R = 0, D_R = 2$.
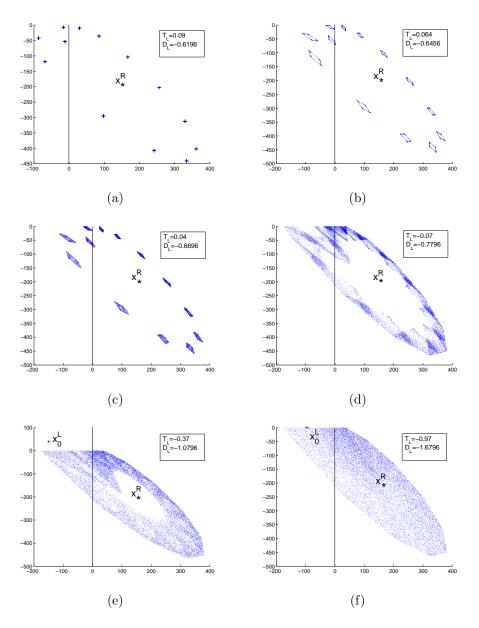
Figure 5.6: Attractors in border collision normal form for various parameter values. $T_R = 1.93, D_R = 1.2204, \mu = 38.36$.

orbit cross the unit circle, the orbit loses its stability and a new attractor is formed in a centre bifurcation mentioned above - a piecewise smooth analogy to the Neimark-Sacker bifurcation. As shown in Figure 5.6 (b) the attractor is a cyclic annular chaotic area, the hole in each part of the attractor contains the periodic point which becomes unstable after the bifurcation.

The bifurcation from Figure 5.6 (b) to (c) is effectively the same as the one from Figure 5.6 (e) to (f), which is a bifurcation from an annular chaotic region to a simply connected attractor. Note that in Figure 5.6 (e) and (f), the outside boundary of the attractor is the polygon formed in the way described before, using the images of the switching surface, and in Figure 5.6 (e) the attractor has a hole which contains the fixed point $\mathbf{x}_*^R$. The fixed point has a preimage $\mathbf{x}_0^L$ in L above the x-axis, and since both L and R are mapped to the bottom half plane, $\mathbf{x}_0^L$ has no preimage, and hence $\mathbf{x}_*^R$ is not a snap-back repeller (see Chapter 3). On the other hand, when $T_L \approx -0.97$ and $D_L \approx -1.6796$, $\mathbf{x}_0^L$ is on the x-axis in L, on the external boundary of the attractor, therefore $\mathbf{x}_*^R$ is contained in the attractor, i.e. the hole disappears, and the attractor becomes a simply connected region.

Lemma 5.3.1. *Let V be a polygonal set constructed as described in Chapter 4 and let V be an attractor. Suppose that V intersects the switching surface, so that $V \cap L$ and $V \cap R$ are non-empty. Let Q be a fixed point and suppose that Q has a preimage $Q_{-1} \neq Q$. Then $Q \in V$ if and only if $Q_{-1} \in V$.*

The proof is almost immediate. Indeed, if $Q_{-1} \in V$, then clearly $Q \in V$ since V maps to itself. Conversely if $Q \in V$, then note that by the construction of V, $F(V \cap R) = V$, thus if $Q \in V \cap L \subset V$, then $Q_{-1} \in V \cap R$. Note also that since V is the attractor, $V = \cup_i F^i(V \cap L)$. If $Q \in V \cap R$, then there exist some $k \geq 1$ such that $Q \in F^k(V \cap L)$, hence there exists some $P \in V \cap L$ such that $F^k(P) = Q$ (and so $F^{k-1}(P) = Q_{-1}$). Then $F(P), \ldots, F^{k-2}(P), Q_{-1}$ are contained in V. Moreover, since $F|_R$ is affine, and Q is already a preimage of Q in R, $Q_{-1} \in V \cap L$.

For the same reasons, V contains a sequence of preimages of Q_{-1}. If Q is repelling

and the sequence of preimages exists and tends toward Q, then the fixed point is a snap-back repeller. When Q_{-1} meets the boundary of the attractor ∂V, a hole containing Q is created inside V and V becomes an annular region. This bifurcation destroys the snap-back repeller and is a snap-back repeller bifurcation [33, 34, 67] (see also Chapter 3). The bifurcation from Figure 5.6 (e) to (f) is a snap-back repeller bifurcation. The bifurcation from Figure 5.6 (b) to (c) is also a snap-back repeller bifurcation but relative to the 13th iterate of the map instead of F itself.

Finally, from Figure 5.6 (c) to (d), the attractor changes from a cyclic chaotic area to a connected chaotic area. This is a boundary crisis we mentioned above that some boundary of the attractor meets the basin boundary, so that after the bifurcation points originally from the cyclic parts eventually map out of the area in a transient, and thus destroy the cyclic chaotic area.

5.4 Some bifurcations of the invariant polygons

So far we have been using the invariant polygons constructed by images of the switching surface, and we show that these polygons often attract orbits. In the example from the previous section, the attractors are either subsets of the polygon (Figure 5.6 (a) to (e)) or the polygon itself (Figure 5.6 (f)). In this section we look at these polygons in more detail.

Recall from the previous chapter, we use the origin and its image $P_1 = F(O)$, and consider successive images of the line segment OP_1, P_1P_2, P_2P_3 and so on. We assume that there exist a finite N such that $P_kP_{k+1} \in R$ for $k = 1, \ldots, N-1$ and P_NP_{N+1} intersects the switching surface, at Q_0. Then the polygon $V = P_1P_2 \ldots P_{N+1}Q_1$ is an $(N+2)$-sided polygon such that $F(V_R) = V$ where $V_R = V \cap R$. Note that the polygon V is determined by T_R and D_R only, and the invariant set depends on the images of $V_L = V \cap L$. If there exists $M \geq 0$ such that $F^M(V) = F^{M+1}(V)$ then $F^M(V)$ is invariant, in particular if P_{N+1} and Q_1 are mapped inside V, so that $F(V_L) \subseteq V$ then V is invariant in F. The number of sides of V is $N + 2$ if $P_k \in R$ for $k = 1, \ldots, N$
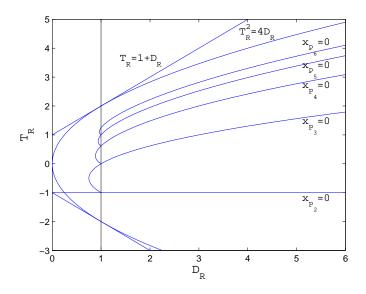
Figure 5.7: For each $n \geq 2$ P_n is on the y-axis when (D_R, T_R) is on the curve $x_{P_n} = 0$.

and $P_{N+1} \in L$, so this number changes when P_N meets the switching surface for each N. We can write down conditions for these changes, $x_{P_k} > 0$ for $k = 1, \ldots, n-1$ and $x_{P_n} = 0$ where x_{P_k} is the x-coordinate of P_k. These conditions depend on T_R and D_R only and they define a family of curves in the (D_R, T_R) parameter space. We have given the conditions in Example 2 from the previous chapter. Suppose that the fixed point $\mathbf{x}_*^R$ is an admissible spiral with complex conjugate eigenvalues $re^{\pm i\theta}, r > 0, 0 < \theta < \pi$, where $T_R = 2r\cos\theta$ and $D_R = r^2$, then P_n has $x = 0$ if

$$r^{n+1}\sin(n\theta) - r^n\sin(n+1)\theta + \sin\theta = 0, \qquad \sin\theta \neq 0. \tag{5.1}$$

These curves, in terms of T_R and D_R, are illustrated in Figure 5.7.

Remark 1: At $D_R = 1$, i.e. $r = 1$, the equation (5.1) for each $n \geq 3$ has two obvious roots, $\theta = 2\pi/(n+1)$ and $\theta = 2\pi/n$. (When $n = 2$, one of the roots $\theta = \pi$ is not allowed.) Hence adjacent curves in the figure intersect at $D_R = 1$. This means that for each n, at the intersection point both P_n and P_{n+1} are on the y-axis, and this is only possible if P_{n+1} is the origin and P_n is the preimage of the origin $(0, -1)^T$. Thus the orbit $O, P_1, \ldots, P_n$ is periodic with period $n + 1$, and $V \subset R$. Note that when $D_R = 1$, $\mathbf{x}_*^R$ is a centre.

Remark 2: At $\theta = 2\pi/(n+1)$, since $\sin n\theta = -\sin\theta$, $r^{n+1}\sin n\theta - r^n\sin(n+1)\theta + \sin\theta < 0$ for all $r > 1$; and at $\theta = \pi/n$, $r^{n+1}\sin n\theta - r^n\sin(n+1)\theta + \sin\theta > 0$ for all $r > 1$. So for any $r > 1$, the root of (5.1) has $\pi/n < \theta < 2\pi/(n+1)$ for each n. Therefore for any $r > 1$, as $n \to \infty$, $\theta \to 0$ and thus the curves $x_{P_n} = 0$ in $D_R > 1$ converge to $T_R^2 = 4D_R$, where the fixed point $\mathbf{x}_*^R$ becomes a node with two real and equal eigenvalues. Also, $\theta = 2\pi/(n+1)$ when $r = 1$ for each $x_{P_n} = 0$, so θ converges to 0 with the rate $1/n$ and the curves converge with $1/n^2$.

Along each curve $x_{P_n} = 0$, the position of P_n is $(0, q_n)^T$, where

$$q_n = \frac{r^{n+1}\sin(n\theta)}{\sin\theta} = -1 + \frac{r^n\sin(n+1)\theta}{\sin\theta} \tag{5.2}$$

and $P_{n+1} = (1 + q_n, 0)^T$. Since for any $r > 1$, $\frac{\pi}{n} < \theta < \frac{2\pi}{n+1}$, $\sin(n+1)\theta$ is negative, hence $q_n < -1$ and $P_{n+1} \in L$. In this case, to show that V is invariant, we only need to check whether $P_{n+2} = F(P_{n+1})$ is inside the polygon V. $P_{n+2} = (T_L(1 + q_n) + 1, -D_L(1 + q_n))^T$, and note that, even though the position of P_{n+2} depends on q_n which is dependent of T_R and D_R, P_{n+2} lies on the straight line

$$y = -\frac{D_L}{T_L}(x - 1). \tag{5.3}$$

When $D_R = r^2 = 1$, $\theta = \frac{2\pi}{n+1}$, $P_{n+1} = O$ and so $P_{n+2} = P_1 = (1, 0)^T$ which is on (5.3). Given D_L and T_L, as we increase r along $x_{a_k} = 0$, a_{k+2} moves along (5.3), possibly monotonically (See Figure 5.8).

We want to show how the set V loses stability. Clearly, in the area expansion case that we have, invariant regions and attractors do not always exist.

Lemma 5.4.1. *If an invariant region exists, then*

$$1 \leq \frac{1}{|D_L|} + \frac{1}{|D_R|}$$

.
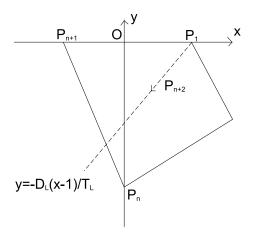
Figure 5.8: The path of P_{n+2} as D_R is increased along $x_{P_n} = 0$.

Proof. Suppose that an invariant region V exists, and V_L and V_R are the areas of the components of V in L and R respectively. Then the areas of their images are $|D_L|V_L$ and $|D_R|V_R$ and they satisfy

$$|D_L|V_L \leq V_L + V_R,$$

$$|D_R|V_R \leq V_L + V_R.$$

Multiply the first inequality by $|D_R|$ and the second by $|D_L|$ and add together gives

$$|D_L||D_R|(V_L + V_R) \leq (|D_L| + |D_R|)(V_L + V_R)$$

$$\Rightarrow \quad 1 \leq \frac{1}{|D_L|} + \frac{1}{|D_R|}.$$

$\square$

This is a very rough condition for D_α, nonetheless it shows that given any D_L the set loses stability if D_R is too large.

Lemma 5.4.2. *Suppose that $\mathbf{x}_*^L$ is an admissible saddle, then for each n, $V = P_1 \ldots P_{n+1}$ loses stability if P_{n+2} crosses the side $P_n P_{n+1}$.*

Proof. Suppose that the fixed point $\mathbf{x}_*^L$ exists in L and is a saddle, which requires $T_L > 1 + D_L$ and $T_L > -(1 + D_L)$, then it has eigenvalues $-1 < s_- < 0 < 1 < s_+$

and the local stable manifold of $\mathbf{x}_*^L$ is the line

$$y = -s_+ x + \frac{s_+ - D_L}{1 - T_L + D_L} \tag{5.4}$$

which has a negative slope.

If P_{n+2} is on (5.4) (note that now (5.3) has a positive slope since $T_L > 0$, $D_L < 0$), P_n and P_{n+1} also have to be on (5.4), so the line segment $P_n P_{n+1}$ coincides with (5.4). Also, P_{n+2} then lies between P_n and P_{n+1} and the images stay on this stable manifold converging to $\mathbf{x}_*^L$. On the other hand, if $\mathbf{x}_*^L$ is on the line $P_n P_{n+1}$, then the image $P_{n+1} P_{n+2}$ has to contain $\mathbf{x}_*^L P_{n+1}$ and so $P_{n+1} P_{n+2}$ is contained in $P_n P_{n+1}$ which coincide with (5.4). If q_n decreases further, P_{n+2} crosses the stable manifold of $\mathbf{x}_*^L$, then the images diverge to infinity. Therefore, given D_L and T_L, as we increase r along $x_{P_n} = 0$ (and hence changes q_n), if P_{n+2} leaves the polygon $V = P_1 P_2 \ldots P_{n+1}$ through the side $P_n P_{n+1}$, then V loses stability. $\square$

Next we want to show that there exist values of T_R and D_R for this to occur.

Lemma 5.4.3. *For each $n \geq 3$, there exists at least one (D_R, T_R) on the curve $x_{P_n} = 0$ where V loses stability. Moreover, these parameter values converge to $D_R = 1$ and $T_R = 2$ as $n \to \infty$.*

Proof. When P_{n+2} is on (5.4), P_n is the y-intercept of (5.4), i.e.

$$q_n = \frac{r^{n+1} \sin n\theta}{\sin \theta} = \frac{s_+ - D_L}{1 - T_L + D_L}. \tag{5.5}$$

Recall that $T_L = s_+ + s_-$ and $s_- < 0 < s_+$, so $\frac{s_+ - D_L}{1 - T_L + D_L} = -\frac{s_- - T_L + D_L}{1 - T_L + D_L} < -1$. When $r = 1$, $q_n = -1$. If we rewrite (5.1) as $r^n(r \sin n\theta - \sin(n+1)\theta) + \sin \theta = 0$, we can see for any given $n \geq 3$, as $r \to \infty$ along $x_{P_n} = 0$, $r \sin n\theta - \sin(n+1)\theta \to 0$ at the same time $\sin n\theta \to 0$, this means that $\theta \to \frac{\pi}{n}$. But $\sin(n+1)\frac{\pi}{n} \neq 0$, so for $r \sin n\theta - \sin(n+1)\theta$ to tend to 0, $\sin n\theta = O(r^{-1})$ as $r \to \infty$ so that $r \sin n\theta$ does not tend to 0. Recall again that $\sin n\theta < 0$ and $\sin \theta \neq 0$ since $\frac{\pi}{n} < \theta < \frac{2\pi}{n+1}$, then $\frac{r^{n+1} \sin n\theta}{\sin \theta} \to -\infty$ as $r \to \infty$ along $x_{P_n} = 0$. Therefore given any T_L and D_L and $n \geq 3$

there must exist at least one pair of parameters D_R and T_R on $x_{P_n} = 0$ where (5.5) holds and the polygon V loses stability.

For the second part of the lemma, we claim that for any $r > 1$, as $n \to \infty$, $q_n \to -\infty$. Suppose not, then as $n \to \infty$, $\sin n\theta$ must tend to 0 much quicker than $\sin \theta$ tending to 0 and r^{n+1} tending to infinity, which means $\theta \sim \frac{\pi}{n}$ as $n \to \infty$. But then $\sin(n+1)\theta \sim -\sin \frac{\pi}{n} \sim \frac{\pi}{n}$ and so $r \sin n\theta - \sin(n+1)\theta$ tends to 0 much slower than r^{-n} that we need in (5.1). Therefore as $n \to \infty$, $q_n \to -\infty$, hence the parameters D_R and T_R on each $x_{P_n} = 0$ where (5.5) holds for given D_L and T_L converge to $r = 1$ and $\theta = 0$, i.e. $D_R = 1$, $T_L = 2$, eventually. $\qquad\square$

Finally, we can show that Lemma 5.4.2 describes the only way the polygon V loses stability.

Proposition 5.4.4. *Suppose that $\mathbf{x}_*^L$ is an admissible saddle and $T_L \geq -D_L$, then along $x_{P_n} = 0$ for each $n \geq 3$, V is invariant and loses stability if and only if P_{n+2} crosses the boundary $P_n P_{n+1}$, when D_R and T_R satisfy (5.5).*

Proof. If $T_L \geq -D_L$, then the y-intercept of (5.3) $\frac{D_L}{T_L}$ is greater than or equal to -1. Since $q_n \leq -1$ along $x_{P_n} = 0$ for $r > 1$, $P_n = (0, q_n)^T$ is below $y = -1$ on the y-axis. Hence the path of P_{n+2} is always above the line $P_1 P_n$, and so P_{n+2} is contained in the polygon V until it meets the boundary $P_n P_{n+1}$. (See Figure 5.8) Therefore, given D_L and T_L as described, the $(n+1)$-sided polygon V is an invariant region, and it loses stability if an only if P_{n+2} is on the boundary $P_n P_{n+1}$, when D_R and T_R satisfy (5.5). $\qquad\square$

So far we have only considered the invariant set V along the curves (5.1), how does this set change as (D_R, T_R) moves across the curves?

Given some parameters D_L, T_L, D_R, T_R and n, so that $P_1, \ldots, P_{n-1} \in R$, P_n is on the critical line, $P_{n+1} \in L$ and P_{n+2} is contained in the polygon V so that it is an invariant region. If we move D_R and T_R across $x_{P_n} = 0$ in the parameter space, P_n moves across the switching surface from one side to another. Suppose that we
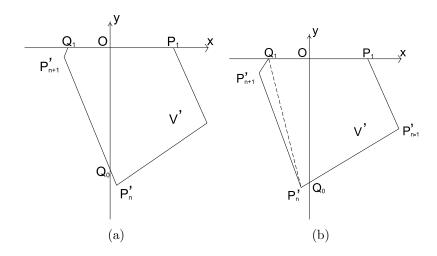
Figure 5.9: The perturbed invariant set V'.

perturb D_R and T_R slightly above the curve $x_{P_n} = 0$ so that the perturbed P'_n is in R, then the line segment joining P'_n and P'_{n+1} intersects the critical line at some point Q_0, which maps to the x-axis at Q_1. Since the map is smooth in the parameters and continuous in the variables, for small changes in the parameters, P'_n and Q_0 are close to the unperturbed position P_n, and the images P'_{n+1} and Q_1 are also close to P_{n+1}, so $Q_1 \in L$. Let V' be the perturbed, $(n+2)$-sided polygon $P'_1 P'_2 \ldots P'_{n+1} Q_1$. (Figure 5.9(a)) Since $P_{n+2} \in int(V)$, for small perturbations, $P_{n+2} \in int(V')$, hence by continuity again P'_{n+1} and Q_1 map to the interior of V' close to P_{n+2}. Therefore V' maps to itself again and the absorbing region is stable.

On the other hand, if the parameters are perturbed so that $P'_n \in L$, then Q_0 is the intersection of the line segment joining P'_{n-1} and P'_n at the critical line. This time, we let $V'_R = OP'_1 \ldots P'_{n-1} Q_0 \subset R$, then $F(V'_R)$ is the polygon $P'_1 P'_2 \ldots P'_n Q_1$. By continuity as before, P'_{n+1} and Q_1 map to the interior of $F(V'_R)$, but note that P'_{n+1} and hence the line segments $P'_{n+1} P'_n$ and $P'_{n+1} Q_1$ are not necessarily contained in $F(V'_R)$. In which case, $F(V'_R)$ maps to $F^2(V'_R) = P'_1 \ldots P'_{n+1} Q_1$ which has $n+2$ sides. (Figure 5.9(b)) $V' = F^2(V'_R)$ then maps to itself and is an invariant region again. If $P'_{n+1} \in F(V'_R)$, then the $(n+1)$-sided polygon $F(V'_R)$ is invariant.

Therefore when $P_1, \ldots, P_{n-1} \in R$, P_n is on the critical line, and P_{n+2} is contained inside the invariant polygon V, then it persists under small perturbations in parameters, along and across the curve $x_{P_n} = 0$. As P_n moves across the critical line from

left to right, the number of sides of the polygon either changes (continuously) from $n + 1$ to $n + 2$, or from $n + 2$ to $n + 1$ to $n + 2$, depending on the position of P_{n+1} when $P_n \in L$.

Chapter 6

An Example: Coupled Systems and Synchronization

In previous chapters we discussed some bifurcation phenomena that occur in piecewise smooth systems, in this chapter we study a particular example which the system is coupled by a piecewise smooth map, and use the theory of border collision bifurcations to explain some of the phenomena first addressed in [73].

6.1   Introduction

Synchronization in coupled dynamical systems and stability of synchronized states have been studied for some time. Many of the examples considered are two-dimensional and involve coupling identical nonlinear systems.

Pikovsky and Grassberger [73] introduced the system

$$
\begin{aligned}
x_{n+1} &= (1 - \epsilon)f_a(x_n) + \epsilon f_a(y_n) \\
y_{n+1} &= \epsilon f_a(x_n) + (1 - \epsilon)f_a(y_n)
\end{aligned}
\tag{6.1}
$$

where $\epsilon \in [0, \frac{1}{2}]$ and $f_a : \mathbb{R} \to \mathbb{R}$ is the skew-tent map

$$f_a(z) = \begin{cases} az & \text{if } z \le a^{-1} \\ \frac{a}{a-1}(1-z) & \text{if } z > a^{-1} \end{cases} \qquad a > 1. \qquad (6.2)$$

This system then has two switching surfaces $x = a^{-1}$ and $y = a^{-1}$.

First note that the unit square $S = [0, 1]^2$ is invariant under (6.1) and (6.2), and henceforth all remarks will be confined to the map restricted to S. The system has a synchronized state in which $x_n = y_n$ for all $n \in \mathbb{N}$, and if $(x_n, y_n)^T = (z_n, z_n)^T$ then $(x_{n+1}, y_{n+1})^T = (f_a(z_n), f_a(z_n))^T$, which geometrically corresponds to motion on the diagonal in $\mathbb{R}^2$, and is governed by the one-dimensional skew-tent map f_a. When $\epsilon = \frac{1}{2}$, then given any starting position $(x_0, y_0)^T$, $x_1 = y_1 = \frac{1}{2}(f_a(x_0) + f_a(y_0))$, so every orbit is mapped to the synchronized state. If a is regarded as fixed, then as ϵ decreases, some orbits in the synchronized state lose stability in the transverse direction although, typical, synchronized orbits remain transversely stable. In other words, the synchronized state loses asymptotic stability and becomes a Milnor attractor (see below) which attracts almost all orbits. As ϵ decreases further the typical orbits in the synchronized state lose stability in the transverse direction through a blowout bifurcation, and finally all synchronized orbits become transversely unstable [73, 3, 48]. In this system it is possible to explicitly determine the bifurcation values and the transverse stability of any periodic orbit in the synchronized state. It is therefore a good example to use in exploring synchronization in coupled systems. Glendinning [40] showed that, for appropriate choices of a, between the parameters of ϵ which the first synchronized orbit loses transverse stability and the blowout bifurcation, where the synchronized state is a Milnor attractor, there is a larger invariant set, containing the synchronized state, which is transitive and where periodic orbits are dense. Moreover, this set becomes the attractor of almost all orbits after the blowout bifurcation.

Recall that a set A is a Milnor attractor if its basin of attraction $B(A)$ has non-zero Lebesgue measure and there is no compact proper subset A' of A whose basin coincides with $B(A)$ up to a set of zero measure. So, even though $B(A)$ may contain no neighbourhood of A, an initial condition taken in a small neighbourhood of A still has a positive probability of being attracted to A.

In this example, there are two switching surfaces and they intersect each other. One would expect the dynamics to be more complicated than when there is only one switching surface. We observe that, as ϵ varies, fixed points or periodic orbits in the system (6.1) and (6.2) may cross or collide the switching surfaces $x = a^{-1}$ or $y = a^{-1}$, and various bifurcations occur. Our aim here is to study the change in the geometry of the topological attractors as the synchronized state loses asymptotic stability, in particular the creation of non-synchronized periodic orbits.

6.2 Blowout bifurcations

Suppose that we have a dynamical system $X_{n+1} = F(X_n), F : \mathbb{R}^m \to \mathbb{R}^m$ with parameter $\nu \in \mathbb{R}$, such that a linear subspace $N \subset \mathbb{R}^m$ is invariant under the map for all $\nu \in \mathbb{R}$. Suppose that A is an attractor contained in N for $\nu < 0$. If A loses stability in the direction transverse to N for $\nu > 0$ and ceases to be an attractor, we say it undergoes a blowout bifurcation at $\nu = 0$. If there are no nearby attractors after the blowout the bifurcation is subcritical, and supercritical if there are attractors that branch from A for $\nu > 0$. Such a bifurcation occurs when the average Lyapunov exponent changes sign. In the system (6.1) and (6.2), it is possible to compute the Lyapunov exponents explicitly and hence all the bifurcation values. As pointed out earlier, the dynamics of a synchronized orbit $x_n = y_n$ may be described by the dynamics of points under the one-dimensional map $z_{n+1} = f_a(z_n)$. The form of the coupling between the maps means that the stability of a synchronized state in the system can be determined from the stability of the corresponding one-dimensional map [28, 86, 29, 30, 31, 38].

Let $z \in [0, 1]$, then the Lyapunov exponent of z under iteration of f_a is the limit

$$\lambda(z) = \lim_{n \to \infty} \frac{1}{n} \sum_{k=0}^{n-1} \log |f_a'(f_a^k(z))| \tag{6.3}$$

provided the limit exists. From Birkhoff's ergodic theorem, if $\mathcal{A}$ is a uniquely ergodic invariant set with invariant measure m, then the Lyapunov exponent of $\mathcal{A}$ is

$$\lambda(\mathcal{A}) = \frac{1}{m(\mathcal{A})} \int_{\mathcal{A}} \log |f_a'(x)| \mathrm{d}m. \tag{6.4}$$

That means, for almost all initial conditions in $\mathcal{A}$, the Lyapunov exponent defined by (6.3) exists and has the value of $\lambda(\mathcal{A})$. From [40], the unit interval $\mathcal{I} = [0, 1]$ is indeed uniquely ergodic and the invariant measure is a Lebesgue measure, furthermore,

$$\lambda(\mathcal{I}) = \log a - (1 - a^{-1}) \log(a - 1). \tag{6.5}$$

In the full two-dimensional system (6.1) and (6.2), the Jacobian matrix has eigenvectors $(1, 1)^T$ and $(1, -1)^T$, which correspond to the synchronized direction and the transverse direction respectively, and the eigenvalues are of the form μ and $(1 - 2\epsilon)\mu$. Therefore a synchronized orbit has two Lyapunov exponents: one, in the synchronized direction, is the Lyapunov exponent under the one-dimensional map f_a. The second one is in the transverse direction,

$$\lambda_\perp(z) = \log |1 - 2\epsilon| + \lambda(z) \tag{6.6}$$

provided $\lambda(z)$ exists. From (6.5) and (6.6) we also obtain $\lambda_\perp(\mathcal{I}) = \log |1 - 2\epsilon| + \lambda(\mathcal{I})$. For $a > 1$, $\lambda(\mathcal{I}) > 0$, thus there are values of ϵ at which $\lambda_\perp(\mathcal{I})$ is positive, which means that the synchronized state is unstable in the transverse direction. We therefore

obtain the blowout bifurcation value where $\lambda_\perp$ changes sign. Let

$$\epsilon_b = \frac{1}{2}(1 - e^{-\lambda(\mathcal{I})})$$

$$= \frac{1}{2}(1 - \frac{(a-1)^{\frac{a-1}{a}}}{a}), \tag{6.7}$$

then the blowout bifurcation occurs as ϵ is reduced through ϵ_b. Note that (6.5) holds only for almost all points. For infinitely many other orbits, in particular for any periodic orbit, the limit in (6.3) also exists, but their values are different from (6.5). For example, consider the fixed points $z = 0$ and $z = \frac{a}{2a-1}$, we have $\lambda(z) = \log a$ and $\lambda(z) = \log \frac{a}{a-1}$ respectively. Also, from (6.3) and (6.6), it is easy to see the bifurcation value at which a synchronized periodic orbit of the full two-dimensional system loses transverse stability. The two fixed points $(0,0)$ and $(\frac{a}{2a-1}, \frac{a}{2a-1})$ become transversely unstable as ϵ is decreased through $\frac{a-1}{2a}$ and $\frac{1}{2a}$ respectively. Since $|f_a'|$ takes either the value a or $\frac{a}{a-1}$, for $a > 1$, $\lambda(z) = \log a$ and $\lambda(z) = \log \frac{a}{a-1}$ are in fact the minimum and the maximum values of the Lyapunov exponent (if $1 < a < 2$ then $\lambda(z) = \log \frac{a}{a-1}$ is maximum, minimum if $a > 2$). Therefore $\epsilon = \frac{a-1}{2a}$ and $\epsilon = \frac{1}{2a}$ are the values of ϵ where the first and the last synchronized orbits lose their transverse stability. The following lemma then comes from [39, 48].

Lemma 6.2.1. *Let* $(\alpha_1, \alpha_2) = (\frac{a-1}{2a}, \frac{1}{2a})$ *if* $a \in (1, 2)$ *and* $(\alpha_1, \alpha_2) = (\frac{1}{2a}, \frac{a-1}{2a})$ *if* $a > 2$. *If* $a > 1$ *and* $a \neq 2$ *then*

(a) if $\epsilon \in (\alpha_2, \frac{1}{2})$ *then the synchronized state is asymptotically stable;*

(b) if $\epsilon \in (\epsilon_b, \alpha_2)$ *then at least some of the synchronized orbits are transversely unstable, but the synchronized state is transversely stable;*

(c) if $\epsilon \in (\alpha_1, \epsilon_b)$ *then at least some of the synchronized orbits are transversely stable, but the synchronized state is transversely unstable;*

(d) if $\epsilon \in (0, \alpha_1)$ *then all synchronized orbits are transversely unstable.*

Recall that the unit square $S = [0,1]^2$ is invariant under (6.1) and (6.2), the critical lines $x = a^{-1}$ and $y = a^{-1}$ divide the square into four regions in which the

map is affine, and so given two points in the same region, the line between them is mapped to the line connecting their images. For convenience we shall give these four regions names (Figure 6.1):

$$S_1 = \{(x, y) \in S \mid x \leq a^{-1}, y \leq a^{-1}\}$$

$$S_2 = \{(x, y) \in S \mid x \leq a^{-1}, y \geq a^{-1}\}$$

$$S_3 = \{(x, y) \in S \mid x \geq a^{-1}, y \leq a^{-1}\}$$

$$S_4 = \{(x, y) \in S \mid x \geq a^{-1}, y \geq a^{-1}\}.$$
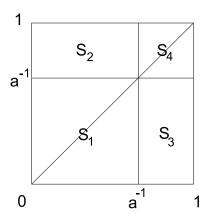
Figure 6.1: The unit square S is divided into four regions by the critical lines.

Lemma 6.2.2. *Let $a < 2$ and $\frac{1}{2a} < \epsilon < \frac{1}{2}$, (Lemma 6.2.1 (a) with $a < 2$) all orbits are attracted to the diagonal.*

Proof. Given a starting point $(x_0, y_0) \in S$, by considering the limit of $|x_n - y_n|$, we want to show that this tends to 0 as $n \to \infty$ and hence the result.

Since

$$x_{n+1} = (1 - \epsilon)f_a(x_n) + \epsilon f_a(y_n)$$

$$y_{n+1} = \epsilon f_a(x_n) + (1 - \epsilon)f_a(y_n),$$

given (x_0, y_0), we have

$$|x_1 - y_1| = (1 - 2\epsilon)|f_a(x_0) - f_a(y_0)| \leq (1 - 2\epsilon).$$

Hence all points in S after one iteration are bounded between the line $ABCD$ and its reflection $A'B'C'D'$ in the diagonal, as shown in Figure 6.2, where $A = (0, 1 - 2\epsilon)$, $B = (a^{-1} - (1 - 2\epsilon), a^{-1})$, $C = (a^{-1}, a^{-1} + (1 - 2\epsilon))$ and $D = (1 - (1 - 2\epsilon), 1)$. Since the map is affine in each region, a line segment in a region is mapped to another line segment. Therefore the image of any point P between $ABCD$ and $A'B'C'D'$ is closer to the diagonal than the image of any point on one of the line segments AB, BC and CD which is in the same region as P. Hence we can get the maximum value of $|x_2 - y_2|$ by considering the images of A, B, C and D.
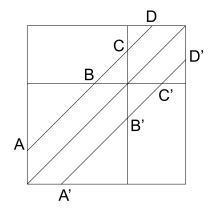
Figure 6.2: The image of any point in S is bounded between the line $ABCD$ and its reflection in the diagonal.

- $A = (0, 1 - 2\epsilon)$, $B = (a^{-1} - (1 - 2\epsilon), a^{-1})$

$$|x_2 - y_2| = (1 - 2\epsilon)|f_a(x_1) - f_a(y_1)|$$
$$= (1 - 2\epsilon)^2 a$$
$$\leq (1 - 2\epsilon)^2 \frac{a}{a - 1} \qquad \text{since } a < 2.$$

A and B have the same value of $|x_2 - y_2|$, and so is every point on AB.

- $C = (a^{-1}, a^{-1} + (1 - 2\epsilon))$, $D = (1 - (1 - 2\epsilon), 1)$

$$|x_2 - y_2| = (1 - 2\epsilon)|f_a(x_1) - f_a(y_1)|$$
$$= (1 - 2\epsilon)^2 \frac{a}{a - 1}$$

Again, every point on CD has the same value of $|x_2 - y_2|$.

For points on BC, the value of $|x_2 - y_2|$ is bounded between $(1-2\epsilon)^2 a$ and $(1-2\epsilon)^2 \frac{a}{a-1}$. Therefore $|x_2 - y_2| \leq (1 - 2\epsilon)^2 \frac{a}{a-1}$. By repeating the same argument inductively, $|x_{n+1} - y_{n+1}| \leq (1-2\epsilon)((1-2\epsilon)\frac{a}{a-1})^n$. For $\epsilon > \frac{1}{2a}$, $(1-2\epsilon)\frac{a}{a-1} < 1$. Hence $|x_n - y_n| \to 0$ as $n \to \infty$. Thus every orbit synchronizes. $\square$

Corollary 6.2.3. *Let $a < 2$, and $\epsilon > \frac{1}{2a}$. If (x, y) is a periodic point then $x = y$. i.e. periodic orbits only exist on the diagonal.*

From now on we will focus on periodic orbits, each of which has its own bifurcation value. The main question comes from the following theorem [40].

Theorem 6.2.4 ([40]). *Let $a \in (\frac{1}{2}(1 + \sqrt{5}), 2)$ and let $O = (0, 0)$, $I = (1, 1)$, $R = (2\epsilon, \frac{1-2\epsilon+2\epsilon^2}{1-\epsilon})$ and $R' = (\frac{1-2\epsilon+2\epsilon^2}{1-\epsilon}, 2\epsilon)$. (See Figure 6.3) If $\mathcal{D}$ is the filled in quadrilateral $ORIR'$ and if $\epsilon \in (\epsilon_b, \frac{1}{2a})$ then*

(i) F is transitive on $\mathcal{D}$ (i.e. there is a dense orbit in $\mathcal{D}$); and

(ii) periodic points are dense in $\mathcal{D}$.
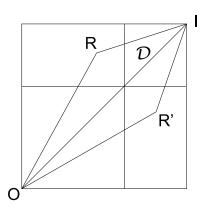
Figure 6.3: For $\epsilon < \frac{1}{2a}$, there is a two-dimensional region where a dense orbit exists.

We have shown that for $\epsilon > \frac{1}{2a}$, periodic orbits only exist on the diagonal, but as soon as ϵ decrease through $\frac{1}{2a}$, off-diagonal periodic orbits are created and there is a two-dimensional region in which these periodic points are dense. By direct calculation, the area of the quadrilateral $\mathcal{D}$ is $(1 - 2\epsilon)^2$. As ϵ tends to $\frac{1}{2a}$ from below,
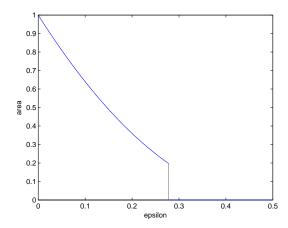
Figure 6.4: At $\epsilon = \frac{1}{2a}$, there is a discontinuous change in the area of the topological attractors. $(a = 1.8)$

this area tends to a non-zero value $(1 - a^{-1})^2$. As shown in Figure 6.4 there is a discontinuous change in the area of the topological attractors as the synchronized state loses asymptotic stability. In the following section we try to explain this sudden change using what we have done on border collision bifurcations. In particular, we show that new off-diagonal periodic orbits (infinitely many in fact) are created in degenerate bifurcations and border collision bifurcations, and it is these orbits and their preimages that fill the two-dimensional region.

6.3 Border collision bifurcations

For our example (6.1) and (6.2), let's take $a \in (\frac{1}{2}(1 + \sqrt{5}), 2)$. Recall that we can label the four regions in S separated by the critical lines $x = a^{-1}$ and $y = a^{-1}$ as $S_i, i = 1, 2, 3, 4$. Then we can rewrite the system as $X_{n+1} = F(X_n)$ where $F(X) =$

$A_i X + b_i$ and

$$
F(X) = \begin{cases}
a \begin{pmatrix} 1-\epsilon & \epsilon \\ \epsilon & 1-\epsilon \end{pmatrix} X & X \in S_1 \\[3ex]
a \begin{pmatrix} 1-\epsilon & -\frac{\epsilon}{a-1} \\ \epsilon & -\frac{1-\epsilon}{a-1} \end{pmatrix} X + \frac{a}{a-1} \begin{pmatrix} \epsilon \\ 1-\epsilon \end{pmatrix} & X \in S_2 \\[3ex]
a \begin{pmatrix} -\frac{1-\epsilon}{a-1} & \epsilon \\ -\frac{\epsilon}{a-1} & 1-\epsilon \end{pmatrix} X + \frac{a}{a-1} \begin{pmatrix} 1-\epsilon \\ \epsilon \end{pmatrix} & X \in S_3 \\[3ex]
-\frac{a}{a-1} \begin{pmatrix} 1-\epsilon & \epsilon \\ \epsilon & 1-\epsilon \end{pmatrix} X + \frac{a}{a-1} \begin{pmatrix} 1 \\ 1 \end{pmatrix} & X \in S_4
\end{cases}
\tag{6.8}
$$

The dynamics of the system can also be described using symbolic representation, as for one-dimensional maps. We define the itinerary of each X as $k(X) = c_0 c_1 \ldots$ where $c_0 = j$ if $X \in S_j$ and $c_i = j$ if $F^i(X) \in S_j$, $j = 1, 2, 3, 4$. So we have an infinite sequence of $1, 2, 3$ and 4 corresponding to each orbit of X. Clearly if we have a periodic orbit, the corresponding itinerary is also periodic. On the other hand, given a periodic code of period n, say, the corresponding periodic orbit X_n, if it exists, is obtained by solving the linear equation $X = F^n(X) = AX + b$ for some A and b. Hence, if A has no eigenvalues equal to 1 or -1, then there exists at most one periodic orbit with that code. For example, if the corresponding Jacobian matrix has no eigenvalues equal to 1 or -1, a periodic orbit that involves only S_1 and S_4 must be the one in the synchronized state, which is the diagonal. If not, suppose that X is a point in the orbit, then by the symmetry of the map for x and y, its reflection in the diagonal X' is also a periodic point with the same period and the same code as X. Moreover, since the map is affine in each region, every point in the line segment XX' is periodic with the same period and the same code. This violates the fact that there is at most one periodic orbit with the same code, unless $X = X'$, which means that X is on the diagonal.

For convenience, we shall refer to periodic orbits in the form of $\{4\}$ (a fixed point

in S_4), $\{24\}$ (a period 2 orbit from S_2 to S_4), $\{2324\}$ and $\{242442\}$ etc..

From Corollary 6.2.3 and Theorem 6.2.4, we know that the first off-diagonal periodic orbit is created at $\epsilon = \frac{1}{2a}$ when the first synchronized periodic orbit loses transverse stability. That is the fixed point in S_4, $P = (\frac{a}{2a-1}, \frac{a}{2a-1})$. P has eigenvalue $\lambda_{syn} = -\frac{a}{a-1}$ with eigenvector in the synchronized direction, and $\lambda_{trans} = -\frac{a}{a-1}(1-2\epsilon)$ in the transverse direction. For $\frac{1}{2a} < \epsilon < \frac{1}{2}$, $\lambda_{syn} < -1$, $-1 < \lambda_{trans} < 0$, therefore P is a saddle. For $\epsilon < \frac{1}{2a}$, $\lambda_{trans} < -1$ and P becomes a repeller. Thus there is a degenerate flip bifurcation at P at $\epsilon = \frac{1}{2a}$ where $\lambda_{trans} = -1$.

For other synchronized orbits, if a periodic orbit involves S_1 m times and S_4 n times, then the Jacobian matrix of F^{m+n} is

$$DF^{m+n} = (-1)^n \frac{a^{m+n}}{(a-1)^n} \begin{pmatrix} 1-\epsilon & \epsilon \\ \epsilon & 1-\epsilon \end{pmatrix}^{m+n}. \tag{6.9}$$

By direct calculation, one can show that the orbit loses transverse stability at

$$\epsilon = \frac{1}{2}\left(1 - \frac{(a-1)^{\frac{n}{m+n}}}{a}\right). \tag{6.10}$$

Furthermore, if n is odd then $\lambda_{trans} = -1$ at the bifurcation value, so there is a degenerate flip bifurcation; if n is even then $\lambda_{trans} = 1$ at the bifurcation value and there is a degenerate pitchfork bifurcation.

Remark: From (6.10), we can see that synchronized periodic orbits with the same value of $\frac{n}{m+n}$ bifurcate at the same value of ϵ. For example, $\{14\}$, $\{1144\}$, $\{111444\}$ and $\{114144\}$ etc. bifurcate at $\epsilon = \frac{1}{2}\left(1 - \frac{(a-1)^{\frac{1}{2}}}{a}\right)$. Similarly for higher period orbits. Also, for $1 < a < 2$, as ϵ decreases from $\frac{1}{2}$, orbits with larger $\frac{n}{m+n}$ bifurcate first, that is, orbits with larger proportion of 4s.

At $\epsilon = \frac{1}{2a}$, since $\lambda_{trans} = -1$, the line of the corresponding eigenvector through P intersects the two critical lines at $Q = (\frac{1}{a}, \frac{2a^2-2a+1}{a(2a-1)})$ and $Q' = (\frac{2a^2-2a+1}{a(2a-1)}, \frac{1}{a})$. Every point X on the segment QQ' except the fixed point P is a period 2 point, with
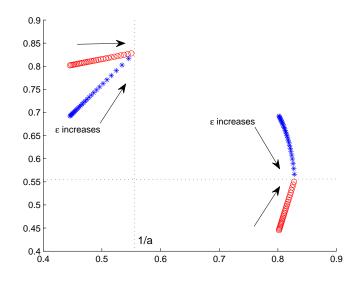
$F(X) = X'$ which is the reflection of X in the diagonal.

As for degenerate flip bifurcations for the border collision normal form described in the previous chapter, one expects that new periodic orbits are created as ϵ decreases further from $\frac{1}{2a}$. At this bifurcation value, instead of having one periodic point on the switching surface, Q and Q' are both on the critical lines. This period-doubled orbit $\{44\}$ can also be labelled as $\{24\}$, $\{43\}$, $\{23\}$ and higher-period combinations of them. When ϵ decreases from $\frac{1}{2a}$, this becomes new periodic orbits, as shown in Figure 6.5. As ϵ increases from 0 to $\frac{1}{2a}$, periodic orbits with these combinations exist and eventually merge on the critical lines at Q and Q' at $\epsilon = \frac{1}{2a}$. Similar diagrams for higher periods are omitted. Note that, these orbits have reflections in the diagonal, so $\{34\}$, $\{3444\}$, $\{3244\}$ and $\{3234\}$ also exist, but are again omitted in the diagram for clearness.
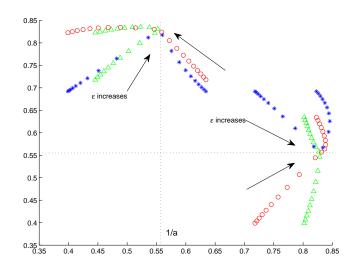
This degenerate bifurcation explains the creation of the set $\mathcal{D}$ in Theorem 6.2.4. At $\epsilon = \frac{1}{2a}$, since the dynamics of the diagonal is governed by the one-dimensional skew-tent map, the preimages of the fixed point P is dense on the diagonal, hence there are infinitely many preimages of P and the line segment QQ' in S_1 and S_4, and each point on them are eventually periodic and not converging to the synchronized state. When ϵ is perturbed below the bifurcation value, the eigenvalue of the fixed point in the transverse direction becomes less than -1. Also, the following lemma has been proved in [40].

Lemma 6.3.1. *Let $a \in (\frac{1}{2}(1 + \sqrt{5}), 2)$ and $\epsilon \in (0, \frac{1}{2a})$. Let U be an open convex polygon in $\mathcal{D}$. Then there exists $k > 0$ and $V \subseteq U$ such that $F^k|_V$ is affine and $F^k(V)$ intersects the diagonal.*

Therefore, for any open convex polygon $U \in \mathcal{D}$, there exists $p \geq 0$ and $V_1 \subseteq V$ such that $F^{k+p}|_{V_1}$ is affine and $F^{k+p}(V_1)$ contains the fixed point P. This set then expands along the transverse direction and contains the new off-diagonal periodic orbits after some iterations. Suppose that U is in the unstable set of one of these periodic orbit, then U contains a homoclinic point to this orbit. Therefore, infinitely

(a) period 2 orbits —- {24} (blue) and {23} (red)

(b) period 4 orbits —- {2444} (blue), {2344} (red) and {2324} (green)

Figure 6.5: As ϵ increases, periodic orbits merge at $\epsilon = \frac{1}{2a}$. ($a = 1.8$)

many periodic orbits, as required in Theorem 6.2.4, are created in the degenerate bifurcation at $\epsilon = \frac{1}{2a}$.

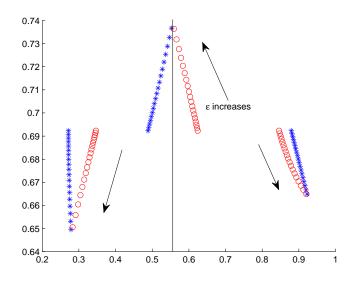As ϵ decreases from $\frac{1}{2a}$, more off-diagonal periodic orbits are created via degenerate bifurcations when other synchronized periodic orbits lose transverse stability. Nonetheless, a lot of other periodic orbits exist and are not created in this way. Note that, at $\epsilon = 0$, the system becomes $x_{n+1} = f_a(x_n)$ and $y_{n+1} = f_a(y_n)$, and since the one-dimensional map f_a is chaotic and the periodic orbits are dense, we have the following lemma.

Lemma 6.3.2. *When $\epsilon = 0$, there exists a periodic orbit for each periodic kneading sequence.*

Therefore, instead of decreasing ϵ from $\frac{1}{2a}$, it is easier to start with some periodic orbit at $\epsilon = 0$, then gradually increase ϵ and see when the orbit is destroyed.

There are 20 distinct period 3 orbits, and they behave in various different ways. $\{114\}$ and $\{144\}$ are in the synchronized state which we have discussed the way they bifurcate above. As the orbit $\{144\}$ loses stability, $\{124\}$ and $\{134\}$ are created in a degenerate fold bifurcation. By calculating the orbits explicitly, one can check that $\{112\}$ and $\{122\}$ (and so $\{113\}$ and $\{133\}$) exist on the y-axis at $\epsilon = 0$ only. For $\epsilon > 0$ these orbits do not exist in S. That leaves 6 pair of orbits, $\{231\}$ and $\{431\}$, $\{232\}$ and $\{432\}$, $\{442\}$ and $\{242\}$, and their reflections in the diagonal. These orbits exhibit border collisions in the same way. We here show the bifurcation of $\{442\}$ and $\{242\}$ in Figure 6.6. There is a border collision pair bifurcation, as the period 3 orbits $\{242\}$ and $\{442\}$ meet on the critical line $x = a^{-1}$ at $\epsilon \sim 0.184$, after which both orbits become virtual and disappear. Higher-period combinations such as $\{(242)(442)\}$ also bifurcate at this value.

In this chapter, we have shown that degenerate bifurcations and border collision bifurcations occur in this coupled piecewise affine system. They are responsible for the creation of the new periodic orbits and the more complicated motion as described in Theorem 6.2.4 [73, 40]. This explains the sudden change in the geometry of the

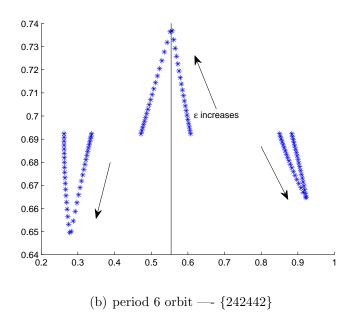(a) period 3 orbits —- {242} (blue) and {442} (red)

(b) period 6 orbit —- {242442}

Figure 6.6: At $\epsilon \sim 0.184$, various orbits of the form {442} and {242} merge on the critical line $x = a^{-1}$

topological attractor as the first synchronized periodic orbit loses transverse stability. (Figure 6.4) We have not yet shown that, when a general synchronized periodic orbit loses stability, which point in the orbit crosses the critical line and enters the other region. This determines the orbits created. But we believe that this point is the one closest to the intersection of the critical lines (a^{-1}, a^{-1}), as the line segment of the transverse eigenvector through the point between the critical lines is shortest. For example, the synchronized $\{14\}$ orbit $P_1 = (\frac{a}{a^2+a-1}, \frac{a}{a^2+a-1}), P_2 = (\frac{a^2}{a^2+a-1}, \frac{a^2}{a^2+a-1})$ bifurcates into period 4 orbit $\{2434\}$ as it loses transverse stability, instead of the orbit $\{1213\}$.

Chapter 7

Conclusions

In this thesis, border collision bifurcations in piecewise smooth discrete-time systems are studied. Piecewise smooth maps have been used as models in various areas. Bifurcations in such maps have little analogue in standard bifurcations in smooth maps, and they are often more complex. We have investigated some of the bifurcation phenomena in two-dimensional continuous piecewise smooth discrete-time systems.

The available results on border collision bifurcations in one and two-dimensional piecewise smooth maps are summarized. For two-dimensional piecewise smooth systems, although some research have been done on their dynamics, usually the maps are assumed to be globally contractive. For maps with area expansions, one might expect divergent motions. We have shown that, by showing the existence of snap-back repellers, such systems can exhibit chaotic dynamics. We have derived sufficient conditions for the existence of simple snap-back repellers. Thus, the dynamics of area expanding systems are not necessarily trivial. Indeed, in Chapter 4 we have shown with some numerical examples that there can exist stable motions in piecewise smooth maps that is area expanding. In particular, there can be stable chaotic motion in a map where both determinants of the Jacobian matrices (one from each side of the border) are greater than one in modulus. We have shown that for appropriate parameter values a polygonal invariant set in the phase space can be constructed. Moreover, we use the results from standard Markov partition theory of dynamical

systems and a generalization of the affine locally eventually onto (ALEO) property to show that this set can be a chaotic attractor so that periodic orbits are dense and there is a dense orbit. We believe that such attractors exist over much larger regions of parameter space, we hope that further research can be done and that the use of the ALEO property will eventually allow us to prove the existence of these attractors.

Various bifurcation phenomena of the stable dynamics of the border collision normal form are then discussed. When an external fixed point changes from a saddle to an unstable node in a degenerate flip bifurcation, new unstable periodic orbits are created on the switching surface. This is different to the standard periodic-doubling bifurcations for smooth systems. If an absorbing region as described exists, the dynamics around these new periodic orbits complicates the geometry of the basin boundary. We have given conditions on the number of sides of the polygon constructed in the way described in Chapter 4. When the basin boundary meets the sides of the polygon, the system loses stability in a boundary crisis.

However, we wish we had had time to study more about these sets. Although for appropriate parameter values we can construct a polygon such that it (or some finite image of it) is invariant, this set is not necessarily the final attracting set. This can involve boundary crises and snap-back repeller bifurcations as described in [33]. (See Figure 5.6) We would also like to connect this to the work of [89, 88, 80, 81].

Finally we have studied a particular example: a two-dimensional system coupled by a piecewise affine map. We have studied its synchronization and the stability of the synchronized state using the theory of border collision bifurcations. We have shown that when a synchronized periodic orbit loses its transverse stability, it undergoes a degenerate bifurcation. Then the presence of the two switching surfaces creates new off-diagonal periodic orbits after the bifurcation. We believe that this bifurcation is responsible for the creation of the quadrilateral where periodic orbits are dense when the first synchronized periodic orbit loses transverse stability, which helps to explain the question originally introduced in [73].

The dynamical behaviour of piecewise smooth systems is incredibly complex and

rich. Even though there have been a lot of research on these systems and their bifurcation phenomena, many aspects of the dynamics of such maps still remain unexplored and to be understood. A detail classification of border collision bifurcations can be a further research direction.

The study on three or higher dimensional piecewise smooth systems is in very preliminary stage and very little is known. So there is a promising research opportunity to study the dynamics of such maps. Also, it would be very useful for analysis to obtain order reduction principles for border collision bifurcations so that the study of the dynamics of multi-dimensional systems can be reduced to the study systems of lower dimension.

Bibliography

[1] R. L. Adler. Symbolic dynamics and Markov partitions. *Bull. Amer. Math. Soc. (N.S.)*, 35(1):1–56, 1998.

[2] K. T. Alligood, T. D. Sauer, and J. A. Yorke. *Chaos: An Introduction to Dynamical Systems.* Springer-Verlag, 1996.

[3] P. Ashwin, J. Buescu, and I. Stewart. From attractor to chaotic saddle: a tale of transverse instability. *Nonlinearity*, 9(3):703–737, 1996.

[4] S. Banerjee and C. Grebogi. Border collision bifurcations in two-dimensional piecewise smooth maps. *Phys. Rev. E*, 59(4):4052–4061, 1999.

[5] S. Banerjee, M. S. Karthik, G. Yuan, and J. A. Yorke. Bifurcations in one-dimensional piecewise smooth maps — theory and applications in switching circuits. *IEEE Trans. Circuits Systems I Fund. Theory Appl.*, 47(3):389–394, 2000.

[6] S. Banerjee, S. Parui, and A. Gupta. Dynamical effects of missed switching in current-mode controlled dc-dc converters. *IEEE Transactions on Circuits and Systems I: Fundamental Theory and Applications*, 51(12):649–654, 2004.

[7] S. Banerjee, P. Ranjan, and C. Grebogi. Bifurcations in two-dimensional piecewise smooth maps — theory and applications in switching circuits. *Circuits and Systems I: Fundamental Theory and Applications, IEEE Transactions on*, 47(5):633 –643, 2000.

[8] S. Banerjee and G. C. Verghese, editors. *Nonlinear Phenomena in Power Electronics: Bifurcations, Chaos, Control, and Applications.* Wiley-IEEE Press, 2001.

[9] S. Banerjee, J. A. Yorke, and C. Grebogi. Robust chaos. *Phys. Rev. Lett.*, 80(14):3049–3052, 1998.

[10] D. Baptista, R. Severino, and S. Vinagre. The basin of attraction of Lozi mappings. *Internat. J. Bifur. Chaos Appl. Sci. Engrg.*, 19(3):1043–1049, 2009.

[11] G. I. Bischi, C. Mammana, and L. Gardini. Multistability and cyclic attractors in duopoly games. *Chaos Solitons Fractals*, 11(4):543–564, 2000.

[12] V. Botella-Soler, J. M. Castelo, J. A. Oteo, and J. Ros. Bifurcations in the lozi map. *Journal of Physics A: Mathematical and Theoretical*, 44(30):305101, 14, 2011.

[13] Y. Cao and Z. Liu. Strange attractors in the orientation-preserving Lozi map. *Chaos Solitons Fractals*, 9(11):1857–1863, 1998.

[14] Y. W. Chang, J. Juang, and C. L. Li. Snap-back repellers and chaotic traveling waves in one-dimensional cellular neural networks. *Internat. J. Bifur. Chaos Appl. Sci. Engrg.*, 17(6):1969–1983, 2007.

[15] G. Chen, S. B. Hsu, and J. Zhou. Snapback repellers as a cause of chaotic vibration of the wave equation with a van del pol boundary condition and energy injection at the middle of the span. *J. Math. Phys.*, 39(12):6459–6489, 1998.

[16] R. L. Devaney. *An Introduction to Chaotic Dynamical Systems.* Westview Press, 2nd edition, 2003.

[17] M. di Bernardo, C. J. Budd, A. R. Champneys, and P. Kowalczyk. *Piecewise-smooth Dynamical Systems. Theory and Applications.* Springer-Verlag, 2008.

[18] M. Di Bernardo, M. I. Feigin, S. J. Hogan, and M. E. Homer. Local analysis of C-bifurcations in n-dimensional piecewise-smooth dynamical systems. *Chaos Solitons Fractals*, 10(11):1881–1908, 1999.

[19] Y. Do. A mechanism for dangerous border collision bifurcations. *Chaos Solitons Fractals*, 32(2):352–362, 2007.

[20] Y. Do and H. K. Baek. Dangerous border-collision bifurcations of a piecewise-smooth map. *Commun. Pure Appl. Anal.*, 5(3):493–503, 2006.

[21] Y. Do, S. D. Kim, and P. S. Kim. Stability of fixed points placed on the border in the piecewise linear systems. *Chaos Solitons Fractals*, 38(2):391–399, 2008.

[22] V. A. Dobrynskiy. On attractors of piecewise linear 2-endomorphisms. *Nonlinear Anal.*, 36(4, Ser. A: Theory Methods):423–455, 1999.

[23] M. Dutta, H. E. Nusse, E. Ott, J. A. Yorke, and G. Yuan. Multiple attractor bifurcations: A source of unpredictability in piecewise smooth systems. *Phys. Rev. Lett.*, 83(21):4281–4284, 1999.

[24] Z. Elhadj. A new chaotic attractor from 2d discrete mapping via border-collision period-doubling scenario. *Discrete Dynamics in Nature and Society*, 2005(3):235–238, 2005.

[25] Z. Elhadj and J. C. Sprott. A new simple 2-D piecewise linear map. *J. Syst. Sci. Complex.*, 23(2):379–389, 2010.

[26] M. I. Feigin. Doubling of the oscillation period with C-bifurcations in piecewise-continuous systems. *Prikl. Mat. Meh.*, 34:861–869, 1970.

[27] M. I. Feigin. The increasingly complex structure of the bifurcation tree of a piecewise-smooth system. *Journal of Applied Mathematics and Mechanics*, 59(6):853–863, 1995.

[28] H. Fujisaka and T. Yamada. Stability theory of synchronized motion in coupled-oscillator systems. *Progr. Theoret. Phys.*, 69(1):32–47, 1983.

[29] H. Fujisaka and T. Yamada. Stability theory of synchronized motion in coupled-oscillator systems. iii. *Progr. Theoret. Phys.*, 72(5):885–894, 1984.

[30] H. Fujisaka and T. Yamada. A new intermittency in coupled dynamical systems. *Progr. Theoret. Phys.*, 74(4):918–921, 1985.

[31] H. Fujisaka and T. Yamada. Stability theory of synchronized motion in coupled-oscillator systems. iv. *Progr. Theoret. Phys.*, 75(5):1087–1104, 1986.

[32] A. Ganguli and S. Banerjee. Dangerous bifurcation at border collision: when does it occur? *Phys. Rev. E (3)*, 71(5):057202, 4, 2005.

[33] L. Gardini. Some global bifurcations of two-dimensional endomorphisms by use of critical lines. *Nonlinear Anal.*, 18(4):361–399, 1992.

[34] L. Gardini. Homoclinic bifurcations in n-dimensional endomorphisms, due to expanding periodic points. *Nonlinear Anal.*, 23(8):1039–1089, 1994.

[35] L. Gardini and F. Tramontana. Snap-back repellers in non-smooth functions. *Regul. Chaotic Dyn.*, 15(2-3):237–245, 2010.

[36] P. Gaspard and X. J. Wang. Homoclinic orbits and mixed-mode oscillations in far-from-equilibrium systems. *J. Statist. Phys.*, 48(1-2):151–199, 1987.

[37] E. Glasner and B. Weiss. Sensitive dependence on initial conditions. *Nonlinearity*, 6(6):1067–1075, 1993.

[38] P. Glendinning. The stability boundary of synchronized states in globally coupled dynamical systems. *Phys. Lett. A*, 259(2):129–134, 1999.

[39] P. Glendinning. Transitivity and blowout bifurcations in a class of globally coupled maps. *Phys. Lett. A*, 264(4):303–310, 1999.

[40] P. Glendinning. Milnor attractors and topological attractors of a piecewise linear map. *Nonlinearity*, 14(2):239–257, 2001.

[41] P. Glendinning. Bifurcations of snap-back repellers with application to border-collision bifurcations. *Internat. J. Bifur. Chaos Appl. Sci. Engrg.*, 20(2):479–489, 2010.

[42] P. Glendinning and C. H. Wong. Border collision bifurcations, snap-back repellers, and chaos. *Phys. Rev. E (3)*, 79(2):025202, 4, 2009.

[43] P. Glendinning and C. H. Wong. Two-dimensional attractors in the border-collision normal form. *Nonlinearity*, 24(4):995–1010, 2011.

[44] C. Grebogi, E. Ott, and J. A. Yorke. Chaotic attractors in crisis. *Phys. Rev. Lett.*, 48(22):1507–1510, 1982.

[45] C. Grebogi, E. Ott, and J. A. Yorke. Crises, sudden changes in chaotic attractors, and transient chaos. *Phys. D*, 7(1-3):181–200, 1983. Order in chaos (Los Alamos, N.M., 1982).

[46] C. Grebogi, E. Ott, and J. A. Yorke. Chaos, strange attractors, and fractal basin boundaries in nonlinear dynamics. *Science*, 238(4827):632–638, 1987.

[47] J. Guckenheimer and R. F. Williams. Structural stability of Lorenz attractors. *Inst. Hautes Études Sci. Publ. Math.*, (50):59–72, 1979.

[48] M. Hasler and Y. L. Maistrenko. An introduction to the synchronization of chaotic systems: coupled skew tent maps. *IEEE Trans. Circuits Systems I Fund. Theory Appl.*, 44(10):856–866, 1997. Special issue on chaos synchronization, control, and applications.

[49] M. A. Hassouneh. *Feedback control of border collision bifurcations in piecewise smooth systems.* PhD thesis, University of Maryland, College Park, U.S.A., 2003.

[50] M. A. Hassouneh, E. H. Abed, and H. E. Nusse. Robust dangerous border-collision bifurcations in piecewise smooth systems. *Phys. Rev. Lett.*, 92(7):070201, 4, 2004.

[51] S. J. Hogan, L. Higham, and T. C. L. Griffin. Dynamics of a piecewise linear map with a gap. *Proc. R. Soc. Lond. Ser. A Math. Phys. Eng. Sci.*, 463(2077):49–65, 2007.

[52] Y. Ishii and D. Sands. Lap number entropy formula for piecewise affine and projective maps in several dimensions. *Nonlinearity*, 20(12):2755–2772, 2007.

[53] P. Jain and S. Banerjee. Border-collision bifurcations in one-dimensional discontinuous maps. *Internat. J. Bifur. Chaos Appl. Sci. Engrg.*, 13(11):3341–3351, 2003.

[54] R. I. Leine and H. Nijmeijer. *Dynamics and Bifurcations of Non-smooth Mechanical Systems*. Springer-Verlag, 2004.

[55] C. Li and G. Chen. An improved version of the marotto theorem. *Chaos Solitons Fractals*, 18(1):69–77, 2003.

[56] T. Y. Li and J. A. Yorke. Period three implies chaos. *Amer. Math. Monthly*, 82(10):985–992, 1975.

[57] Z. Li, Y. Shi, and C. Zhang. Chaos induced by heteroclinic cycles connecting repellers in complete metric spaces. *Chaos Solitons Fractals*, 36(3):746–761, 2008.

[58] W. Lin. *Some theoretical problems in complex systems and their applications*. PhD thesis, Fudan University, Shanghai, People's Republic of China, 2002.

[59] W. Lin and G. Chen. Heteroclinical repellers imply chaos. *Internat. J. Bifur. Chaos Appl. Sci. Engrg.*, 16(5):1471–1489, 2006.

[60] W. Lin, J. Ruan, and W. Zhao. On the mathematical clarification of the snap-back-repeller in high-dimensional systems and chaos in a discrete neural network model. *Internat. J. Bifur. Chaos Appl. Sci. Engrg.*, 12(5):1129–1139, 2002. Chaos control and synchronization (Shanghai, 2001).

[61] W. Lin, J. Wu, and G. Chen. Generalized snap-back repeller and semi-conjugacy to shift operators of piecewise continuous transformations. *Discrete Contin. Dyn. Syst.*, 19(1):103–119, 2007.

[62] Z. R. Liu, H. M. Xie, Z. X. Zhu, and Q. H. Lu. The strange attractor of the Lozi mapping. *Internat. J. Bifur. Chaos Appl. Sci. Engrg.*, 2(4):831–839, 1992.

[63] Y. Maistrenko, I. Sushko, and L. Gardini. About two mechanisms of reunion of chaotic attractors. *Chaos Solitons Fractals*, 9(8):1373–1390, 1998.

[64] Y. L. Maistrenko, V. L. Maistrenko, and L. O. Chua. Cycles of chaotic intervals in a time-delayed Chua's circuit. *Internat. J. Bifur. Chaos Appl. Sci. Engrg.*, 3(6):1557–1572, 1993.

[65] F. R. Marotto. Snap-back repellers imply chaos in $\mathbf{R}^n$. *J. Math. Anal. Appl.*, 63(1):199–223, 1978.

[66] F. R. Marotto. On redefining a snap-back repeller. *Chaos Solitons Fractals*, 25(1):25–28, 2005.

[67] C. Mira, L. Gardini, A. Barugola, and J. C. Cathala. *Chaotic Dynamics in Two-Dimensional Noninvertible Maps*. World Scientific, 1996.

[68] C. Mira, C. Rauzy, Y. Maistrenko, and I. Sushko. Some properties of a two-dimensional piecewise-linear noninvertible map. *Internat. J. Bifur. Chaos Appl. Sci. Engrg.*, 6(12A):2299–2319, 1996.

[69] M. Misiurewicz. Strange attractors for the Lozi mappings. In *Nonlinear dynamics (Internat. Conf., New York, 1979)*, volume 357 of *Ann. New York Acad. Sci.*, pages 348–358. New York Acad. Sci., New York, 1980.

[70] H. E. Nusse, E. Ott, and J. A. Yorke. Border-collision bifurcations: an explanation for observed bifurcation phenomena. *Phys. Rev. E (3)*, 49(2):1073–1076, 1994.

[71] H. E. Nusse and J. A. Yorke. Border-collision bifurcations including "period two to period three" for piecewise smooth systems. *Phys. D*, 57(1-2):39–57, 1992.

[72] H. E. Nusse and J. A. Yorke. Border-collision bifurcations for piecewise smooth one-dimensional maps. *Internat. J. Bifur. Chaos Appl. Sci. Engrg.*, 5(1):189–207, 1995.

[73] A. S. Pikovsky and P. Grassberger. Symmetry breaking bifurcation for coupled chaotic attractors. *J. Phys. A*, 24(19):4587–4597, 1991.

[74] T. Puu and I. Sushko, editors. *Business Cycles Dynamics: Models and Tools.* Springer, 2006.

[75] B. Rakshit. *Studies on some atypical bifurcation phenomena in continuous and discontinuous piecewise smooth maps.* PhD thesis, Indian Institute of Technology, Kharagpur, India, 2009.

[76] A. N. Sharkovsky and L. O. Chua. Chaos in some 1-d discontinuous maps that appear in the analysis of electrical circuits. *IEEE Transactions on Circuits and Systems I: Fundamental Theory and Applications*, 40(10):722–731, 1993.

[77] Y. Shi and G. Chen. Chaos of discrete dynamical systems in complete metric spaces. *Chaos Solitons Fractals*, 22(3):555–571, 2004.

[78] Y. Shi and P. Yu. Chaos induced by regular snap-back repellers. *J. Math. Anal. Appl.*, 337(2):1480–1494, 2008.

[79] D. J. W. Simpson. *Bifurcations in Piecewise-Smooth, Continuous Systems.* PhD thesis, University of Colorado, 2008.

[80] D. J. W. Simpson and J. D. Meiss. Neimark-Sacker bifurcations in planar, piecewise-smooth, continuous maps. *SIAM J. Appl. Dyn. Syst.*, 7(3):795–824, 2008.

[81] D. J. W. Simpson and J. D. Meiss. Shrinking point bifurcations of resonance tongues for piecewise-smooth, continuous maps. *Nonlinearity*, 22(5):1123–1144, 2009.

[82] I. Sushko and L. Gardini. Center bifurcation for two-dimensional border-collision normal form. *Internat. J. Bifur. Chaos Appl. Sci. Engrg.*, 18(4):1029–1050, 2008.

[83] I. Sushko and L. Gardini. Degenerate bifurcations and border collisions in piecewise smooth 1D and 2D maps. *Internat. J. Bifur. Chaos Appl. Sci. Engrg.*, 20(7):2045–2070, 2010.

[84] J. Tseng. Schmidt games and Markov partitions. *Nonlinearity*, 22(3):525–543, 2009.

[85] M. Urbański. The Hausdorff dimension of the set of points with nondense orbit under a hyperbolic dynamical system. *Nonlinearity*, 4(2):385–397, 1991.

[86] T. Yamada and H. Fujisaka. Stability theory of synchronized motion in coupled-oscillator systems. II. The mapping approach. *Progr. Theoret. Phys.*, 70(5):1240–1248, 1983.

[87] Z. T. Zhusubaliyev and E. Mosekilde. *Bifurcations and Chaos in Piecewise-Smooth Dynamical Systems*. World Scientific, 2003.

[88] Z. T. Zhusubaliyev, E. Mosekilde, S. De, and S. Banerjee. Transitions from phase-locked dynamics to chaos in a piecewise-linear map. *Phys. Rev. E (3)*, 77(2):026206, 9, 2008.

[89] Z. T. Zhusubaliyev, E. Mosekilde, S. Maity, S. Mohanan, and S. Banerjee. Border collision route to quasiperiodicity: numerical investigation and experimental confirmation. *Chaos*, 16(2):023122, 11, 2006.